NORM FASTENERS
AR-GE MERKEZİ YAYINLARI

R&D CENTER PUBLICATIONS

2024

VOLUME 10

NORM
FASTENERS

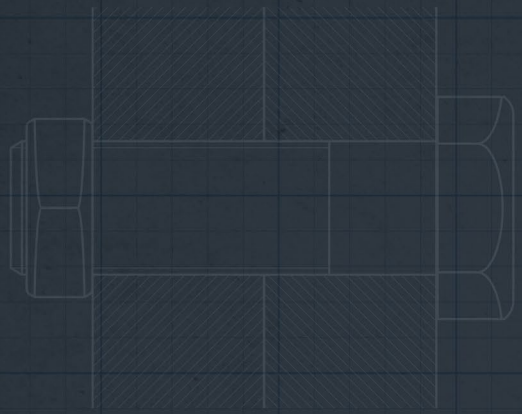

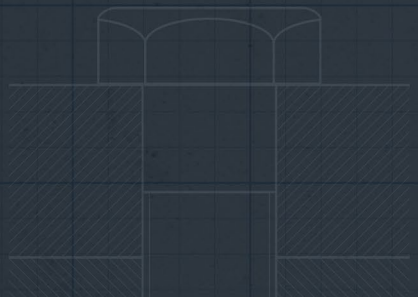

NORM FASTENERS

AR-GE MERKEZİ YAYINLARI

R&D CENTER PUBLICATIONS

ÖN SÖZ

Umut İnce
Norm Fasteners Ar-Ge ve Mühendislik Direktörü

Norm Holding'in sürdürülebilir gelecek vizyonuyla hareket eden bir ekip olarak, her geçen gün Ar-Ge ve inovasyon alanında ivme kazanan yatırımlarımızla sektördeki gelişimi desteklemeye odaklanıyoruz. Değerli iş ortaklarımızla birlikte, geleceğe değer katma misyonumuzu sürdürmek adına kararlı adımlarla ilerliyoruz.

Akademik geçmişe sahip, uzman Ar-Ge ekibimiz ve güçlü iş birliklerimizle birlikte, müşterilerimizin talepleri doğrultusunda katma değeri yüksek çözümler geliştirmenin yanı sıra ulusal ve uluslararası alanda sektöre öncülük eden çalışmalar yürütüyoruz. Her bir projemizde artan motivasyon ve azimle hedeflerimize doğru ilerlerken, teknolojik ilerlemelere katkıda bulunmayı ve sektörümüzde birlikte güçlenerek ilerlemeyi bir sorumluluk olarak görüyoruz.

2024 yılı içerisinde gerçekleştirdiğimiz çalışmaların meyvesini sizlerle paylaşmaktan büyük mutluluk ve gurur duyuyoruz. Bu kitapçık ile birlikte, ortak hedeflerimiz doğrultusunda yürüttüğümüz Ar-Ge faaliyetlerinin sonuçlarını siz değerli iş ortaklarımızla paylaşarak geleceğe değer katmaya devam etmekten memnuniyet duymaktayız.

FOREWORD

Umut İnce
Norm Fasteners R&D and Engineering Director

Driven by a vision of a sustainable future of Norm Holding, we are a team focused on supporting the development of the sector with our investments gaining momentum in R&D and innovation day by day. Together with our valued business partners, we are moving forward with determined steps to continue our mission of adding value to the future.

With our R&D team of expert researchers with strong academic backgrounds, and strong partnerships, we develop high added value solutions in line with the demands of our customers as well as we conduct pioneering work both nationally and internationally. As we move towards our goals with increasing motivation and determination in each of our project, we see it as a responsibility to contribute to technological advancements and grow stronger together in our industry.

We are thrilled and proud to share with you the fruits of our efforts in 2024. With this booklet, we are pleased to continue adding value to the future by sharing the results of the R&D activities we carry out in line with our common goals with you, our valued business partners.

EFFECTS OF CO RATIO ON FATIGUE LIFE OF WC-CO DIE INSERTS USED IN COLD FORMING OPERATIONS

Burak HIZLI
Kübra ÖZTÜRK
Umut İNCE

ESAFORM 2024

EFFECTS OF CO RATIO ON FATIGUE LIFE OF WC-CO DIE INSERTS USED IN COLD FORMING OPERATIONS

Burak HIZLI[1,2,a*], Kübra ÖZTÜRK[1,2,b] and Umut İNCE[2,c]

[1]Department of Metallurgical and Materials Engineering, Dokuz Eylul University, İzmir, Türkiye
[2]R&D Center, Norm İzmir Cıvata San. ve Tic. A.Ş., AOSB, İzmir, Türkiye
[a*]burak.hizli@normfasteners.com, [b]kubra.ozturk@normfasteners.com, [c]umut.ince@normfasteners.com([*]corresponding author)

Abstract

Production of fasteners via cold forming requires high forming forces, which induce significant stresses in dies. Therefore, die performance becomes a critical parameter of the fastener production process. Estimation of die life with high accuracy allows to enhance production efficiency and reduce die-related expenditures. Generally, WC-Co hardmetals consisting of 4-30% Co content as a binder are highly preferred in cold forming operations. WC-Co metal-ceramic composite materials offer high wear resistance against frictional forces, high compressive strength, and lower elastic deformation to resist excessive contact pressures, which are primary requirements for cold-forming dies. In this study, experimental investigations were conducted for the determination and comparison of fatigue performance at three different stress amplitudes, utilizing three-point bending fatigue testing with two different grades of WC-Co hardmetals. After the experiments, Goodman-Haigh diagrams were obtained from the experimental results to be utilized in predictive die-life calculations.

Keywords: WC-Co, Co ratio, Fatigue life, Cold forming.

1. Introduction

Tungsten carbide-cobalt materials are ceramic-matrix composite materials with high wear resistance, consisting of a WC as a hard phase and Co as a soft binding phase. Low cobalt content in a hardmetal causes large gaps between WC grains, resulting in a material with lower toughness and resistance to fatigue [1]. Various combinations are formed depending on the content of the Co binder, and they are used in different industries according to the needs, ranging from automotive parts production to the mining sector [1, 2]. Die materials used in the cold forming process require high fracture toughness to prevent crack propagation, wear resistance, and high fatigue strength due to the high forming forces that create significant stresses in the dies. [2]. As a consequence, die life has a direct and significant impact on several factors, including mass production, production plans, costs, and customer satisfaction. In the studies conducted in the literature on this subject, Tanrikulu et al. examined three-point bending fatigue tests on specimens of WC-20 wt.% Co, which are often used in cold forging dies, with a loading ratio (R) of 0.1, and constructed Morrow-Haigh diagrams to determine the fatigue life. Through comparison of three-point bending test results with production line dies, their model accurately predicted fatigue life with a deviation of only 5.6 % [3]. The research conducted by Klünser et al. investigated various grades with variations in WC grain size and Co binder content, ranging from 0.2 to 1.3 µm and 6 to 12 wt.%, respectively. They demonstrated that the fatigue crack growth behavior of a hardmetal alloy with an ultra-fine WC grain size showed a dependency on the stress ratio. The threshold stress intensity factor range for fatigue crack growth from inhomogeneities was found to vary with stress ratios, with values of 4.3, 6.2, and 9 MPa for R=0.1, -1, and -3, respectively [4]. Ferreira et al. examined the mechanical behavior of WC-Co materials with different Co ratios (R=0.05 and R=0.5) and demonstrated the influence of Co content on ductility and brittleness [5]. Mikado et al. investigated the fatigue strength of WC-Co materials using a three-point bending test with R=0.5 and analyzed S-N diagrams [6]. A study by Torres et al. aimed to assess the fatigue behavior of a fine-grained WC-10 wt.% Co hardmetal. It specifically examined the influence of mean stress on the fatigue limit of hardmetals, suggesting that this influence could be elucidated through a Goodman-like relationship [7]. Li et al. examined the fatigue strengths of WC-Co samples with Co binder contents ranging from 3 to 20 wt. % were compared based on their Co content. Having an in-depth knowledge of the mechanical properties of WC-Co will enable companies to determine the most suitable composite structure for various types of industrial processes [8]. Therefore, the fatigue performance of two different grades of WC-Co hardmetals was meticulously investigated and compared in this study. Experimental investigations were conducted for the determination and comparison of fatigue performances at three different stress amplitudes, utilizing three-point bending fatigue testing with two different grades of WC-Co hardmetals. After the completion of experiments, Goodman-Haigh diagrams were obtained from the experimental results.

2. Materials & Method

In this study, different grades of WC-Co materials that have Co contents of 19 and 26% were used in the experiments in order to reveal the fatigue life performance of die inserts used in heading and upsetting operations. Referenced grades were supplied from Boehlerit GmbH & Co.KG with corresponding product range numbers of GB40 and GB56, respectively. The chemical compositions, and mechanical and physical properties of these grades shared by the supplier are given in Table 1. All the test samples were produced by sintering WC powder with Co binder using special molds and HIPed to fabricate the test samples without machining.

Table 1. Properties of referenced grades.

Grade	Chemical Composition [wt. %]			Density [g/cm3]	Hardness HV 30 [MPa]	Copressive Strength [MPa]	Transverse Rupture Strength [MPa]	Fracture Toughness [$MNm^{3/2}$]	Elastic Modulus [GPa]	Thermal Expansion Coefficient [10-6 / K]
	WC	Co	Other							
GB40	Balanced	19	<0.2	13.60	950	4,000	2800	≥ 24	530	6
GB56	Balanced	26	<0.2	13.05	815	3,200	2700	≥ 24	490	6.5

It is crucial to decrease the surface roughness of forming dies in order to prevent excessive frictional effects that could cause high forming forces and, in return, lower the die life during cold forming. Therefore, prior to testing stage, the surfaces of the test samples were grinded and polished to obtain surface conditions similar to forming dies. Surface preparations were completed in two steps: (i) grinding of each surface with 220+ grid diamond disc under 40 N for 3 min. at 400 rpm, and (ii) polishing of each surface with 9 – 3 µm diamond disc under 25 N for 5 min. at 400 rpm. Surface preparation steps were carried out using Metkon Forcipol 102 grinding and polishing machine with Metkon Forcimat 102 automatic head. Following the microstructural observations, the surface roughness of grinded and polished surfaces of samples was measured by Mitutoyo Surftest SJ 210 portable surface roughness measurement instrument in terms of Ra, Rq, and Rz values. During the measurements, roughness values of the polished surfaces were measured with a straight line pattern over a sampling length of 4.8 mm, in accordance with ISO 1997. Additionally, microstructural observations were conducted on samples of both grades using Zeiss Axio Imager.M2m optical microscope on the polished surfaces.

Fatigue life tests were carried out on prismatic test samples using a three-point bending test apparatus adapted to Zwick Roell Amsler 250 FP 5100 high-frequency fatigue testing machine. Test samples were produced according to Type B as given in ISO 3327:2009, whose nominal dimensions are 20x6.5x5.25 mm [9]. Test samples and fatigue testing stage are illustrated in Fig. 1a and Fig. 1b, respectively. Stress amplitudes in fatigue tests were determined as 750, 800, and 850 MPa in order to observe the fatigue behavior in a wide range of loading conditions. Stress ratios (R) were determined using minimum stress (σ_{min}) and maximum stress (σ_{max}) values in a cycle as given in Eq. 1. Mean stresses (σ_m) and stress amplitudes (σ_a) were sequentially calculated by the formulas in Eq. 2 and Eq. 3 as given below.

$$R = \frac{\sigma_{min}}{\sigma_{max}} \quad (1)$$

$$\sigma_m = \frac{\sigma_{max} + \sigma_{min}}{2} \quad (2)$$

$$\sigma_a = \frac{\sigma_{max} - \sigma_{min}}{2} \quad (3)$$

Maximum and minimum loads in fatigue tests were calculated for corresponding maximum and minimum stress values based on stress ratios of R=0.1 and R=0.2 by using Eq. 4 which is given in ISO 3327:2009 as;

$$R_{bm} = \frac{3kFl}{2bh^2} \quad (4)$$

where R_{bm} is transverse rupture strength in MPa, F is the force applied to the test piece in N, k is the correction factor to compensate for the chamfer, l is the distance between supports, b is the width of test piece perpendicular to its height, and h is the height of test piece parallel to the direction of application of the test force, respectively. k value was taken as 1, as described in the standard for test samples having chamfer of 0,15 to 0,2 mm.

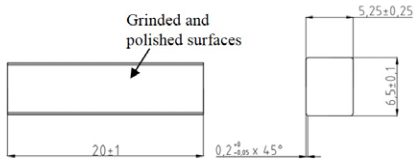

(a)

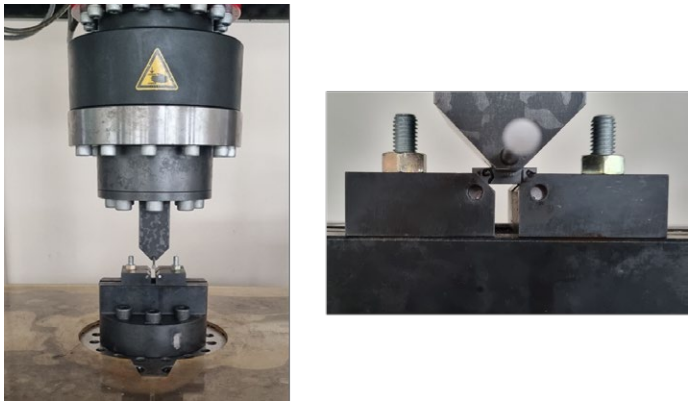

(b)

Fig. 1. (a) Dimensions of prismatic samples used in the testing stage and (b) testing fixtures used in fatigue tests and sample positioning.

Calculated static and dynamic forces in fatigue tests corresponding to maximum, minimum, and mean stress values are given in Table 2. The endurance limit for fatigue tests was accepted as 5,000,000 cycles. The average fatigue performance of each set was determined from consistent 3 test results. S-N curves and Goodman-Haigh diagrams were obtained and compared from test results of each grade in order to correlate test results with life cycles of forming dies during the cold forming operations.

Table 2. Fatigue test parameters and corresponding static and dynamic loads.

Stress Ratio [R]	Stress Amplitude, σa [MPa]	Min.Stress σmin [MPa]	Max Stress, σmax [MPa]	Mean Stress, σm [MPa]	Static Load [kN]	Dynamic Load [kN]
0.1	850	188.9	1,888.9	1,038.9	6.20	5.08
	800	177.8	1,777.8	977.8	5.84	4.78
	750	166.7	1,666.7	916.7	5.47	4.48
0.2	850	425	2,125	1,275	7.61	5.08
	800	400	2,000	1,200	7.17	4.78
	750	375	1,875	1,125	6.72	4.48

3. Results & Discussions

OM micrographs of both grades are shown in Fig 2a and 2b, respectively. WC powders in Co binder exhibited homogenous distributions regardless of the amount of Co binder. However, the difference in the amount of Co binder depending on grade was identified from the micrographs. WC powders with an average particle size of 6.6 µm were used during the fabrication of GB40 samples. For GB56 samples, the average particle size of WC particles was found as 6.1 µm.

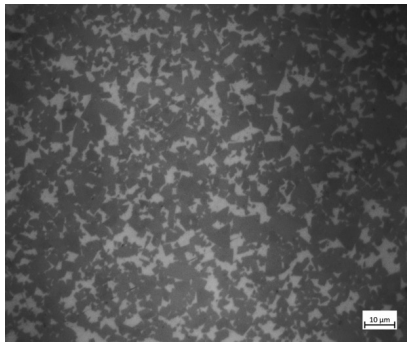

(a)

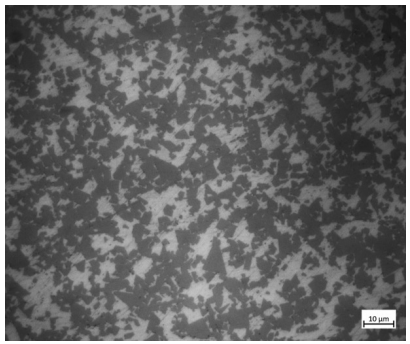

(b)

Fig. 2. OM micrographs of (a) GB40 and (b) GB56.

Surface roughness results obtained from grinded and polished samples are given in Table 3. According to the results, it was seen that values exhibited convergent and even superior values compared to those of forming dies. Also, surface roughness results were in well-conforming manner to surface conditions outlined in ISO 3327:2009, which is defined as not exceeding R_a limit of 0,4 µm. These findings are evident that failure in fatigue tests is expected to originate from inner defects rather than surface conditions.

Table 3. R_a, R_q, and R_z values of test samples.

Grade	R_a (µm)	R_q (µm)	R_z (µm)
GB40	0.036 ± 0.010	0.044 ± 0.05	0.255 ± 0.031
GB56	0.046 ± 0.021	0.058 ± 0.026	0.275 ± 0.098

Three-point bending fatigue test results of GB40 and GB56 insert materials are listed in Tables 4 and 5 in detail, respectively. For both grades, fatigue test results showed a consistent manner with each other considering stress ratio, stress amplitude, and hardness increase with Co content decrease.

Table 4. Fatigue test results of GB40 samples.

Stress Ratio [R]	Static Load [kN]	Dynamic Load [kN]	Stress Amplitude [MPa]	Cycles to Failure	Average Cycles to Failure
0.1	6.20	5.08	850	268,396	438,316 ± 221,767
	6.20	5.08	850	357,366	
	6.20	5.08	850	689,185	
	5.84	4.78	800	772,647	2,144,884 ± 2,473,221
	5.84	4.78	800	662,006	
	5.84	4.78	800	5,000,000	
	5.47	4.48	750	5.000.000	5,000,000
	5.47	4.48	750	5.000.000	
	5.47	4.48	750	5.000.000	
0.2	7.61	5.08	850	179,076	174,419 ± 74,119
	7.61	5.08	850	98,081	
	7.61	5.08	850	246,101	
	7.17	4.78	800	431,630	310,732 ± 136,040
	7.17	4.78	800	163,423	
	7.17	4.78	800	337,144	
	6.72	4.48	750	463,139	700.656 ± 205,850
	6.72	4.48	750	811,459	
	6.72	4.48	750	827,372	

Table 5. Fatigue test results of GB56 samples.

Stress Ratio [R]	Static Load [kN]	Dynamic Load [kN]	Stress Amplitude [MPa]	Cycles to Failure	Average Cycles to Failure
0.1	6.20	5.08	850	114,737	87,383 ± 36,755
	6.20	5.08	850	45,603	
	6.20	5.08	850	101,808	
	5.84	4.78	800	208,056	127,365 ± 73,225
	5.84	4.78	800	65,142	
	5.84	4.78	800	108,896	
	5.47	4.48	750	97,394	269,746 ± 205,725
	5.47	4.48	750	497,502	
	5.47	4.48	750	214,342	
0.2	7.61	5.08	850	22,276	25,083 ± 8,244
	7.61	5.08	850	34,365	
	7.61	5.08	850	18,609	
	7.17	4.78	800	100,492	74,994 ± 22,536
	7.17	4.78	800	66,745	
	7.17	4.78	800	57,744	
	6.72	4.48	750	122,389	123,889 ± 53,824
	6.72	4.48	750	70,831	
	6.72	4.48	750	178,448	

According to fatigue test parameters given in Table 2, maximum, minimum and mean stress levels considerably altered as the stress ratio increased to R=0.2. Because of this reason, cycles to failure in R=0.2 were significantly decreased compared to cycles acquired from R=0.1 tests. It is generally anticipated that WC-Co grades with higher binder content exhibit greater toughness than grades with lower binder content, resulting in improved performance in resisting higher forming loads during cold forming operations. Consequently, WC-Co grades with higher binder content demonstrate increased resistance to cyclic loads, as evidenced by an extended cycle-to-failure capability. Additionally, lower binder content leads to increased brittleness, so toughness decreases. However, in contrast to having a lower binder content than the other grade, the results of GB40 grade were well above those obtained from GB56 grade, considering both stress ratios and each stress amplitude. Despite GB56 tests, several tests on GB40 grade which were conducted at various stress amplitudes and stress ratios resulted in run-out and reaching the endurance limit. These results were attributed to the probability of the existence of <0.2 % other elements such as Cr and Mo in GB40 grade that improve the material properties. As comparing the two referenced grades, GB40 results exhibited noticeable scattering in all test sets, even higher in test sets of low mean stress-stress amplitudes. It is noteworthy to be said that inner defects and their severeness become critical influencing criteria in terms of fatigue performance and eventual cycles to failure. For any stress combinations lying within the limit areas of R=0.2 with stress amplitude of 750 MPa and R=0.1 with stress amplitude of 800 MPa evidently showed the effect of the previous statement. Additionally, having slightly bigger sized WC powders by GB40 was predicated as an accompanied factor to result in better fatigue performance than GB56 due to lowering crack propagation rates. These outcomes would be further investigated and verified through elemental analysis and examination of fracture surfaces. Also, test results would be confirmed in real-world applications for usage in die life simulations and production trials of die inserts built by using GB40 and GB56 grades.

Following the testing stage, obtained test results were employed to draw Goodman-Haigh diagrams that would be utilized in die life estimations of WC-Co die inserts. Respective diagrams for both GB40 and GB56 grades are illustrated in Fig. 3 and Fig. 4. With the help of these diagrams, die lifes and safe stress limits could be estimated based on determined areas separated by fitted lines of cycle-to-failure limits, also identifying the corresponding mean stress-stress amplitude ranges in which the die insert could perform reliably.

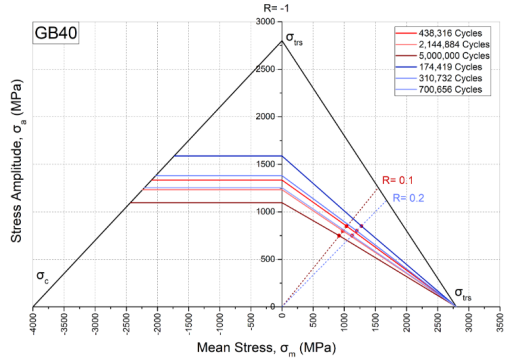

Fig. 3. Goodman-Haigh diagram of GB40 grade for R=0.1 and R=0.2.

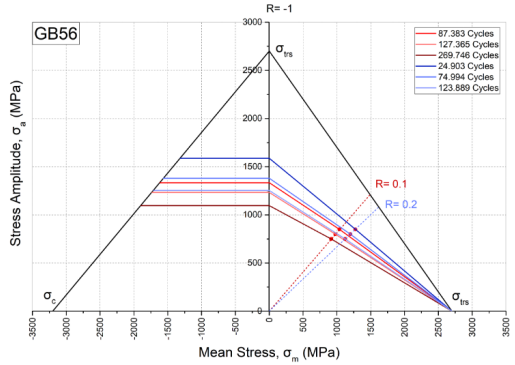

Fig. 4. Goodman-Haigh diagram of GB56 grade for R=0.1 and R=0.2.

As the fatigue tests at R=-1 stress ratio could not be conducted for the three-point bend samples of hardmetals, the transverse rupture strength of such hardmetals was utilized as static failure strength instead of the ultimate tensile strength value in the Goodman-Haigh graph. In contrast to diagrams that are drawn for materials with infinite fatigue life, diagrams for hardmetals help to define stress limits and corresponding fatigue life limits. Therefore, fitted lines based on mean stress-stress amplitude values illustrate the most probable cycles until failure due to fatigue and life zones placed on each fitted line are restricted with other lines that show a lower fatigue life. The Goodman-Haigh diagrams were extended to include the compression zone, facilitating the adjustment of the acquired lines to the compression characteristics of the material. With the utilization of the shrink-fitting process in cold forming dies, there is a need for a comprehensive fatigue life map that takes into account the compressive stresses present in the core material of WC-Co die inserts due to shrink-fitting. The compressive strength of the material represents the static failure strength on the compression zone of the diagram, which was taken as 4,000 MPa and 3,200 MPa for GB40 and GB56, respectively. The diagrams given in Fig. 3 and Fig. 4 would directly be used to predict the most probable fatigue lifes of GB40 and GB56 in the case of being exposed to several means stress and stress amplitude combinations. Additionally, fatigue life limits for the R=-1 stress ratio could be determined from where the fitted limit lines meet the stress amplitude axis and then S-N diagrams would be drawn for each stress amplitude accordingly. Though the fatigue endurance limit of GB40 was found as 1096 MPa directly from diagrams for zero mean stress condition, the determination of the fatigue endurance limit of GB56 required further tests in lower mean stress-stress amplitude values rather than those reported above.

Conclusions

In the scope of this study, two different grades of WC-Co materials that sequentially have Co contents of 19 and 26% were tested and investigated to understand the effects of Co content on the fatigue life of WC-Co die inserts, which are highly preferred materials in heading and upsetting operations due to high resistance against frictional forces and high contact pressures, superior compressive strength, and lower elastic deformation under forming forces. The following conclusions can be extracted from the experimental results and Goodman-Haigh diagrams:

- Fatigue tests were conducted after reaching lower surface roughness values in order not to cause failure by the surface defects, originating from inner flaws and defects.
- GB40 (WC-19 wt.% Co) grade exhibited better fatigue performance compared to GB56 (WC-26 wt.% Co) in contrast to its increased sensitivity to brittleness due to less binder content and higher hardness.
- Superior test results obtained from GB40 grade were attributed to the probability of existence of <0.2 % other elements such as Cr and Mo. The addition of such elements in WC-Co grade is likely to improve the material properties including fatigue resistance.
- As the Co content decreased, the standard deviation for the same sets increased.
- Goodman-Haigh diagram of both GB40 and GB56 grades were drawn by utilizing experimental results. Die life estimations and determination of safe stress limits could be made based on determined areas separated by fitted lines of cycle-to-failure limits, also identifying the corresponding mean stress-stress amplitude ranges in which the die insert could perform reliably.
- Stress amplitude values read for R=-1 stress ratio conditions when the respective limit lines cross the vertical axis in Goodman-Haigh diagrams could be used to construct an S-N diagram of zero mean stress condition.

The aforementioned experimental outcomes would be further investigated and verified through elemental analysis, and examination of fracture surfaces. Fatigue test results are planned to be confirmed in real-world applications for usage in die life simulations and production trials of dies built by using GB40 and GB56 grade die inserts as a part of future investigations.

References

[1] H.M. Ortner, P.Ettmayer, H. Kolaska, I.Smid, The history of the technological progress of hardmetals, International Journal of Refractory Metals and Hard Materials, 49 (2015) 3-8. https://doi.org/10.1016/j.ijrmhm.2014.04.016

[2] J.García, V.C. Ciprés, A. Blomqvist, B. Kaplan, Cemented carbide microstructures: a review, International Journal of Refractory Metals and Hard Materials, 80 (2019) 40-68. https://doi.org/10.1016/j.ijrmhm.2018.12.004

[3] B.Tanrikulu, R. Karakuzu, Fatigue life prediction model of WC-Co cold forging dies based on experimental and numerical studies, Engineering Failure Analysis, 118 (2020) https://doi.org/10.1016/j.engfailanal.2020.104910

[4] T.Klünsner, S.Marsoner, R. Ebner, R. Pippan, J. Glätzle, A.Püschel, Effect of microstructure on fatigue properties of WC-Co hardmetals, Procedia Engineering 2 (2010) 2001-2010. https://doi.org/10.1016/j.proeng.2010.03.215

[5] J.A.M. Ferreira, M.A. Pina Amaral, F.V. Antunes, J.D.M. Costa, A study on the mechanical behaviour of WC/Co hardmetals, International Journal of Refractory Metals and Hard Materials 27 (2009) 1-8. https://doi.org/10.1016/j.ijrmhm.2008.01.013

[6] H. Mikado, S.Ishira, N. Oguma, K.Masuda, S. Kitawaga, S.Kawamura, Effect of stress ratio on fatigue lifetime and crack growth behavior of WC–Co cemented carbide, Transactions of Nonferrous Metals Society of China 24(2014) 14-19. https://doi.org/10.1016/S1003-6326(14)63282-9

[7] Y.Torres, M. Anglada, L.Llanes. Fatigue mechanics of WC–Co cemented carbides, International Journal of Refractory Metals and Hard Materials, 19(2001) 341-348. https://doi.org/10.1016/S0263-4368(01)00032-4

[8] A.Li, J.Zhao, D.Wang, X. Gao, H. Tang, Three-point bending fatigue behavior of WC–Co cemented carbides, Materials & Design 45(2013) 271-278. https://doi.org/10.1016/j.matdes.2012.08.075

[9] Hardmetals - Determination of transverse rupture strength, ISO 3327:2009 (2009)

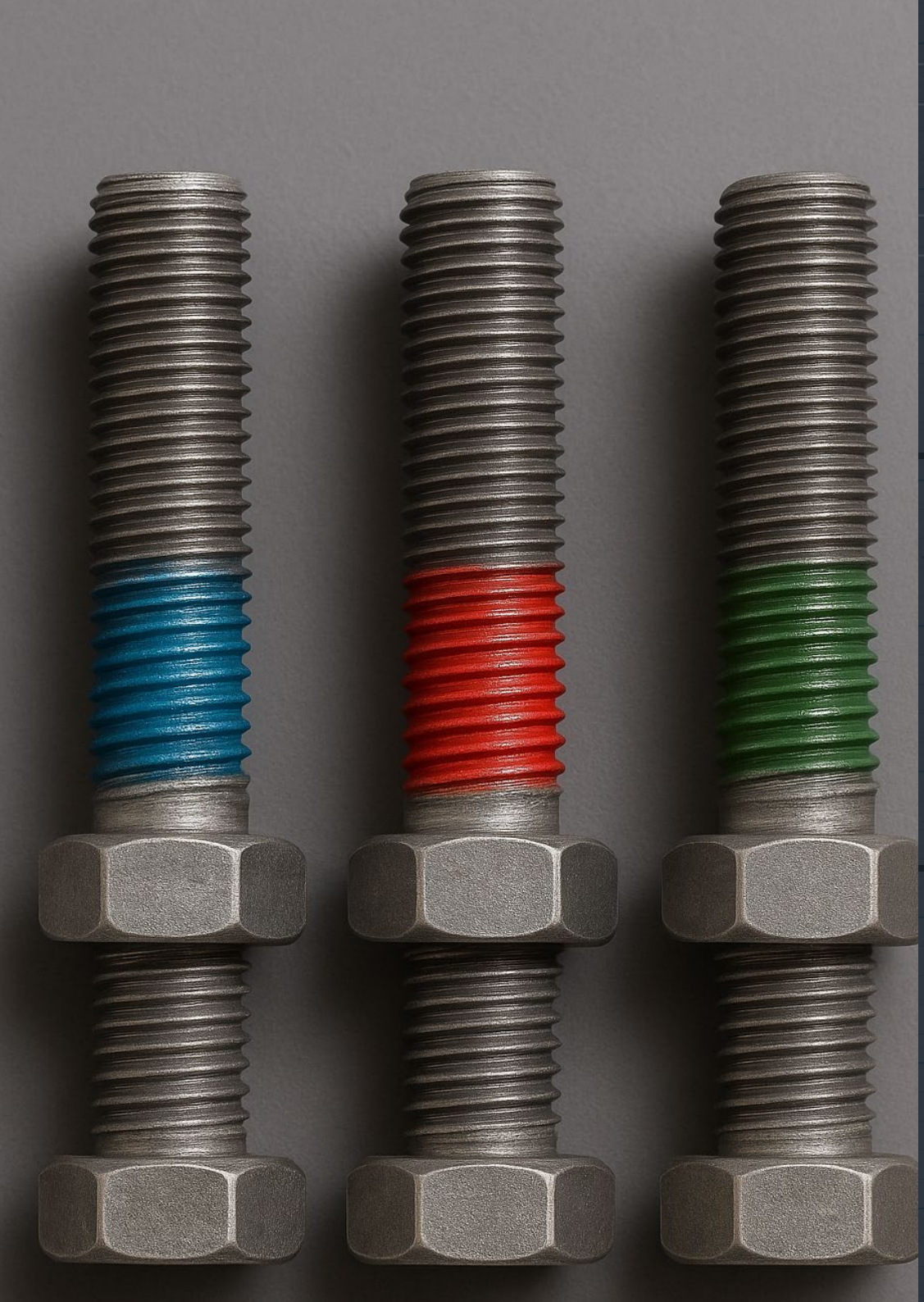

INVESTIGATION OF LOOSENING RESISTANCE UNDER ASSEMBLY CONDITIONS USING DIFFERENT LOCKING CHEMICALS AND LOCK NUTS

Baybars SARICA
Tolga AYDIN
Samed ENSER
Umut İNCE

The International Journal of Materials and Engineering Technology

INVESTIGATION OF LOOSENING RESISTANCE UNDER ASSEMBLY CONDITIONS USING DIFFERENT LOCKING CHEMICALS AND LOCK NUTS

Baybars Sarıca[1] , Tolga Aydın[1] , Samed Enser*[1] and Umut Ince[1]

[1]Norm Fasteners, R&D Center, AOSB, Cigli, İzmir, Türkiye

Abstract

Fasteners are subjected to repetitive and variable loads in the areas where they are used. This situation creates some risks such as loosening or fracture of fasteners, result the failure of the joint. Locking chemicals applied on the bolt to prevent loosening that may occur under assembly conditions are used extensively, especially in the automotive industry. By using locking chemicals selected in accordance with the assembly area and fastener, it is aimed to prevent the loosening of the assembly parts under vibration. There are commercial products that offer different properties that can be used in the mass production of locking chemicals. Within the scope of the study, the performance of three different commercial locking chemicals against loosening was investigated and used standard M8 bolts and nuts. In addition, the M8 DIN 980 lock nut, which is used in joints that are at risk of loosening in vibrating areas, was also added to the studies. Due to the effect of the coefficient of friction on the clamping load, all fasteners were coated with the same coating to ensure equivalence in installation conditions. The vibration performances of the locking chemicals were investigated with the Junker vibration test. The results were analyzed comparatively and the joint condition with the highest vibration resistance was determined. As a result, it was observed that the use of locking chemicals and lock nuts increased the loosening resistance.

Keywords: Bolt, Lock Nut, Locking Chemical, Assembly, Junker vibration test

1. Introduction

Bolt-nut connections are one of the oldest and most frequently used joint methods. Bolt-nut connections, which are preferred in many sectors including automotive and white goods, are exposed to loads and displacements at high cycle numbers and for long periods. If the appropriate clamping load is not created during the tightening process, loosening may occur at low cycle numbers. Even if there is no problem in the tightening process, it is exposed to dynamic and static loads according to the conditions of the application area. As a result of the radial contraction of a bolt subjected to dynamic loads and radial expansion of the nut with the amount of Poisson's ratio deformation, the bolt produces a radial micro-slip at both the bolt-nut thread interface and the bearing surface during axial stress variation and the loosening problem occurs over time (Figure 1) [1].
Especially in the critical design points, loosening of the joint must not occur. The introduction of robotic systems in mass production factories in Industry 4.0 applications, is aimed to minimize the errors that may occur in the assembly area.

The performance of the joint is affected by the bolt-nut parts as well as the assembly conditions. The yield point, friction coefficient, clamping length and moment of inertia of the fasteners are the main parameters of the fractures/loosening that may occur in the connection. In the assembly area, proper tightening in accordance with the bolt-nut quality class is of great importance. In a study conducted in 2010, it was stated that the coefficient of friction changes due to wear during repeated tightening of the fastener and therefore, when tightened at a certain torque value, the clamping load realized in the assembly decreases. Furthermore, if an axial load is also acting on a joint that is experiencing radial slippage, it has been reported that lock nut can continue to self-loosen, leading to loosening [2].

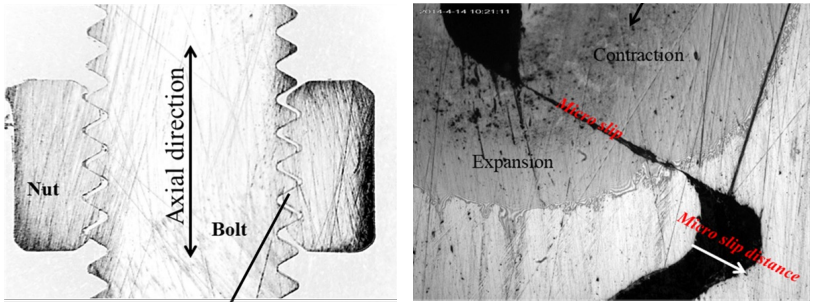

Figure 1. Sliding zones in nut-bolt threads under vibration

In another study conducted by NASA, vibration tests were carried out by simulating the rocket conditions of a bolt-nut connection mechanism with a safety wire that would not lose its preload, considering the vibrations generated in a rocket. As a result of the study, it was stated that radial movement caused by vibration and structural forces was the main cause of loosening [3]. There are also studies in the literature on modeling the self-loosening behavior and thus predicting the loosening behavior of bolted joints without a test. In a 2021 study, the self-loosening behavior of bolted joints was investigated by numerically and experimentally. The numerical analysis showed that the existing analytical model was unable to predict the experimental loosening behavior therefore the analytical model was modified with the help of a finite element model. In this way, the prediction of self-loosening behavior was increased from 58.3% to 73% [4]. In a study at Toyota Automotive Co., the self-loosening behavior of bolt-nut connections subjected to tensile load was investigated and the loosening behavior was described with the fundamental material strength equations. As a result of the study, it was suggested that the clamping load on the joint is removed as instant due to the tensile force, and in the absence of this load, the bolt rotates counterclockwise due to the torque generated by the axial stress and loosening occurs. However, it is said that this type of loosening rarely occurs in steel bolt-nut connections [5]. In another study in 2022, a radial anti-loosening precision locked-nut was used and tested under three different target axial force conditions. With this test, the stiffness of the assembly was measured. At the end of the study, the authors concluded that the use of precision locked-nuts in fastener systems has improved assembly properties by providing stable design stiffness under dynamic vibration. The authors tested parameters such as tightening-loosening torque, axial force ratio and anti-loosening ratio of the nut in different vibration conditions and showed that the precision locked-nut improves the dynamic stability of the system [6]. In a 2021 review article, systems and methods to prevent loosening are listed. While this study was carried out, methods were categorized under two headings; traditional methods and newly developed methods. While, the authors have categorized the traditional methods evaluated and compared as anti-loosening structures in the form of a washer and nut, the new-style anti-loosening structures methods under three different headings.

These are; changing the thread of the nut or bolt, changing the bearing surface of the nut or bolt head, and changing the material type of the nut or bolt. At the end of the study, it was mentioned that the methods have advantages/disadvantages against each other and it was suggested that there is no single method that can solve all loosening problems yet. The authors did not mention the use of locking chemicals in the anti-loosening method [7]. In 2021, another paper investigated how to improve both the anti-loosening and fatigue strength of a bolt-nut connection at low cost. M12 pitch 1.75mm bolts and nuts were used in the study. Different nut lengths and standard pitch length of 1750 µm were given different length (α) deviations and the fatigue and loosening performance of the connection was investigated. At the end of the study, the authors reported that the joints with longer nuts and smaller pitch deviations had both improved fatigue performance and increased loosening resistance [8]. A study in 2007 investigated the self-loosening performance of Teflon and adhesive coatings. Two different adhesive coatings and two different Teflon coatings were studied and compared with uncoated scenarios. The main objective of the study was to find a relationship between the self-loosening resistance of the tested scenarios and the friction coefficients. Teflon coatings were found to reduce the coefficient of friction, but not the loosening resistance of the joint. Adhesive coatings were said by the authors to increase the loosening resistance of the assembly. However, it was reported that the adhesive coatings used lost their properties over time under transverse loading [9].

Vibration loads are the major factor determining the loosening behavior of a bolt. Under certain conditions, tightened bolts are observed to have a loosening problem. The sliding behavior of the bolt-nut connection and the transverse rotation of the nut under transverse load is shown in Figure 2. When an external shear force acts on the joint, time-varying forces in the form of tension and compression act on the parts tightened between the bolt head and the nut. The external load is divided into three components due to the inclination angle of the threads and the flange angle. The first of these components along the axis of the bolt, the other in the radial direction and the last one acts tangentially to the surfaces. The force component acting along the bolt axis extends and deforms the shaft, while the radial force bends the thread profile. The radial force creates a moment in the opposite direction to prevent warping from occurring [10, 11].

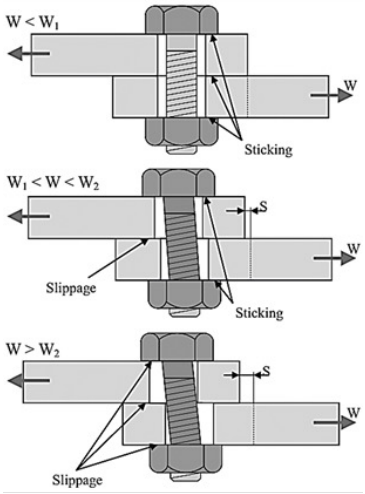

Figure 2. Sliding behavior of bolted joint under vibration [10]

In addition to the appropriate bolt-nut joint, locking chemicals are also used to prevent loosening caused by both bolt-nut and assembly area conditions in the joint areas and to increase the operating performance of the fittings in cases where sealing is desired. Figure 3 shows the method of application of a commercial locking chemical. Each commercial locking chemical has its own specific application which methods are specified by the manufacturer [9, 12].

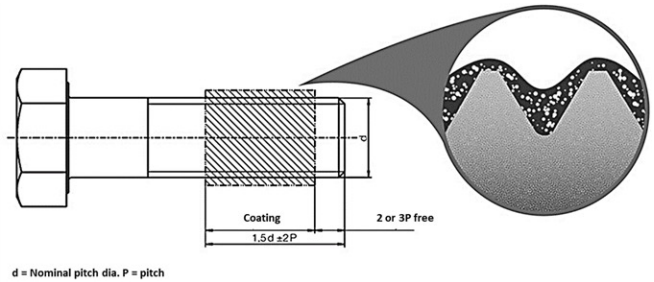

Figure 3. Locking chemical distribution on the bolt [13]

As can be seen, there are many studies on resistance to loosening in the literature. However, there is no comparative study that reveals the performance differences between newly locking chemicals. Moreover, it is also unknown how the locking chemicals perform compared to mechanical locking methods. In this study, bolts, standard nuts and lock nuts with the same coating and constant coefficients of friction were used. In order to investigate the effect of locking chemicals on vibration resistance, three different commercial locking chemicals were applied to the bolts and vibration tests were performed. After clamped load was applied with a digital wrench, the bolts were subjected to vibration in the transverse direction for a certain displacement and cycle duration with Junker tester. During the Junker vibration test, cycle-based changes in the clamping load value were recorded so that the loosening rate data of the assembly combination were obtained and compared with each other. The combination giving the highest vibration resistance among the two different nuts and three different locking chemical applications used in the study was determined after the comparative results.

2. Materials and methods

In order to compare the performance of locking chemicals, the loosening resistance of bolt-nut connections was evaluated by the Junker vibration test. The bolts used for the test are M8x1,25 8.8 DIN 933 standard bolts produced by Norm Fasteners. M8x1,25 8.8 DIN 934 standard hex nuts and DIN 980 lock nuts tightened hex nuts produced within Norm Fasteners were also used for fastening. The bolts and nuts used in the tests were coated with a zinc-plated coating by dip-spin method and then top-coated to ensure that their surface quality and roughness were the same. In this way, a constant coefficient of friction in the range of 0.09-0.12 was obtained in the bolts and nuts. The clamping length ofthe bolts was kept constant at 53 mm. This ensured that the internal threads of the nuts were in full contact with the applied chemicals under assembly conditions. The test procedure to be followed throughout the study is shown in Table 1.

Table 1. Test Procedure.

Locking Chemicals	Bolt	Nut	Test Condition
Lock. Chem. 1	DIN 933	DIN 934 / DIN 980	5 Hz, 53 mm clamp length
Lock. Chem. 2	DIN 933	DIN 934 / DIN 980	2000 cycle
Lock. Chem. 3	DIN 933	DIN 934 / DIN 980	0,7 mm displacement

Technical specifications of the locking chemicals used are shown in Table 2.

Table 2. Technical Specification of Locking Chemicals.

Locking Chemicals	Active Substance	Friction Coefficient	Micro-Capsule Content
Lock. Chem. 1	Toluen	0,16	+
Lock. Chem. 2	Acrylic	0,24	+
Lock. Chem. 3	Polyamide	0,3	-

Although the coefficient of friction of the bolted joint is constant through the coating of the bolts and nuts, the joints tightened to the same torque value do not reach the same clamping load due to the friction values of the locking chemicals being compared and the prevailing torque values of the lock nuts. Since the clamping load is the main factor observed in the loosening resistance, the bolted joint was tightened to reach a constant clamping load for comparison in all scenarios. A digital wrench was used as a tightening tool. When calculating the constant clamping load, the minimum breaking torque value of 33 Nm specified in the ISO 898-7 standard was taken as a reference [14]. The maximum safe clamping load $10_{-(-0)}^{\wedge(+0.5)}$ kN was tightened for the scenario with the highest coefficient of friction (μ=0.3). When calculating this value, the Equation 1 from ISO 16047 "Fasteners - Torque/clamp force testing" standard was used [15];

$$\mu = \frac{T/F - P/2\pi}{0{,}577 d_2 + 0{,}5 D_b} \quad (1)$$

Where T, F, P, d2 and Db are torque (Nm), clamping load (N), pitch (mm), basic pitch diameter of the thread and effective bearing surface (mm) respectively.

Each locking chemical used in the tests was applied in the method and range recommended by its manufacturer. Bolts with three different locking chemicals are shown in Figure 4. Locking Chemical 1, fastener adhesive, are microencapsulated, room temperature curing locking chemicals that improve the loosening resistance of threaded fasteners. The adhesives are designed to be poured onto fasteners and dried. Locking Chemical 1 contains a microencapsulated epoxy resin suspended in form. When the fastener is tightened, the microscopic capsules of the epoxy resin are reacted by the force between the threads and the reactant components initiate a chemical reaction that locks the parts together. An image of Locking Chemical 1 applied to the bolts used in the project is given in Figure 4 (a). Locking Chemical 2, like Locking Chemical 1, contains epoxy resin suspended in its own form. The microcapsules are released by compression and shear stress during assembly and create a coating on the bolt threads (Figure 4 (b)). Locking Chemical 3, like Locking Chemicals 1 and 2, is applied on the bolt threads to create resistance to vibration in the clamping area. The radial tension created by the elastic deformation of the product causes the locking chemical 3 to maintain the clamping position through increased friction. Locking Chemical 3 has some differences compared to Locking Chemicals 1 and 2. Locking Chemicals 1 and 2 have an adhesive effect where the epoxy granules in their structure spread over the bolt threads after torque is applied into the clamping area. The dispersed epoxy granules need to be cured at room temperature in the assembly area. Locking Chemical 3 is a powder sprayed on bolt and nut threads and can be used in the assembly area without the need for curing. This is because Locking Chemical 3 does not have epoxy granules in its structure like the other chemicals, but it is a locking chemical that forms an elastic, wear-resistant blue polyamide coating on the threads by spraying (Figure 4 (c)).

In this study conducted at Norm Fasteners R&D Center, tests were carried out in the Junker test machine with $10_{-(-0)}^{\wedge(+0.5)}$ kN preload, 500 rpm speed and 2000 cycle test parameters. At least 5 tests were performed for each group. The test setup illustration and test machine of the Junker tester are shown in Figures 5 (a) and (b) respectively [16].

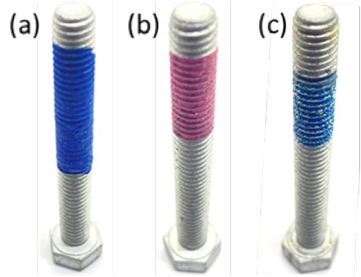

Figure 4. Bolts with Locking Chemicals (a) 1, (b) 2 and (c) 3

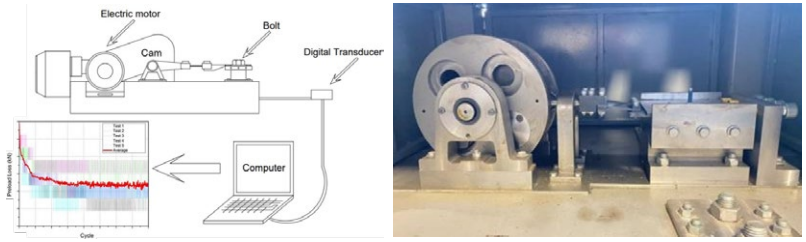

Figure 5. (a) Test set-up illustration and (b) Junker tester

3. Results and discussion

In the first step of the study, vibration tests were performed using DIN 933 (standard hex bolt) bolts and DIN 934 (standard nut) and DIN 980 (lock nut) nuts without locking chemical for reference. The average test results for the tests without locking chemicals are shown in Figure 6. Here the results are shown as a graph of clamping force versus cycle. It was observed that after the operation with the standard nut, the initial clamping load decreased from 10 kN to 7.2 kN due to loosening in the transverse direction. When the results obtained after the vibration test with the lock nut are

compared with the test with the standard nut, it is seen that the reduction in the clamping loads is quite limited and there is no complete relaxation in 2000 cycles. Unlike standard nuts, while tightening, lock nuts are assembled encountering a mechanical resistance on the bolt threads which is prevailing torque. The additional mechanical resistance creates a structure that is resistant to loosening. Compared to standard nuts, the positive effect of the mechanical resistance obtained with lock nuts on the loosening resistance can be seen.

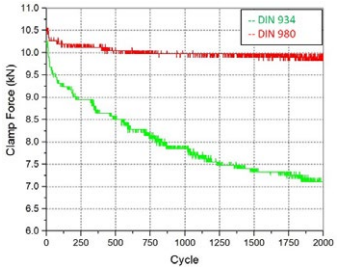

Figure 6. Average results of locking chemical-free vibration test with two different nuts.

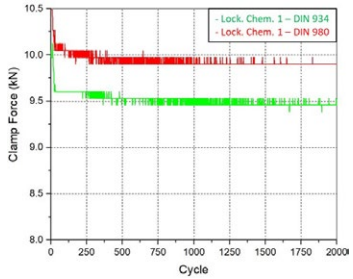

Figure 7. Average results of vibration test with Locking Chemical 1

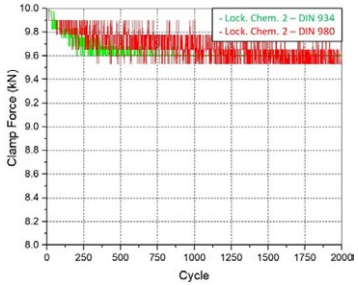

Figure 8. Average results of vibration test with Locking Chemical 2

After the reference test which has no locking chemical, Locking Chemical 1 was tested first. After the microcapsules in the epoxy structure were tightened and dispersed on the bolt, they were left for 1 day as they needed to cure. The average test results for the tests where Locking Chemical 1 was applied are shown in Figure 7. When the results with standard nut and Locking Chemical 1 are examined, it is seen that the clamping load decreased up to 9.4 kN but never went below this value. If we look at the result of the lock nut, it is seen that the clamping load decreased up to 9.8 kN values but never went below this value. There was also some difference between the average initial clamping load levels in the tests.
The results of the studies using Locking Chemical 2 are shown in Figure 8. Locking Chemical 2, like Locking Chemical 1, is a chemical that requires curing to achieve the desired mechanical properties. After the test with the standard nut and Locking Chemical 2, it was seen that the clamping load loosened up to 9.5 kN, but on average, the clamping load remained constant after 1000 cycles. When the vibration test with the lock nut and Locking Chemical 2 is examined, it is seen that it does not go below the clamping load of 9.6 kN, similar to the results of the standard nut.

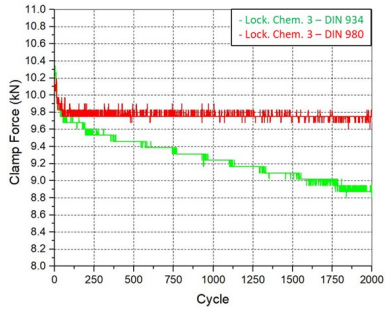

Figure 9. Average results of vibration test with Locking Chemical 3

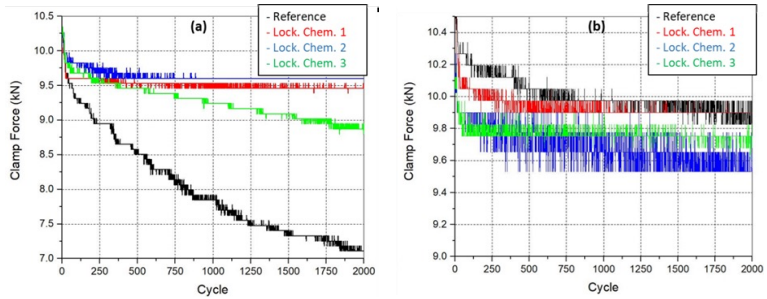

Figure 10. Vibration test results of (a) standard and (b) lock nuts with 3 different locking chemicals

After the applications of Locking Chemicals 1 and 2, which were cured and ready for use, the studies continued with Locking Chemical 3, which is a locking chemical that is ready for use directly after tightening. The test results with Locking Chemical 3 are given in Figure 9. It was observed that the clamping load value in the Locking Chemical 3 application with the standard nut showed different results after 5 tests. In four tests, it was observed that it oscillated with a relatively large amplitude between 9.5 – 8.8 kN, while in one test, the clamping load value decreased to 6.0 kN. Considering the studies conducted with the standard nut, it was clearly observed that it exhibited more inconsistent loosening performance than the cured Locking Chemicals 1 and 2 applications. When the results of the Locking Chemical 3 application

with the lock nut were examined, it was observed that unlike the test results with the standard nut, the combination of Locking Chemical 3 and the lock nut showed both consistent results and the clamping load remained above 9.6 kN throughout the cycles.

Table 3. Result of locking chemicals and lock nut performances

Locking Chemicals	Nut	Loosening Ratio %
No Chem. (ref)	934	29
No Chem. (ref)	980	2
Lock. Chem. 1	934	6
Lock. Chem. 2	934	5
Lock. Chem. 3	934	12
Lock. Chem. 1	980	2
Lock. Chem. 2	980	4
Lock. Chem. 3	980	4

4. Conclusions

Within the scope of the project, the resistance to loosening of three different locking chemicals, which are frequently used with bolted joints in automotive, was investigated. The test results of standard nuts and lock nuts are shown in Figures 10 (a) and (b) together with all locking chemicals for comparison. In addition, the performances of the locking chemicals are tabulated in Table 3. When the results were analyzed;

- When standard nut without locking chemicals is used, the clamping loads decreased approximately 30% after 2000 cycles in vibration tests. Whereas the clamp load decreased by only 2% when the lock nut was used.
- When locking chemicals were used, the maximum loosening rate was approximately 5% for Locking Chemicals 1 and 2, which contain microcapsules, provide locking with adhesive properties and therefore require curing time. On the other hand, a 12% loss in the clamping load was realized with Locking Chemical 3, which provides only a mechanical locking to improve the loosening resistance.
- Considering these results, locking chemicals applied to standard nuts have been shown to successfully improve loosening resistance.
- When the tests with lock nut and locking chemicals together were examined, it was observed that the effect of locking chemical applications on the loosening resistance did not provide a significant difference in the test conditions compared to the standard nut applications. Although it was expected that the using of a lock nut and locking chemicals together would have a positive effect on the loosening resistance, it was clearly seen that it gave similar results to the scenarios with only used one of the solutions.

In short, it was observed that the use of only the lock nut provided as much loosening resistance as the standard nut and locking chemical application. Interpretation of the performance of locking chemicals could only be done for the installation scenarios with standard nuts where significant differences could be observed.

Acknowledgments

The authors would like to thank Norm Holding for the opportunity to conduct and present the study.

Author contributions

All authors reviewed and approved final version of the manuscript. Baybars Sarıca: Investigation, Validation, Data curation, Formal analysis. Tolga Aydın: Conceptualization, Visualization, Formal analysis. Samed Enser: Writing – editing & original draft, Resources, Supervision. Umut İnce: Investigation, Resources, Methodology, Supervision.

References

1. Goodier, J., Loosening by Vibration of Threaded Fastenings, Mech. Engg. 1945, 67, 798

2. Eccles, W. Tribological aspects of the self-loosening of threaded fasteners. University of Central Lancashire, 2010

3. DellaCorte, C., Howard, S. A., Hess, D. P., Preload Loss in a Spacecraft Fastener via Vibration-Induced Unwinding, 2018

4. Umut, İ., Güden, M., An experimental and comparative study of the self-loosening of bolted-joints under cyclic transverse loading, Sakarya University Journal of Science 2021, 25 (2):498-512

5. Sakai, T., Mechanism for a bolt and nut self loosening under repeated bolt axial tensile load, Journal of Solid Mechanics and Materials Engineering 2011, 5 (11):627-639

6. Chen, C., Chang, H., Syu, J., In Study on advanced assembly characteristics of locking with radial anti-loosening precision locked-nut while maintaining the design rigidity under dynamic precision fastening system, Journal of Physics: Conference Series, IOP Publishing: 2022, 012025

7. Hao, G., Jianhua, L., Huihua, F., Review on anti-loosening methods for threaded fasteners. Chinese Journal of Aeronautics 2022, 35 (2):47-61

8. Wang, B., Noda, N.-A., Liu, X., Sano, Y., Inui, Y., Oda, K., How to improve both anti-loosening performance and fatigue strength of bolt nut connections economically, Engineering failure analysis 2021, 130, 105762

9. Ganeshmurthy, S., Housari, B., Nassar, S. A., Investigation of the effect of adhesive coating on the performance of threaded fasteners, SAE Transactions 2007, 707-717

10. Çavdar, K., Öngerilmeli Cıvata Bağlarında Çözülme Problemleri. Uludağ Üniversitesi Mühendislik Fakültesi Dergisi 2015, 20 (1):103-118

11. Hattori, T., Yamashita, M., Mizuno, H., Naruse, T., In Loosening and sliding behaviour of bolt-nut fastener under transverse loading, EPJ Web of Conferences, EDP Sciences: 2010, 08002

12. Haviland, G. S., Machinery adhesives for locking, retaining, and sealing. Routledge: 2019

13. Boellhoff Kimyasal Diş Tutma Yöntemleri, https://www.boellhoff.com/tr-tr/urunler-ve-hizmetler/ozel-baglanti-elemanlari/kimyasal-dis-tutma-yontemleri.php (accessed 13.09.2023)

14. ISO, ISO 898-7 Mechanical properties of fasteners - Part 7. International Organization for Standardization Geneva, Switzerland: 1992

15. ISO, ISO 16047 Fasteners-Torque/Clamp Force Testing. International Organization for Standardization Geneva, Switzerland: 2005

16. Junker, G. H., New criteria for self-loosening of fasteners under vibration. Sae Transactions 1969, 314-335

OPTIMIZING HEAT TREATMENT FOR ENHANCED MECHANICAL PERFORMANCE OF ULTRA-HIGH STRENGTH BOLTS

Burak HIZLI
Umut İNCE
Şerife HELVACIOĞLU
C. Can ERDOĞAN
Ayşe ERKAN
Ümmihan T. YILMAZ

22. Uluslararası Metalurji ve Malzeme Kongresi (IMMC 2024)

OPTIMIZING HEAT TREATMENT FOR ENHANCED MECHANICAL PERFORMANCE OF ULTRA-HIGH STRENGTH BOLTS

BURAK HIZLI[1,3*], UMUT INCE[1], SERIFE HELVACIOGLU[2,4], C. CAN ERDOGAN[2], AYSE ERKAN[2], UMMİHAN T. YILMAZ[4]

[1]Norm İzmir Cıvata San. ve Tic. A.Ş, İzmir, Türkiye
[2]Döksan Isıl İşlem ve ArGe Merkezi A.Ş., Ankara, Türkiye
[3]Dokuz Eylul University, İzmir, Türkiye
[4]Ankara Hacı Bayram Veli University, Ankara, Türkiye

Keyword: Ultra-high strength bolts, austempering, bainite, martensite, mechanical properties

Abstract

In recent years, ultra-high strength bolts have gained significant interest in the automotive industry in terms of complying with environmentally sustainable regulations, enabling the reduction of total vehicle weight by lessening the required quantity of bolts and allowing the utilization of reduced-size bolts. Compared to quenching and tempering, cold-formed bolts require precisely controlled heat treatments for isothermal bainitic transformation to achieve high tensile strengths above 1200 MPa and good ductility. In this study, M10x150 hexagon flange bolts produced from low alloy DIN 1.7225 (AISI 4140) steel were subjected to heat treatment cycles, including conventional austempering above the martensite initial temperature Ms, at Ms, and low-temperature isothermal transformation below Ms. The bainite morphology greatly was affected from the austempering temperature and austempering time. Tensile test results revealed that higher transformation temperatures and holding times led to higher bainitic phase fraction in lower bainite dominant dual isothermal martensite/lower bainite microstructure, resulting in relatively higher mechanical properties in terms of yield strength, tensile strength, and elongation as 1332 ± 3 MPa, 1506 ± 4 MPa, and around 13,7 ± 0,2%. It was identified that partial decarburization in the thread zones of the bolts caused the erroneous elongation values.

1. Introduction

Different strength-graded fasteners from 4.8 up to 12.9 are crucial structural members that are intensively used to assemble components of main systems and subsystems, functioning to maintain structural integrity. In recent years, regulations and related measures regarding sustainable future policies have been driving increasing attention to innovative material technologies based on lightweightness, high performance, and endurance [1]. Ultra-high strength fasteners are thus seen as corresponding products within the fasteners industry considering requirements of the sustainable materials. Ultra-high strength fasteners are one of the pioneering components for weight reduction studies especially within the automotive industry in order to accelerate the transformation to electric vehicles and enable energy-efficient traveling in long distances by allowing usage of downsized assembled parts and reduced overall quantity of fasteners in need [2]. However, manufacturing of ultra-high strength fasteners stands as a challenging process in terms of achieving desirable mechanical properties with good ductility.

Fasteners are generally manufactured by cold forming process with subsequent heat treatment application using low and medium carbon steels as a raw material. Quenching and tempering (Q&T) processing of cold-formed fasteners is the most common form of hardening and strengthening heat treatment in order to obtain strength grades of 8.8 or above, having the final microstructure of tempered martensite. Although the tempered martensite phase offers the potential for exceptional strength, its toughness severely diminishes at ultra-high strength levels, which causes brittleness and reduction in deformation capability. Therefore, it possesses a significant challenge in achieving a combination of ultra-high strength and high toughness [2]. In contrast to Q&T processes, it is necessary to apply of precisely controlled isothermal heat treatments to cold-formed bolts that results in bainitic transformation as the bainite phase is characterized by having better toughness compared the tempered martensite at equal strength levels [3]. Bainitic transformation generally isothermally occurs at the temperatures above Ms, however, several studies reported even better mechanical properties by forming mixed martensite/bainite phase than both tempered martensite and bainite because of prior austenite grain partitioning by athermal martensite and fine bainitic plate formation at low temperatures [4-6].

In this study, M10x150 hexagon flange bolts produced from low alloy DIN 1.7225 (AISI 4140) steel, which is widely used as a raw material in cold forming process, were subjected to heat treatment cycles, including conventional austempering above the martensite initial temperature Ms, at Ms, and low-temperature isothermal transformation below Ms in order to investigate austempering temperature-holding time-mechanical property relations. Following the heat treatment stage, the obtained properties were evaluated in the aspects of microstructural features, the volume fraction of bainite in the microstructure, and mechanical performance in comparison with property grades given in standards and industrial specifications for automotive.

2. Experimental Procedure

M10 bolts having 150 mm length were produced by cold forming process using five-staged bolt former machine and final product form is given in Figure 1. The raw material for this study is AISI 4140 steel in the wire-drawn form, whose chemical compositions are tabulated in Table 1.

Figure 1. Final bolt form after the production.

Table 1. Chemical composition of AISI 4140 steel.

Element	C	Cr	Mo	Ni	Mn	Si	Fe
wt (%)	0.4	1.1	0.23	≤0.15	0.75	≤0.2	bal.

Prior to the production of sample bolts, steel wire was subjected to spheroidization annealing in order to facilitate the cold forming process by decreasing the hardness values into the desired range. Thereafter, surface of the wires was coated with polymer to adjust the frictional effects to avoid excessive forming forces during cold forming. As a final process after production by cold forming, bolts were subjected to heat treatment under two steps; austenization, and conventional austempering. Austempering was applied to sample bolts for the isothermal bainitic transformations at the temperatures above Ms, at Ms, and below Ms. During the processes, austenization process was first optimized in terms of process time, thereafter austempering process was optimized to understand the effect of holding time on isothermal transformation below Ms. Following these, austempering processes were applied at Ms and above Ms to obtain optimum isothermal transformation. Process parameters regarding temperature and time are listed in Table 2. Relations between temperatures and holding times within the salt bath were as $T_1<T_2=Ms<T_3<T_4$ and $t_1<t_2<t_3<t_4<t_5$, respectively. T_4 corresponds to austenization temperature. It was mainly aimed to obtain higher tensile strength above 1200 MPa, yield/tensile strength ratio of minimum 0.80, and at least 10% elongation, which complies with property grades stated in standards and industrial specifications.

Table 2. Process parameter based on process numbers.

Stage	Process	Austenization	Austempering	Ni	Mn
		Temp. (°C)	Time (min)	Temp. (°C)	Time (min)
Austenization Time Optimization	Process #3	T_4	t_1	T_1	t_5
	Process #4	T_4	t_3	T_1	t_5
Austempering Optimization (Below Ms)	Process #2	T_4	t_1	T_1	t_2
	Process #1	T_4	t_1	T_1	t_5
Austempering Optimization (Ms and Above Ms)	Process #5	T_4	t_3	T_2	t_3
	Process #6	T_4	t_3	T_2	t_4
	Process #7	T_4	t_3	T_3	t_3

Microstructural observations were conducted on specimens for each grade using Leica DM 2700 optical microscope after metallographic preparations via grinding and polishing, and sequential etching with 3 vol% nital solution for 3-5 s and 10 vol% aqueous solution of sodium metabisulfite to control the microstructure and volume fraction of bainite. Uniaxial tensile tests using special test fixtures with a loading rate of 0,166 mm/s were carried out on Zwick Roell Z400RED universal testing machine at room temperature to determine the mechanical properties. Three tests from each process were performed. Hardness measurements in $HV_{0.3}$ and HV_{10} were sequentially carried out from the surface of the bolts and core to determine hardness ranges and their conformity to desired values.

3. Results and Discussion

The micrographs taken from each process showed that bainite microstructure was formed at the temperatures below Ms, Ms, and above Ms. The microstructures of bolts from Process #5 and Process #6 are sequentially given in Figure and 2 and Figure 3 in order to illustrate the effectiveness of bainitic transformations depending on heat treatment processes. It was identified that the amount of bainite decreased as the holding temperature below Ms decreased. It was attributed to the formation of more prior martensite. It is known mechanism that larger amount of prior martensite leads to inhibiting the transformation of residual austenite to bainite. Additionally, increasing holding time had a positive effect on the transformation rate as the amount of lower bainite increased with increasing holding time.

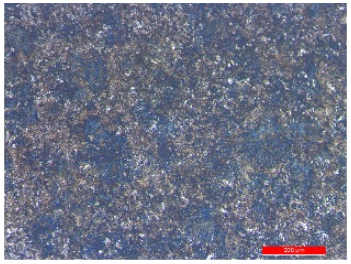

Figure 2. Microstructure of Process #5 at 100x.

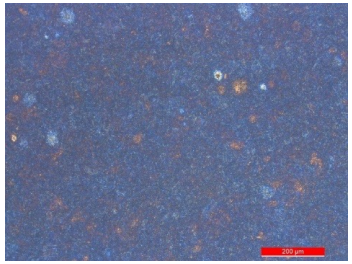

Figure 3. Microstructure of Process #6 at 100x.

The highest bainite content (blue zones) was achieved in Process #6 compared to other processes, which was confirmed by examining micrographs of all processes. On the contrary, Process #5 provided the least bainite content than other processes as the austempering temperature and time were selected as lower than the other applied processes. Thus, higher austempering temperature and longer holding time facilitated the bainitic transformation and increased the transformation ratio. Additionally, partially decarburized regions in the thread zones of the sample bolts were identified in all processes except for Process #6. Decarburization issues were more prone to occur at high strength levels and these issues were intended to be overcome during the austenization optimization studies for conducting highly controlled austempering process in terms of microstructural features and hardness homogeneity. Micrographs of partially decarburized and non-decarburized zones in the threads of sample bolts are given in Figure 4 and Figure 5, respectively.

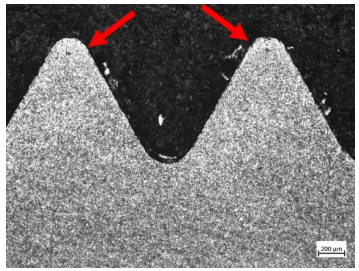

Figure 4. Decarburization in the thread zone at 5x. (Process #1)

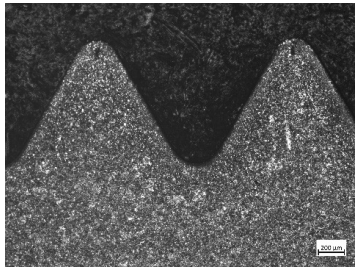

Figure 5. No decarburization in the thread zone at 5x. (Process #7)

Mechanical properties of the sample bolts in terms of yield strength, tensile strength, elongation at fracture, average hardness in the core, and hardness range in the surface are tabulated in Table 3 and Table 4, respectively. The mechanical strength of the bolts was inversely proportional to fracture at elongation i.e. ductility. The reason could be incorporated with the decrease in the deformation capability of the material due to increased strength and hardness. Higher strength properties with austempering lead to restriction of dislocation movements due to high dislocation density within the bainite and cause brittleness in the material structure. However, enhanced ductility-toughness allows to ensure high performance and increased resistance to fracture under static and fatigue loading conditions. In some cases in the literature, it is reported that increase in bainite amount in the microstructure generally increases the ratio of yield strength to tensile strength, reduction of area, and fatigue endurance limit [7]. Additionally, yield strength and elongation values appeared in more susceptible properties depending on heat treatment parameters as they altered in wide ranges. Therefore, the isothermal heat treatment process parameters and the amount of bainite in the microstructure had a significant influence on these properties.

Table 3. Mechanical properties of the sample bolts in terms of yield strength, tensile strength, elongation at fracture.

Process Nunber	Yield Strength (MPa)	Tensile Strength (MPa)	Elongation at Fracture (%)
Process #1	1211 ± 17	1606 ± 4	20,6 ± 1,1
Process #2	1119 ± 40	1617 ± 15	22,4 ± 0,5
Process #3	1075 ± 21	1545 ± 21	20,2 ± 1,0
Process #4	1200 ± 17	1626 ± 2	17,5 ± 1,0
Process #5	902 ± 5	1267 ± 22	21,9 ± 0,3
Process #6	1332 ± 3	1506 ± 4	13,7 ± 0,2
Process #7	1143 ± 11	1334 ± 6	20 ± 1,0

Table 4. Mechanical properties of the sample bolts in terms of average hardness in the core and hardness range in the surface.

Process Nunber	Core Hardness (HV)	Hardness Range in Surface (HV)
Process #1	513 ± 12,1	285 - 517
Process #2	502 ± 7,8	260 - 506
Process #3	514 ± 4,6	274 - 454
Process #4	524 ± 35,2	284 - 503
Process #5	428 ± 7,5	354 - 419
Process #6	483 ± 8,9	485 - 520
Process #7	431 ± 3,6	367 - 473

Mechanical test results showed that Process #6 provided the optimal results complying with the property grade of 15.8U according to the standards and industrial specifications as the yield strength of at least 1200 MPa, tensile strength of 1500-1650 MPa, at least 9% elongation, and hardness of 455-515 HV. Although hardness deviations seen in Process #6 resulted in the lowest range compared to other applied processes, deviation range exceeded the maximum allowable hardness deviation of 30 HV as in the frame of ISO 898-1 [8]. This finding confirms that the best hardness homogeneity was achieved in Process #6 in which isothermal temperature and holding time were selected as T_2 equal to Ms and t_4, respectively. The tensile strength results of all processes were determined as well-conforming with the required strength level, however, the ratios of yield strength to tensile strength were found between 0.69-0.75 as not to meet general requirements for ultra-high strength grades except Process #6 and #7. Nevertheless, the mechanical results of Process #7 did not match the required properties in terms of insufficient yield and tensile strength values. Additionally, it was observed that relatively greater elongation values in contrast to higher hardness values in the core but excessively lowered in the surface caused by decarburization near the surface of the threads due to adverse effects originating from further softening of these zones. Considering the mechanical properties and microstructural features, increasing isothermal transformation temperatures starting below Ms through Ms temperature had a positive effect on yield strength, though passing over the temperatures above Ms caused a decrease in yield strength values. Low-temperature isothermal transformation below Ms during the austempering induced to decrease the bainitic transformation ratio and promote the amount of retained austenite. On the other hand, increase in holding time within the salt bath negatively affected the tensile strength values. Austenizing temperature and time were seen not having significant impact on the final microstructure, as well as mechanical properties. These outcomes revealed that isothermal heat treatment parameters should be carefully determined by combining optimal temperature and holding time in order to obtain the required mechanical properties for the property grades of 12.9 and above.

4. Conclusion

In the scope of this study, the effects of austempering parameters on phase transformation-microstructure-mechanical property relations of ultra-high strength bolts subjected to heat treatment cycles, including conventional austempering above the martensite initial temperature Ms, at Ms, and low-temperature isothermal transformation below Ms were investigated. The following conclusions could be drawn from this study:

1. Process #6 exhibited the best mechanical properties complying with 15.8U property grade with the highest bainite content in the microstructure. Therefore, austempering process parameters of T_2 equal to Ms as isothermal transformation temperature and holding time of t_4 process resulted in optimal properties compared to other processes.
2. Higher strength properties with austempering were attributed to high dislocation density within the bainite which led to restriction of dislocation movements and caused brittleness.
3. Decarburization issues should be avoided during the austenization in order to provide similar microstructural features and hardness homogeneity.
4. Partial decarburization in the thread areas of the bolts caused the improper elongation values due to the negative effect caused by the further softening of these zones.
5. Increasing isothermal transformation temperatures starting below Ms through Ms temperature increased the yield strength, though passing over the temperatures above Ms caused a decrease in yield strength values. Low-temperature isothermal transformation below Ms during the austempering induced to decrease the bainitic transformation ratio.
6. Increase in holding time within the salt bath negatively affected the tensile strength values.

Acknowledgment

The authors would like to thank Norm Holding and Döksan Isıl İşlem ve ArGe Merkezi A.Ş. for the collaborative opportunity to carry out this work.

References

[1] H. Lee, Y. Jo, and B. Jang, Metals and Materials International, 2023.

[2] D. Zeren, B. Hizli, D. Sarper, M. B. Toparli, and U. Ince, "A Comparison Of Static And Fatigue Performance Of High-Strength Bolts Depending On Heat Treatment Process," 3rd International Materials Technologies and Metallurgy Conference-2023, 11-13 Ekim 2023, İstanbul, Türkiye.

[3] N. E. Nanninga, "Effet of Microstructure and Alloying Elements on the Resistance of Fastener Grade Steels to Hydrogen Assisted Cracking," M.Sc. Thesis, Michigan Technology University, 2005, Michigan, USA.

[4] S. Dhara, S. M. C. van Bohemen, and M. J. Santofimia, Materials Today Communications, vol. 33, p. 104567, 2022.

[5] J. Feng, T. Frankenbach, and M. Wettlaufer, Materials Science and Engineering: A, vol. 683, pp. 110-115, 2017.

[6] J. W. Jo, H. J. Seo, B.-I. Jung, S. Choi, and C. S. Lee, Materials Science and Engineering: A, vol. 814, p. 141226, 2021.

[7] R. Bakhtiari and A. Ekrami, Materials Science and Engineering: A, vol. 525, no. 1, pp. 159-165, 2009.

[8] ISO 898-1:2013; Mechanical properties of fasteners made of carbon steel and alloy steel - Part 1: Bolts, screws and studs with specified property classes - Coarse thread and fine pitch thread, 2013.

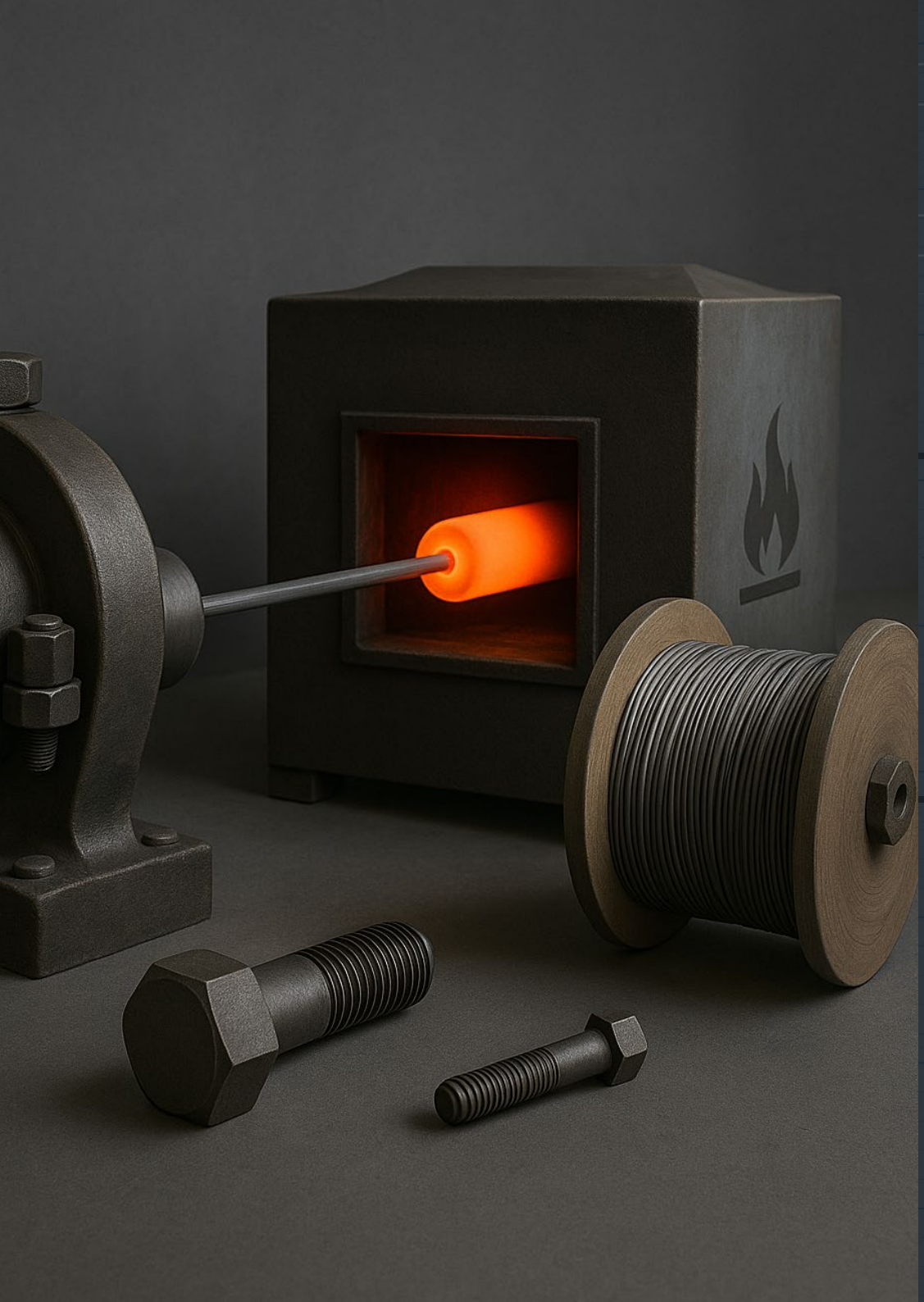

MICROSTRUCTURE AND MECHANICAL PROPERTIES OF CARBON STEEL FOR SEQUENTIAL WIRE DRAWING AND ANNEALING

Doğuş ZEREN
Samed ENSER
Umut İNCE

22. Uluslararası Metalurji ve Malzeme Kongresi (IMMC 2024)

MICROSTRUCTURE AND MECHANICAL PROPERTIES OF CARBON STEEL FOR SEQUENTIAL WIRE DRAWING AND ANNEALING

DOGUS ZEREN[1], SAMED ENSER[2*], UMUT INCE[2]

[1]Norm Additive, AOSB, Çiğli, İzmir, Türkiye
[2]Norm Fasteners, R&D Center, AOSB, Çiğli, İzmir, Türkiye

Keyword: Wire drawing, Steel, Annealing, Cold forming

Abstract

A sequential wire drawing and annealing processes were applied to a medium carbon steel wire used for fastener production in order to investigate for better formability compared to starting material as annealed without pre-wire drawing. The sequential wire drawing process consisted of 14.3%, and 24.9% total cross sectional area reductions respectively. The wire was subjected to spheroidizing annealing above the subcritical temperature of the material after each wire drawing pass. According to hardness and compression test results, the material showed lower hardness values and lower yield strength compared to the starting material. Scanning electron microscope (SEM) images were taken to investigate the microstructure after annealing and wire drawing. SEM images showed that spheroidizing was improved after sequential wire drawing and annealing process. According to this study, it is expressed that the workability of medium carbon steels for fastener production can be increased by sequential wire drawing and annealing by enhancement of spheroidizing.

1. Introduction

Cold forging is one of the widely used production methods in fastener production. According to the application area, fasteners are produced in different shapes, strength classes and sizes. The first step in the process is started with the selection of raw materials suitable for these specifications. The raw materials used in this study procured from Norm Fasteners are steels produced according to ISO 9002 certificate and consist of low and medium carbon steels produced by hot rolling. The annealing process is frequently used processes to prepare the raw material for cold forming to reduce the hardness of the material and increase the tool life. The type of annealing used in Norm Fasteners is spheroidizing. During the annealing, the needlelike cementites in the pearlite phase achieve a spherical morphology which is resulted in ductility. In spheroidizing, steels in the pearlitic structure are first subjected to the annealing process at a temperature below the subcritical temperature (Ac1) temperature (723 °C) and converted from ferrite-cementite lamellae microstructure to spherical cementite particles dispersed in a continuous ferrite matrix with phase transformation [1]. After the annealing, the raw materials are subjected to surface treatment in order to minimize the frictional forces during the cold forging stage. Then, wire drawing is applied to obtain the desired diameter of the raw material and increase the circularity of the material. The process is done by pulling the wire through a die in a tapered form to plastically deform the metal within the confinement of the die. The size reduction is dependent on the die geometry, the material properties of the wire, the friction coefficient between the die and material [2]. During the wire drawing, the mechanical properties of the steel is improved due to the microstructural changes with the plastic deformation [3, 4]. The improvement of the properties is mainly related to the microstructural refinement occurred during the wire drawing [5-9]. During wire drawing, decrease of the interlamellar thickness of the steel is attributed to the increase of the strength of the steel.

Hwang et al. suggested twinning-induced plasticity (TWIP) steels for high strength wire raw material applications for fastener production. By using TWIP steels, fine twins occur during the plastic deformation and dislocation mobility is reduced by the grain refinement and obtain high tensile properties [10].
In order to accelerate spheroidizing behavior of materials, various studies have been carried out. [11-14]. Joo et al. [12] improved the spheroidization behavior of a medium carbon steel wire by increasing the pre-straining of the wire by a non-circular drawing sequence.
In this study, hardness, microstructure and compression tests were compared in the process of reducing a Ø13.5 mm cold forging wire to Ø11.7 (24.9% area reduction ratio) gradually after repeated wire drawing and annealing processes. Thanks to sequential wire drawing and annealing processes, higher formability of the raw material will be achieved, and it will be possible to produce fasteners with complex head geometries.

2. Experimental Procedure

42CrMo4 in Ø13.5 mm annealed steel wire was used in the study. The chemical composition of the raw material is shown in Table 1. For the annealing process, Tenova Loi thermopress furnace was used. The wire drawing process was applied to wire rod a wire drawing machine with deformation rate of 24 mm/min was used. In order to minimize the friction between the wire drawing dies and the raw material, a surface treatment, which includes sand-blasting and polymer coating steps, is applied to the raw material. For the raw material with a diameter of 13.5 mm, the following steps were applied respectively so that the diameter was reduced to 11.7 mm:

i. Annealing of Ø13.5 mm raw material (sample 1)
ii. Surface treatment of annealed Ø13.5 mm raw material
iii. Wire drawing of Ø13.5 mm raw material to Ø12.5 mm (14.3% of cross sectional area reduction) (sample 2)
iv. Annealing of Ø12.5 mm raw material (sample 3)
v. Surface treatment of annealed Ø12.5 mm raw material
vi. Wire drawing of Ø12.5 mm raw material to Ø11.7 mm (total 24.9% of cross sectional area reduction) (sample 4)
vii. Annealing of Ø11.7 raw material (sample 5)
viii. Surface treatment of annealed Ø11.7 mm raw material ready for cold forming

Wire specimens were cut through cross-section for hardness measurements and microstructural examination. Then the samples were grinded and polished before hardness measurements. In microstructural analysis, sanding with 240, 400, 600, 800, 1000 grits, respectively, and polishing with a diamond solution up to 1 µm were performed. Indentation tests were carried out with Digi-load micro-hardness tester. The tests were performed 9.807N (HV10) 10 ms and repeated 5 times. Optical microscopic examinations were carried out with Zeiss Axio Imager M2M microscope. Scanning electron microscope (SEM) images were taken in Quanta FEG in secondary electron and back-scattered electron mode. In order to obtain the mechanical properties of the samples, compression tests were carried out on the prepared cylindrical samples of these materials in ZWICK/ROELL universal tension/compression test device at room temperature according to ASTM E9-89a "Standard Test Methods of Compression Testing of Metallic Materials at Room Temperature" standard. The deformation rate was determined as 5 mm/min, which corresponds to the quasi-static strain rate.

Table 1. Chemical composition of the 42CrMo4 material.

C	P	S	Mn	Cr	Si	Ti	Cu	Ni	Mo	Al
0.42	0.02	0.015	0.9	1.2	0.2	0.05	0.15	0.15	0.3	0.05
0.38	max	max	0.6	0.9	max	max	max	max	0.15	0.015

3. Results and Discussion

The measured hardness values for every five steps are summarized in Table 2. Also, the measured hardness values were given in Figure 1 for annealed and wire drawn samples. Five hardness measurements were taken for each case. All hardness measurements were taken from the longitudinal wire section. According to the hardness measurement results, there is an increased tendency in the hardness of the wire drawn samples and a decrease in the hardness after annealing. In the first step, hardness reduction is about 17 HV (10%) and hardness reduction in the second step is about 21 HV (14%). After sequential wire drawing and annealing, there is a decrease of approximately 38 HV (~%23) raw material hardness compared to the first annealed state of the material.

Table 2. Hardness measurements of the samples of five steps.

Sample	Average Hardness	Standard Deviation
1- Ø13.5-Annealed	163	0.63
2- Ø12.5 Wire drawn -(14.3% Area reduction)	210.4	1.02
3- Ø12.5-Annealed	146.6	1.35
4- Ø11.7 Wire drawn -(24.9% Area reduction)	177.8	2.04
5- Ø11.7-Annealed	125.8	2.30

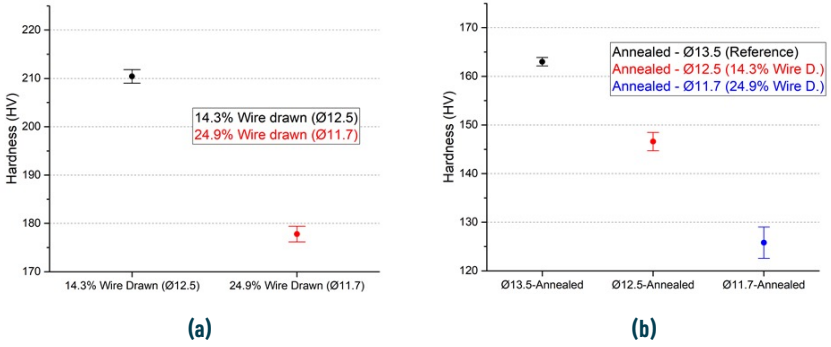

Figure 1. Hardness measurements: (a) wire drawn samples, (b) annealed samples.

SEM images of wire drawn Ø12.5 (14.3% area reduction) and Ø11.7 (24.9% area reduction) samples are shown in Figure 2 (a) and (b), respectively. As indicated in Figure 2 (a) the ferrite grains in the microstructure are elongated in the direction of the wire drawing. However, there is no grain orientation in the wire drawn Ø11.7 sample (Figure 2 (b)). Compared to the two wire-drawn samples each other, grain growth can be seen clearly.

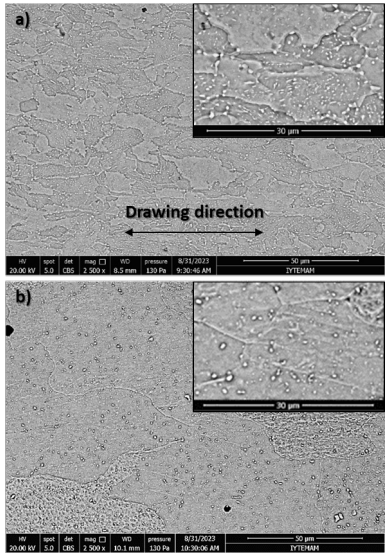

Figure 2. SEM of the wire drawn samples: (a) 14.3% (Ø13.5) and (b) 24.9% (Ø11.7).

SEM images of annealed Ø13.5, Ø12.5 and Ø11.7 samples are shown in Figure 3 (a), (b) and (c), respectively. After annealing, spheroidized Fe_3C spheres (spheroidite) homogeneously dispersed in the ferrite matrix can be seen. The microstructure of the starting material (annealed Ø13.5) clearly shows the randomly oriented pearlitic grains, which include cementite in lamellae form and spheroidites. As the diameter reduction ratio increases with the wire drawing, the lamellae form is in disappearing tendency after annealing. The lamellar cementite and pearlite grains were more effectively transformed into spheroidite cementite and wide ferrite grains, which is clearly seen in Figure 3 (c). As a result of the annealing processes applied after each wire drawing step, grain growth is attributed more than in the first case. The inclination to increase in grain size can be observed more clearly with SEM images. Moreover, the size of precipitated spheroidite particles increasing can be observed. The spheroidization might be accelerated by the plastic deformation since the morphological defects such as kinks, holes and fissures in the cementite can be initiated by higher plastic deformation with the wire drawing and led them to break up of large cementite plates into small spheroidite particles [15].

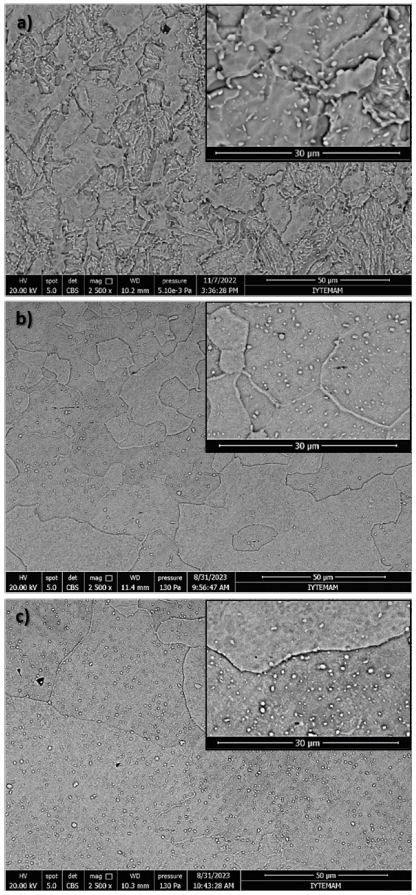

Figure 3. SEM of the annealed samples: (a) Ø13.5, (b) Ø12.5 and (c) Ø11.7 samples.

Compression test results of each sample are given in Figure 4. According to the results, a similar effect on the hardness decrease with sequential wire drawing and annealing was also observed in the compression tests. Lower yield strength (~350 MPa) in the annealed Ø11.7 sample was obtained than the starting material annealed Ø13.5 sample (~410 MPa) and a 14.6% yield strength reduction occurred.

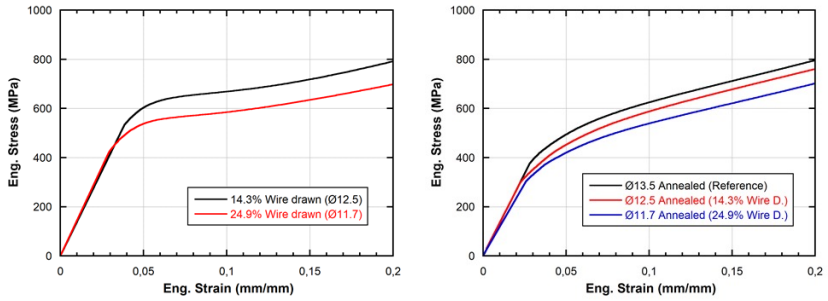

(a) (b)

Figure 4. Compression test results of (a) wire drawn and (b) annealed samples.

4. Conclusion

In this study, the effect of diameter reduction of raw materials with sequential wire drawing and annealing on the formability of a medium carbon steel raw material used for fastener production was investigated. The specimen subjected to multiple wire drawing and annealing processes showed lower yield strength and lower hardness values. Compression test results represent that the specimen subjected to multiple wire drawing and annealing process showed better formability (cold workability). The SEM images showed that the grain size of the final material is greater than the starting material. These images exhibited that spheroidization of lamellae cementite in the final material was greater than the starting material. As a conclusion, the formability of medium carbon steels can be increased by sequential wire drawing and annealing by improvement of spheroidization.

Acknowledgment

The authors would like to thank Norm Holding for the opportunity to conduct and present the study.

References

[1] S. Goto, R. Kirchheim, T. Al-Kassab, C. Borchers, Application of cold drawn lamellar microstructure for developing ultra-high strength wires, Transactions of Nonferrous Metals Society of China 17(6) (2007) 1129-1138.

[2] J. Wistreich, The fundamentals of wire drawing, Metallurgical Reviews 3(1) (1958) 97-142.

[3] P. Kumar, N.P. Gurao, A. Haldar, S. Suwas, Progressive changes in the microstructure and texture in pearlitic steel during wire drawing, ISIJ international 51(4) (2011) 679-684.

[4] W.J. Nam, C.M. Bae, Void initiation and microstructural changes during wire drawing of pearlitic steels, Materials Science and Engineering: A 203(1-2) (1995) 278-285.

[5] G. Langford, A study of the deformation of patented steel wire, Metallurgical and Materials Transactions B 1 (1970) 465-477.

[6] G. Langford, Deformation of pearlite, Metallurgical Transactions A 8 (1977) 861-875.

[7] W.J. Nam, C.M. Bae, S.J. Oh, S.-J. Kwon, Effect of interlamellar spacing on cementite dissolution during wire drawing of pearlitic steel wires, Scripta materialia 42(5) (2000) 457-463.

[8] J.J. Pepe, Deformation structure and the tensile fracture characteristics of a cold worked 1080 pearlitic steel, Metallurgical Transactions 4 (1973) 2455-2460.

[9] D. Porter, K. Easterling, G. Smith, Dynamic studies of the tensile deformation and fracture of pearlite, Acta metallurgica 26(9) (1978) 1405-1422.

[10] J.-K. Hwang, I.-C. Yi, I.-H. Son, J.-Y. Yoo, B. Kim, A. Zargaran, N.J. Kim, Microstructural evolution and deformation behavior of twinning-induced plasticity (TWIP) steel during wire drawing, Materials Science and Engineering: A 644 (2015) 41-52.

[11] J.-K. Hwang, The microstructure dependence of drawability in ferritic, pearlitic, and TWIP steels during wire drawing, Journal of materials science 54(11) (2019) 8743-8759.

[12] H.S. Joo, S.K. Hwang, H.M. Baek, Y.-T. Im, I.-H. Son, C.M. Bae, Manufacturing of medium carbon steel wires with improved spheroidization by non-circular drawing sequence, Procedia Engineering 81 (2014) 682-687.

[13] D. Wei, X. Min, X. Hu, Z. Xie, F. Fang, Microstructure and mechanical properties of cold drawn pearlitic steel wires: Effects of drawing-induced heating, Materials Science and Engineering: A 784 (2020) 139341.

[14] X. Zhang, A. Godfrey, N. Hansen, X. Huang, W. Liu, Q. Liu, Evolution of cementite morphology in pearlitic steel wire during wet wire drawing, Materials Characterization 61(1) (2010) 65-72.

[15] Y.L. Tian, R.W. Kraft, Mechanisms of pearlite spheroidization, Metallurgical transactions A 18 (1987) 1403-1414.

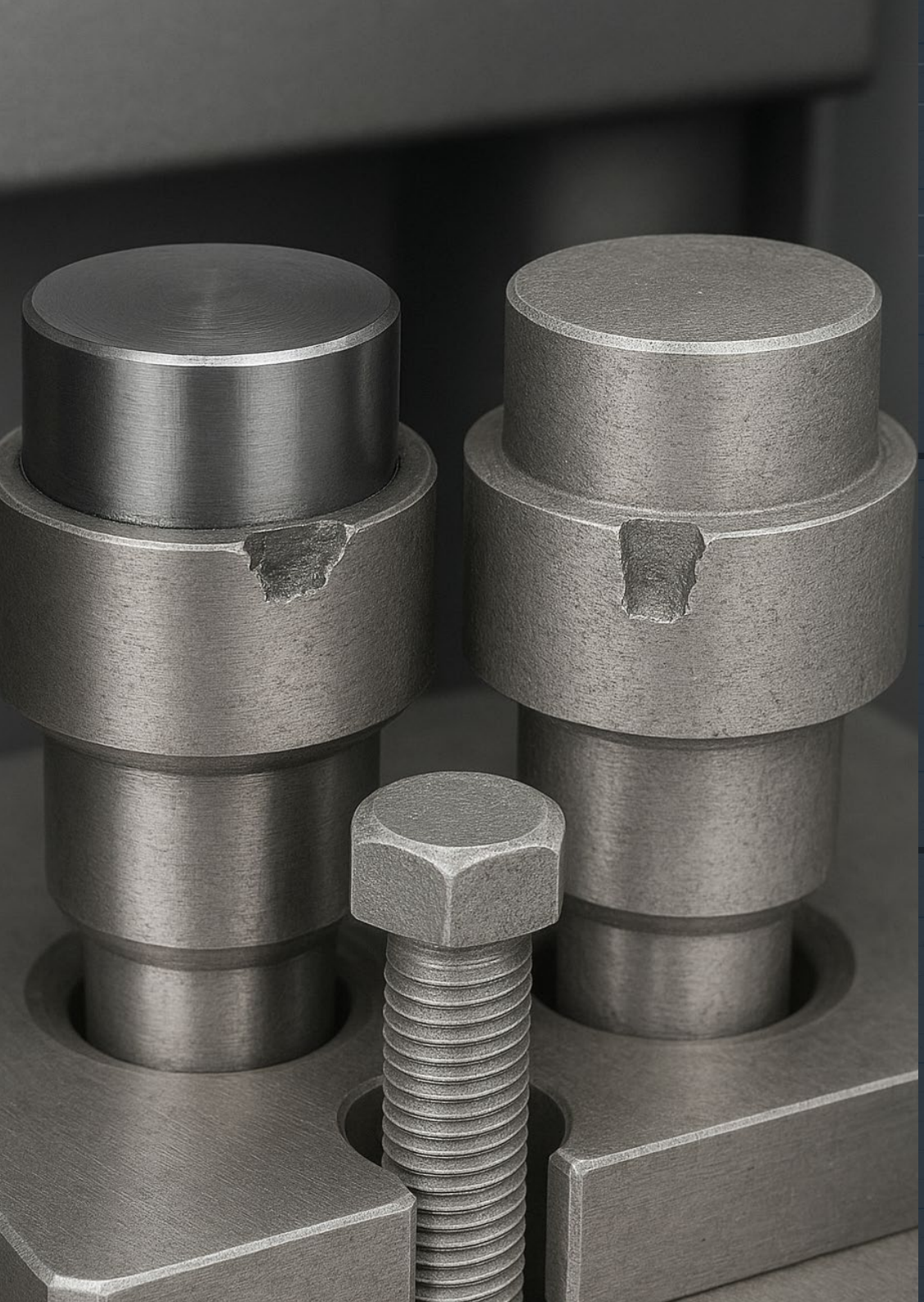

ENHANCING TRIMMING DIE LIFE: THE IMPACT OF MATERIAL PROPERTIES, GEOMETRY AND COATINGS IN COLD FORGING PROCESSES

Tolga AYDIN
Tayfur YAVUZBARUT
Umut İNCE

22. Uluslararası Metalurji ve Malzeme Kongresi (IMMC 2024)

ENHANCING TRIMMING DIE LIFE: THE IMPACT OF MATERIAL PROPERTIES, GEOMETRY AND COATINGS IN COLD FORGING PROCESSES

TOLGA AYDIN[1*], TAYFUR YAVUZBARUT[2], UMUT INCE[1]

[1]R&D Center, Norm Cıvata San. ve Tic. A.Ş., AOSB, Çiğli, İzmir, Turkey
[2]R&D Center, Nedu Bağlantı Elemanları San. ve Tic. A.Ş., AOSB, Çiğli, İzmir, Turkey

Keyword: Bolt Forming, Die Life, Chipping Resistance.

Abstract

The life of trimming dies with different geometries and material properties was analyzed in this study. After a preliminary numerical study of the stresses arising in the cold forging trimming dies using Simufact Forming®, an experimental test setup was determined with different combinations. Combinations with different types of materials and finish coatings were used in the initial installation. The aim was to observe the effect of using powder metallurgical material and nanolayer coating on trimming die life. The examined die set was used in the cold forging process of M16x90 bolts until chipping or fracture was observed. Failure modes, surface morphologies and cycle data were evaluated. Based on the cycle data obtained from the first cold forging trial, a second testing set was created to observe the effects of geometry, material hardness and coating composition on trimming die performance. As a result, it has been determined that the chipping resistance of the HSS material containing relatively high Co has competitive results with PM materials and that the use of nanolayer coating increases the trimming die life by up to 57%.

1. Introduction

Cold forging is a preferred method for the production of fasteners due to its speed, ability to work within tight dimensional tolerances, and the lack of need for preheating. Despite these advantages, there are certain challenges associated with using this manufacturing method. One of the most significant challenges identified in this study is the relatively higher forces acting on the forging dies. The high forging load leads to high principal stresses on cold forging dies, which can result in low cycle failures. This issue, which affects production efficiency in terms of both die consumption and active production time, is a common subject of study in the literature. There are studies examining parameters affecting die life under the headings of raw material surface treatment and annealing, optimal station design, and die design. In order to reduce the load on critical dies, the high stress values can be minimised by improving the station design [1]. It is possible to increase the fatigue life of a die even when the forging load is not reduced, provided that the stress amplitude is reduced. In cases where alterations to the die design and station design are not feasible, or where efficiency is a priority, preparation processes has been identified as a potential avenue for improvement. Annealing of the raw material, surface treatment, wire drawing process affect the formability and die life [2-4].
In the literature, a significant portion of studies on cold forging dies focus on stationary dies. These studies generally address the interference fit optimization of dies made from WC-Co material, which has high compressive strength, the die manufacturing parameters affecting life, and the structural design of the die [5-7]. In contrast, studies focusing on the efficiency improvement of trimming dies are relatively few. Kocatürk et al. conducted a die-life analysis of hexagonal trimming dies with different edge radius and cutting widths [8]. Trimming process was modelled using Simufact Forming software and outputs of FEA simulations compared with production trials to validate. The results showed that cutting width and stopping distance had a significant impact on peak trimming load, while edge radius was found to be effective in reducing peak damage value. In accordence with the findings of Kocatürk and colleagues, many studies have shown that the dominant parameters affecting the life of trimming dies are stopping distance and edge radius [9-13]. However, there are processes where, despite performing the shearing operation, the stopping distance and edge radius parameters should not be influenced to achieve product dimensional requirement. In this condition, there is a need to optimize the parameters in the design conditions of the die.
In this study, the effects of geometry, material, and coating on the life of a trimming die used in a different operation from those in the literature were investigated. The results provide experimental data on parameter effects that are difficult to predict with finite element programs for the specified process.

2. Experimental Procedure

In this study, the fourth station moving die used for the cold forming of an M16x70 bolt was examined. Due to the high ratio of the wrench size to the flange diameter and the low head thickness of the forged product, it is produced using the trimming process. Station design to be used for the cold forging process is given in Figure 1(a). As shown in station design, reduction process is conducted in stage 1. Furthermore, head section of the part is prepared for hexagonal shape in stage 2. In the fourth station, the hexagonal head shape and flange angle are formed using the trimming die discussed in this study. Finally, in the fifth station, excess material is cut off to produce the final product. The trimming die used in the fourth station is shown in Figure 1(b).

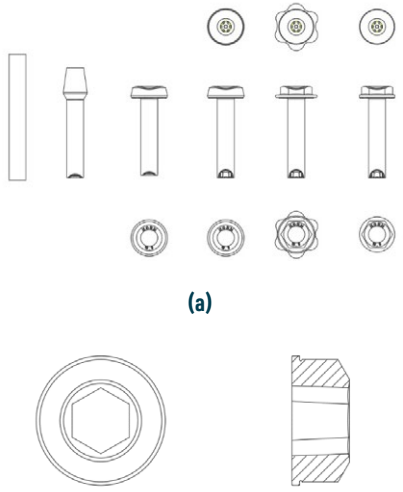

Figure 1. (a) Stage design, (b) Trimming die geometry.

At the beginning of the study, forming simulations were performed using Simufact Forming to modify the test set, and then the principal stresses occurring in the die were examined. Since the FEA results were predicted to be inefficient for the parameters to be tested, the study was designed to test different die types on the production line. In the two-stage

planned study, the second test set was created based on the data obtained from the first test set. Five dies were produced for each die type to be tested. First test set, including material and coating variables, is shown in Table 3. The chemical composition of the die materials is shown in Table 1 and Table 2.

Table 1. Chemical composition of the 1.3247 material (%wt)

C	Si	Mn	Cr	Mo	V	Co
1.05	-	-	3.5	9	0.9	7.5
1.15	0.07	0.4	4.5	10	1.3	8.5

Table 2. Chemical composition of powder metallurgical materials (%wt)

	C	Si	Mn	Cr	Mo	V	W
PM-1	1.28	-	-	5	6,40	4,20	3,10
PM-2	1.40	0.4	0.4	4.7	3.5	3.7	-

Table 3. Experimental Set - 1

No	Material	Coating Type	Material Hardness (HRC)
1	PM - 1	TiAlCN	60-62
2	PM - 1	AlCrN	60-62
3	PM - 2	TiAlCN	62-64
4	PM - 2	AlCrN	62-64
5	CWS	TiAlCN	60-62
6	CWS	AlCrN	60-62
7	1.3247	TiAlCN	60-62
8	1.3247	AlCrN	60-62

In the test set created in the first stage, the aim was to determine the optimum material and understand the effect of nanolayer coating on die life. With the use of powder metallurgy material, the goal was to enhance the chipping resistance due to increased toughness, while minimizing the loss of wear resistance compared to high-speed steel material. Also, cold work steel (CWS) is evaluated for further chipping resistance. The coating given as TiAlCN in Table 3 is a nanolayered, multi-layer PVD coating. This type of coating was compared with the commonly used AlCrN coating in trimming dies to examine the cost/performance ratio. After monitoring the performance of the die types in Table 3 on the production line, dies will be produced using the determined material for the combinations in Table 4, and production trials will be conducted.

Table 4. Experimental Set - 2

No	Coating Type	Material Hardness (HRC)
1	TiSiN	60-62
2	AlCrN	64-66
3	TiSiN	60-62
4	AlCrN	64-66
5	Polished	64-66

In the second test set, the effects of coating usage, coating composition, and hardness on die life and cost were examined. Additionally, the dies were subjected to heat treatment to be manufactured at different hardness values, aiming to observe the dominance of wear and chipping mechanisms relative to each other.

3. Results and Discussion

3.1 FEA Studies

In the die analysis conducted to determine the ability of making inferences based on the obtained data that can be examined by FEA, it was observed that compressive stresses close to the static limit of the material were found at the edges of the hexagonal form. However, no tensile stresses approaching critical levels were observed (Figure 2).

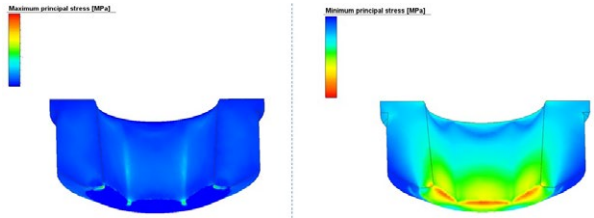

Figure 2. Principal stresses occuring on the die.

3.2 First Experimental Set

The average die life of the dies tested, with five samples of each die type, are given in Table 5. It was observed that all dies, except those made from 1.3247 material, failed due to chipping. Real-time inspections on the production line showed that the dies primarily wore out – the wrench size increased – and then chipped. One of the chipped dies is shown in Figure 3.

Table 5. Results of first cold forging trials

No	Material	Coating Type	Material Hardness (HRC)	Die Life (Cycle)	Failure Mode
1	PM - 1	TiAlCN	60-62	12600	Chipping
2	PM - 1	AlCrN	60-62	9340	
3	PM - 2	TiAlCN	62-64	11900	Chipping
4	PM - 2	AlCrN	62-64	8520	
5	CWS	TiAlCN	60-62	2500	Wear
6	CWS	AlCrN	60-62	1100	
5	1.3247	TiAlCN	60-62	16180	Chipping, Fracture
6	1.3247	AlCrN	60-62	10300	

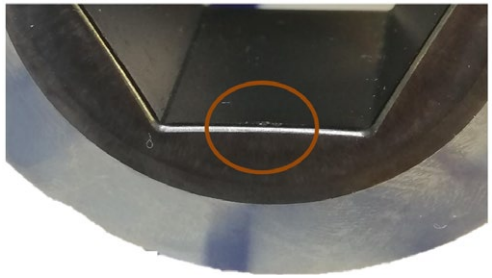

Figure 3. Chipped sample.

The obtained results showed that the use of nanolayer coating improved die life by up to 57%. However, the TiAlCN coating was not used in the secondary test set due to its cost increase outweighing the improvement. The cause of multiple failure modes experienced under conditions using 1.3247 material was investigated. Examination of the crack in Figure 4(a) and the fracture surface in Figure 4(b) revealed that the crack initiation area was not on the forming surface of the die. This finding leaded to a geometric modification for the secondary test samples (Figure 4(c)).

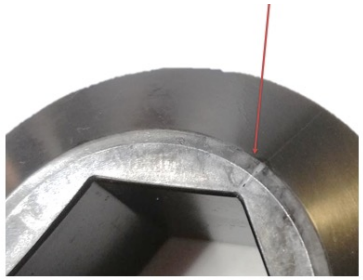

(a)

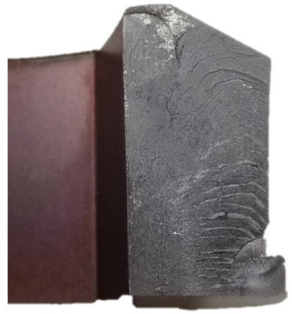

(b)

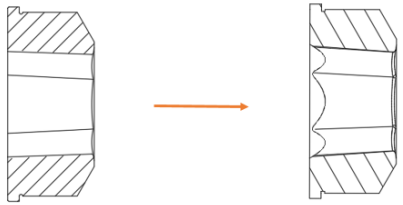

(c)

Figure 4. 1.3247 die sample (fractured): (a) fracture area, (b) fracture surface, (c) revision.

3.3 Second Experimental Set

Results of secondary cold forging trials shown in Table 6.

Table 6. Results of second cold forging trials

No	Coating Type	Material Hardness (HRC)	Die Life (Cycle)
8	AlCrN	60-62	13900
9	AlCrN	64-66	22900
10	TiSiN	60-62	10400
11	TiSiN	64-66	9950
12	Polished	64-66	12400

In the second cold forging trial, all dies were failed due to chipping. Due to the geometric revision, the die life of die type number 8 increased by 34%. According to the results in Table 4, the uncoated polished dies had a 45% shorter life compared to the AlCrN coated ones.

4. Conclusion and Discussion

In this study, the effect of material, coating, and geometry on the die life of a reference trimming die used for the shearing process were investigated. The data obtained from two test sets with different parameters can be summarized as follows:

- The use of nano-coatings has been found to increase die life excessively. However, as the high cost of coating outweighs the increase in tool life, its use in mass production conditions may reduce financial efficiency.
- Due to its relatively high Co content, the 1.3247 material performed better chipping resistance compared to PM materials. However, cold work steel should not be preferred for trimming dies subjected to high wear because of its low wear resistance.
- In the operating conditions of the trimming die examined in this study, wear is observed first, followed by failure due to chipping. As wear increases, the surface profile deteriorates and roughness increases, triggering the chipping mechanism. It is believed that by increasing material hardness, the wear process can be prolonged and chipping delayed, thereby extending die life.
- In the FEA analysis, no high tensile stresses were observed at the corner points of the hexagon; however, in cold forging trials, the dies fractured from these points. Under operating conditions, the multi-axial loads acting on the die created stress concentrations in the corners at the back of the die. It was found that this problem could be solved by chamfering the area.

Acknowledgment

The authors would like to thank Norm Holding for the opportunity to conduct and present the study.

References

[1] Kılıçaslan, C., & İnce, U. Tool life enhancement in cold bolt forging process: effect of forging stage design. Sakarya University Journal of Science, 21(5) (2017) 961-967.

[2] Akyıldız, A. K., & Bayraktar, G. Experimental and numerical analysis of residual stresses in cold forging. Journal of Manufacturing Processes, 78 (2023) 31-45.

[3] Karunathilaka, N., Sunil, T., & Karunathilaka, S. Finite element analysis of metal flow in cold forging of a high-strength steel. Materials Science Forum, 96 (2019) 183-189.

[4] Andreas, K., & Merklein, M. Influence of surface integrity on the tribological performance of cold forging tools. Procedia CIRP, 13 (2014) 61-66.

[5] Killmann, M., & Merklein, M. Analysis of stress pins for the local prestressing of cold forging tools. Production Engineering, 15 (2021) 119-131
.
[6] Lee, H. C., Saroosh, M. A., Song, J. H., & Im, Y. T. The effect of shrink fitting ratios on tool life in bolt forming processes. Journal of Materials Processing Technology, 209(2) (2009) 3766-3775.

[7] Yuangen, Q., & Cho, H. Y. A split die design for forging of hexagonal bolt head. Journal of the Korean Society of Manufacturing Process Engineers, 19(5) (2020) 91-97.

[8] Kocatürk, F., Tanrıkulu, B., Doğan, S., Kılıçaslan, C., Yurtdaş, S., & İnce, U. Optimization of trimming process in cold forging of steel bolts by Taguchi method. International Journal of Pressure Vessels and Piping, 194, Part A (2021) 104503

[9] McCormack, C., & Monaghan, J. Failure analysis of cold forging dies using FEA. Journal of Materials Processing Technology, 117 (2001) 209-215.

[10] McCormack, C., & Monaghan, J. A finite element analysis of cold-forging dies using two- and three-dimensional models. Journal of Materials Processing Technology, 118 (2001) 286-292.

[11] Park, S.-C., & Lee, K.-H. Design of the trimming process of an Al6061 alloy bolt head using finite element analysis and the taguchi method. Journal of the Korean Society of Marine Engineering, 42 (2018) 800-806.

[12] Lee, Y. C., & Chen, F. K. Fatigue life of cold-forging dies with various values of hardness. Journal of Materials Processing Technology, (2001) 539-543.

[13] Hilditch, T. B., & Hodgson, P. D. Development of the sheared edge in the trimming of steel and light metal sheet. Journal of Materials Processing Technology, 169 (2005) 184-191.

DEBRİYAJ SİSTEMLERİNDE KENDİNDEN DİŞ AÇAR CIVATA KULLANIMININ İNCELENMESİ: VAKA ANALİZİ

Tolga AYDIN
Samed ENSER
Ceren ÇELİK
Gökçenur TİMİNCİOĞLU
Caner EŞ
Umut İNCE

6. Ulusal Üniversite-Sanayi İşbirliği, Ar-Ge ve İnovasyon Kongresi

DEBRİYAJ SİSTEMLERİNDE KENDİNDEN DİŞ AÇAR CIVATA KULLANIMININ İNCELENMESİ: VAKA ANALİZİ

TOLGA AYDIN[1*], SAMED ENSER[1], CEREN ÇELİK[2], GÖKÇENUR TİMİNCİOĞLU[2], CANER EŞ[2], UMUT İNCE[1]

[1]Norm Cıvata San. ve Tic. A.Ş. Ar-Ge Merkezi, AOSB, Çiğli, İzmir, Türkiye
[2]Dönmez Debriyaj A.Ş. Ar-Ge Merkezi, BOSB, Kemalpaşa, İzmir, Türkiye
Email*: tolga.aydin@normfasteners.com

Özet

Otomotiv alt sistemlerinde kullanılan sökülmeyen bağlantı elemanları, düşük maliyet ve tedarik kolaylığı gibi avantajlar sunmasına rağmen belirsiz servis koşulları ve ilk montaj sırasında oluşabilecek hatalara müdahale edilememesi gibi dezavantajlar nedeniyle tercih edilebilirliğini kaybetmektedir. Bu çalışmada, bahsi geçen dezavantajlara çözüm olarak debriyaj sisteminde yer alan baskı montaj bölgesine montajlanan perçin ve tahdit yüzüğünün diş açar cıvata ile ikame edilmesi konu alınmıştır. Titreşim ve çok eksenli kuvvetlerin etkisi altında çalışan debriyaj sistemlerinde, diş açar cıvata kullanımı konusunda literatürde ve endüstride yeterli bilgi ve deneyim bulunmamaktadır. Parça sayısını azaltarak montaj sürecini kolaylaştırmak amacıyla, perçin yerine kullanılmak üzere diş açar cıvata tasarımları geliştirilmiş ve numune üretimleri yapılmıştır. Bu çalışma kapsamında, baskı plakası montaj noktası için özel olarak tasarlanıp üretilen diş açar cıvataların debriyaj sistemindeki karşı parçaya diş açma uygunluğu test edilmiştir. Sıyırma/sıkma tork oranı gibi ürün performansını ifade eden parametreler hesaplanmıştır. Çalışmanın devamında Dinamometre performans testi ve bilgisayar destekli mühendislik programı ile mekanik analizler gerçekleştirilerek bulgular raporlanmıştır. Gerçekleştirilen sistem testlerinde, simüle edilen çalışma ortamdaki cıvatanın gevşeme davranışı ve şok testlerindeki dayanımı detaylı bir şekilde analiz edilmiştir.

Anahtar Kelimeler: Diş açar cıvata, Sıyırma torku, Debriyaj sistemleri, Dinamometre testi, Bilgisayar destekli mühendislik programı.

1. Giriş

Günümüz otomotiv endüstrisinde, araç alt sistemlerinin güvenilirliği ve verimliliği, optimum araç performansına ulaşmak için kritik bir öneme sahiptir. Bu alt sistemler arasında, bağlantı elemanlarının seçimi, hem yapısal bütünlük hem de sistem verimliliği sağlamak için önemli bir rol oynamaktadır. Perçin gibi sökülmeyen bağlantı elemanları, düşük maliyetleri, tedarik kolaylığı ve güçlü, kalıcı bağlantılar sağlama yetenekleri nedeniyle yaygın bir şekilde kullanılmaktadır. Ancak, bu avantajlarına rağmen, sökülemeyen bağlantı elemanları; belirsiz servis koşulları ya da ilk montaj sırasında oluşabilecek hataları düzeltememe gibi zorluklar nedeniyle bazı uygulamalarda tercih edilmemektedir. Bu zorlukların belirgin bir şekilde görüldüğü alanlardan biri de araç debriyaj sistemleridir (Şekil 1).

Debriyaj sistemi, motor gücünü vites kutusuna ileterek aracın hareketini başlatan ve durdurulmasını ya da vites değiştirilmesini sağlayan bir aktarma organıdır. Motor ile şanzıman arasında yer alan bu sistem, özellikle ilk harekette titreşimsiz bir geçiş sağlarken, vites değişimlerinde güç iletimini geçici olarak keser. Ayrıca aşırı torka karşı şanzımanı koruma görevini üstlenir. Kuru sürtünmeli debriyaj, otomobillerde yaygın olarak kullanılır ve tork iletimi, disk yüzeylerindeki sürtünme kuvvetiyle gerçekleşir. Kuru sürtünmeli debriyajda kavrama ayrım işlemi, sürücünün debriyaj pedalını kullanmasıyla başlar. Kavramayı ayırmak için pedala basıldığında, mekanik ya da hidrolik bir aktüatör aracılığıyla baskı ünitesindeki diyafram yayına eksenel bir kuvvet uygulanır [1]. Bu kuvvet, diyafram parmaklarının eksenel hareketine

neden olur ve baskı plakası, mesnet lamaları yardımıyla geri çekilerek disk komplesindeki tork iletimi kesilir. Pedaldan ayağın çekilmesiyle, aktüatör tarafından eksenel kuvvet serbest bırakılır ve disk grubu baskı plakası ile volan arasında sıkışarak balatalar üzerinden kavrama sağlanır. Böylece, şanzıman miline tork iletimi tekrar başlar [2]. Diskteki helezon yaylar, motor titreşimlerini ve aşırı torkları sönümleyerek şanzımanın zarar görmesini engeller [1].
Metal bir gövdeden oluşan debriyaj baskısı volana cıvata yardımı ile montajlanır. Motor devri volana aktarılır.

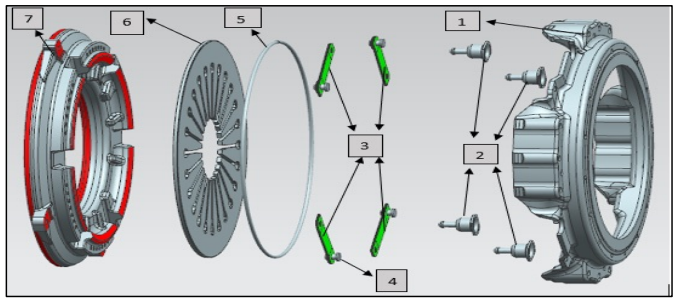

Şekil 1. Baskı Komplesi Alt Bileşenleri [3]

Kafes (1), tahdit perçini (2), mesnet lamaları (3), mesnet laması tespit perçini (4), fulcrum ring (5), diyafram yay (6) ve baskı plakası (7) oluşmaktadır. Debriyaj araca bağlanırken, diyafram yay (6), kafes (1) ve fulcrum ring (5) arasına ön gerilmiş halde bağlanır. Tork iletimi esnasında, diyafram yay aynaya basmaktadır. Debriyaj pedalına basılmasıyla birlikte baskı rulmanının diyafram yayı esnemeye zorlamasıyla birlikte ayna (7) ile disk teması kesilir böylece ayırma gerçekleşir [3].

Ayna esneklik modülü düşük mesnet laması ile debriyaj kafesine bağlıdır. Ayna genellikle iyi aşınma ve ısı taşınım özelliklerine sahip olan gri dökme demirden yapılmaktadır. Kavrama için gerekli sürtünme yüzeyleri ayna ile diskteki balata arasında sağlanır. Debriyajın en önemli parçalarından diyafram yay, debriyaj kafesi içinde bulunur. Diyafram yay, kafesteki yuvaya yerleştirilmiş olup serbest halde bulunmaktadır [3].

Bu sistemlerde geleneksel olarak kullanılan perçinler, kalıcı bağlantı sağlamada etkili olsa da montaj veya servis sorunlarına yönelik kolaylık sunmamaktadır. Bu durum, daha pratik ve güvenilir bağlantı teknolojilerinin araştırılmasının önünü açmıştır. Geleneksel sökülebilir bağlantı elemanları olan cıvatalarda ise karşılaşılabilecek gevşeme problemleri, kesme yüklerine karşı performans düşüşleri, montaj bölgesine diş açma operasyonları veya somun kullanma ihtiyaçları nedeniyle diş açar cıvatalar geliştirilmiş ve özellikle otomotiv sektöründe giderek fazla kullanılmaya başlanmıştır. Montaj bölgesine kendi dişini açması nedeniyle hem operasyon azaltma hem de kendi oluşturduğu dişlerdeki temas alanı sayesinde gelişmiş gevşeme direnci ve kesme mukavemetine sahip diş açar cıvatalar sektörde araştırma konusu olmuştur.

Bu bağlamda, parça sayısını azaltmak, montaj sürecini kolaylaştırmak ve servis kolaylığı sağlamak hedefiyle geliştirilmiş diş açar cıvatalar, araç alt sistemlerinde umut verici bir alternatif olarak ortaya çıkmaktadır. Ancak, bu teknolojinin debriyaj sistemleri gibi kritik otomotiv bileşenlerinde kullanımı henüz yeterince araştırılmamıştır. Mevcut çalışmalar daha çok geleneksel bağlantı elemanları ve uygulamalarına yönelik olup otomotiv alt sistemlerinde karşılaşılan zorlu koşullar altındaki performanslarına yönelik önemli bir bilgi ve tecrübe eksikliği mevcuttur. Örneğin, literatürde gerçekleştirilen çalışmada otomobil ön tampon orta braketinin nümerik analizleri gerçekleştirilmiş olup mekanik değerlendirmesi yapılmıştır. Çalışma, analizi gerçekleştirilen braket parçası için kaliteyi iyileştiren parametrelerin belirlenmesini

ve bu parametreler arasından en etkili olanlarını ortaya koymayı hedeflemişlerdir [4]. Başka bir çalışmada ise, binek araçlar için koltuk kızak bağlantı braketi tasarımı ve ürün regülasyon testlerini gerçekleştirmiştir. Çalışma sonucunda analizler test ile doğrulanmış olup topografya iyileştirme çalışmaları gerçekleştirilerek geliştirilen braket parçasında %20 ağırlık azaltımı sağlanmıştır [5]. Görüldüğü gibi araç sistemlerinde kullanılan bağlantı elemanı çalışmaları geleneksel ürünlere yöneliktir. Diş açar cıvataların diş açma performansına yönelik çalışmalar da mevcuttur. Bir çalışma, diş açar cıvataların diş açma performansının, montajlanacak iş parçasının malzeme özellikleri ve delik çapı ile ilişkisini analitik olarak incelemiştir [6]. Yine diş açar cıvatalarla ilgili başka bir çalışmada, diş açar cıvataları sonlu elemanlar modeli kurarak diş açma performansını analitik olarak incelemiş, diş açma prosesi boyunca gerçekleşen malzeme akışı ve diş açma torklarını deneysel sonuçlar ile kıyaslamışlardır [7]. Son olarak diş açar cıvatalarla ilgili gerçekleştirilen başka bir çalışmada, bu cıvataların diş açma torkları dikkate alınarak montaj torkunun belirlenmesi için deneysel çalışmalar yürütülmüş, çalışma sonucunda sıyırma torku testleri verilerine göre tasarım gerçekleştirilmiştir [8]. Görüldüğü gibi diş açar cıvataların gerçek bir sistemde nasıl performans göstereceğine yönelik bir çalışma yok ya da çok kısıtlıdır.

Tahdit yüzüğünün operasyonel süreçlerde yarattığı sınırlamalar, bu parçanın sistemden çıkarılmasını gerekli kılmaktadır. Ayrıca perçin varyasyonlarının baskı plakasında çatlamalara yol açması sistemin dayanıklılığı üzerinde olumsuz etkiler yaratmaktadır. Bunun yanı sıra, sökülemez bağlantıların tercih edilmesi, hatalı montaj durumlarında operasyonel süreçleri zorlaştırarak maliyetlerin artmasına neden olmaktadır. Bu çalışma, söz konusu sorunları ele alarak debriyaj sisteminin baskı montaj bölgesindeki perçinlerin yerine diş açar cıvataların kullanılmasının montaj operasyonu ve sistem performansı üzerine etkisini incelemeyi amaçlamaktadır. Araştırmada, bu uygulama için özel olarak tasarlanıp geliştirilen diş açar cıvataların prototip üretimleri gerçekleştirilmiş ve montajlanabilirlik değerlendirmeleri yapılmıştır. Tasarımın uygunluğunu belirlemek için sıyırma ve sıkma tork oranları gibi parametreler incelenmiş; dinamometre performans testleri ve bilgisayar destekli mühendislik (CAE) analizleri ile gerçek çalışma koşulları simüle edilmiştir. Ayrıca, cıvataların gevşeme davranışları ve şok testlerindeki dayanımı detaylı bir şekilde analiz edilmiş ve elde edilen sonuçlar test verileriyle karşılaştırılmıştır.

2. Malzeme ve Yöntem

2.1 Geometrik ve Kavramsal Tasarım

Çalışma kapsamında, ağır vasıta debriyaj sisteminde, perçin ve tahdit yüzüğünün cıvata bağlantısı ile ikame edilebilirliğine yönelik tasarım çalışması yapılmıştır. Şekil 2'de, debriyaj sistemine ait baskı montajının 3D modeli gösterilmektedir. Şekil 3'te ise bağlantı noktalarının görüntüleri verilmiştir. Şekil 3'te 1 numaralı kısım baskı plakasındaki tahdit yüzüklü tarafı, 2 numaralı kısım ise kafes tarafındaki perçini göstermektedir.

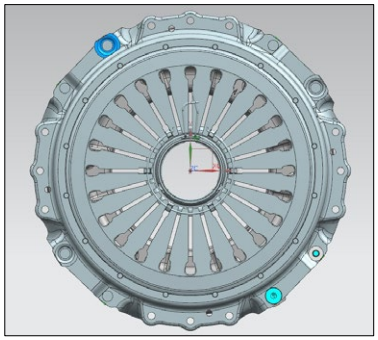

Şekil 2. Debriyaj Sistemine Ait Baskı Montajının 3D Modeli

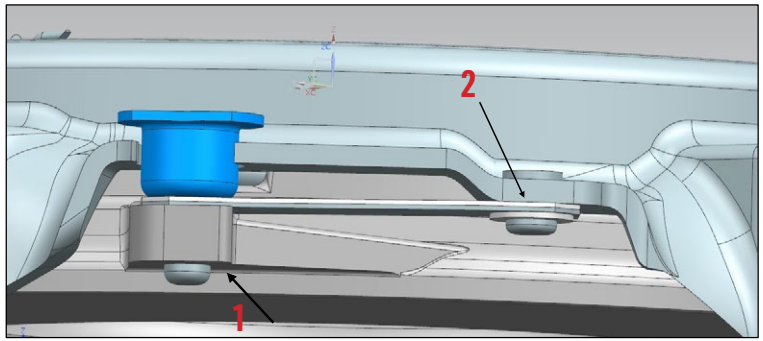

Şekil 3. Tahdit Yüzüğü ve Perçin Kullanılan Baskı Modeli

Perçin bağlantılarının yerine ikame olarak tasarlanan cıvata bağlantılarında, bağlantı noktasındaki kritik tasarım parametreleri dikkate alınmıştır. Bu parametreler; bağlantıya etki eden tork ve kuvvet değerleri, montaj yapılacak karşı parçanın sertlik ve malzeme özellikleri, karşı parçanın et kalınlığı ve bağlantı parçası ölçülerini sınırlayan alt parçaların tolerans değerleri gibi unsurları içermektedir. Parça ve proses çeşitliliğini artırmamak ve montaj ile demontaj işlemlerini kolaylaştırmak amacıyla diş açar cıvataların her iki montaj noktasında kullanımı öncelikli olarak değerlendirilmiştir. Mevcutta kullanılan tahdit yüzüğü ve perçin yerine her iki montaj noktasında da diş açar cıvataların kullanımı denenmiştir. İlgili parçanın diş açar cıvatalar ile montajlanmış hali Şekil 4'te gösterilmektedir.

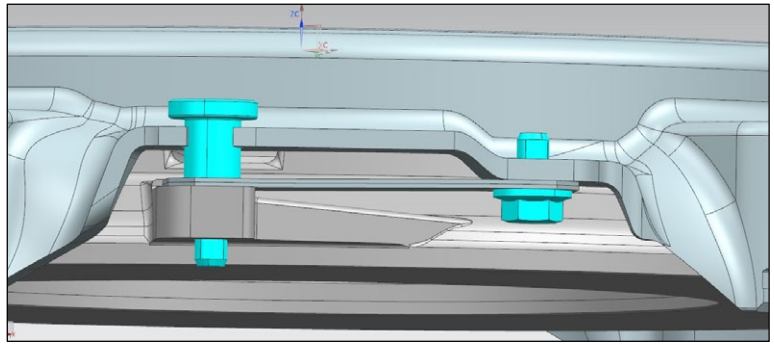

Şekil 4. Tahdit yüzüksüz Diş Açar Cıvata kullanılan Baskı Modeli

2.2. Bilgisayar Destekli Sayısal Analiz

Debriyaj sistemindeki boyutsal ölçüler ve teknik gereksinimler göz önünde bulundurularak, baskı montajında diş açar cıvata kullanımının sisteme olan etkileri, bilgisayar destekli sayısal analiz yöntemleriyle simüle edilmiştir. Bu kapsamda, cıvatalar üzerindeki yükleme koşullarını değerlendirmek için gerilme, moment ve toplam deformasyon analizleri detaylı bir şekilde gerçekleştirilmiş ve elde edilen veriler sistem performansını değerlendirmek amacıyla incelenmiştir.
Debriyaj sisteminde 3200 Nm'lik bir tork öngörülmüş ve bu değere 1.5 emniyet katsayısı uygulanarak 4800 Nm'lik bir maksimum tork değeri hesaplanmıştır. Analiz, sistemin yalnızca dörtte bir parçası için gerçekleştirildiğinden, bu doğrultuda tork parametresi 1200 Nm olarak belirlenmiştir. Gerçekleştirilen analizde cıvatalara montaj sonrası üzerinde gerçekleşmesi beklenen kuvvet uygulanmıştır. Uygulanan kuvvet Şekil 5'te görüldüğü gibidir. Şekil 5'te bileşene belirli bir noktada uygulanan dönme kuvveti görülmektedir. Uygulanan moment değeri 1200 Nm olarak belirtilmiştir.

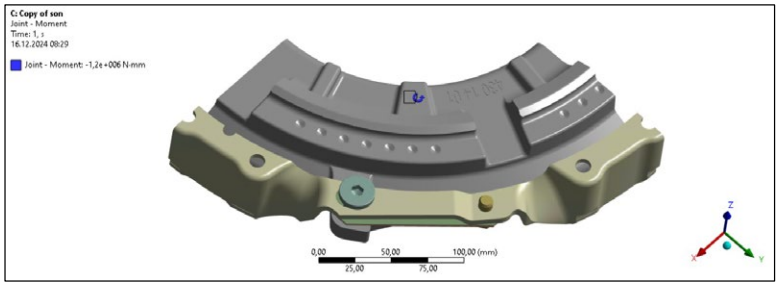

Şekil 5. Bilgisayar Destekli Analizde Uygulanan Moment

2.3 Cıvata Ön Testleri

Bu çalışmada, M10x20 altıköşe flanşlı diş açar cıvatanın diş açma performansını değerlendirmek amacıyla deneysel testler gerçekleştirilmiştir. Performansı incelenen diş açar cıvata, Norm Cıvata firması tarafından patentli olan ve Normest® adıyla bilinen dörtlü lobular kesite sahip bir üründür. Testlerde, montaj noktasına uygun olarak StW 24 malzemeden, 6 mm levha kalınlığına ve 130 HV sertliğe sahip karşı parçalar kullanılmıştır (Şekil 6).

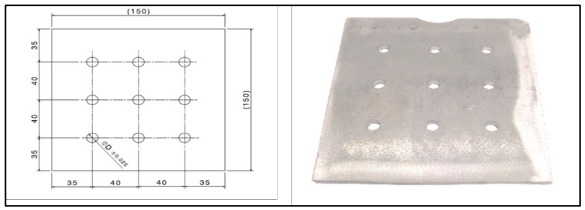

Şekil 6. Test Levhası ve Bağlantı Parçaları

Testlerde cıvataların fonksiyonelliği onaylanarak, bağlantı üzerindeki "prevailing" tork değeri tespit edilmiş, çalışılması gereken yüzey sertliği, delik çapı gibi değerler kesinleştirilmiştir. Dökme demir parça için olası diş açar cıvata kullanımını denetlemek adına ek test gerçekleştirilmiştir. Deneyler, 9.20 mm, 9.30 mm ve 9.40 mm olmak üzere üç farklı delik çapında gerçekleştirilmiştir. Test için üretilen bağlantı parçasının 3D görseli Şekil 7'de sunulmuştur.

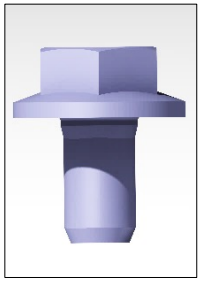

Şekil 7. Diş açar cıvata tercih edilen ürün

2.4. Baskı Montajı Performans Testi

Sistem, maksimum 3500 Nm tork üretebilecek kapasiteye sahiptir ve bu güç, 1000 devir/dakika (rpm) motor hızıyla sağlanmaktadır. Araç, maksimum 60 ton yük taşıma kapasitesine sahip olup, bu yük altında dahi 12° eğime kadar olan rampalarda çalışabilmektedir. Bu veriler, dinamometre cihazına sistemin sınır koşulları olarak tanımlanmıştır. Sınır koşulları, cihazın araca veya sisteme uygun bir test ortamı sağlayabilmesi için temel referans değerler olarak kullanılmaktadır. Böylece, dinamometre testleri sırasında sistemin gerçek çalışma koşullarına en yakın performansı sergilemesi sağlanır. Özellikle ağır yük taşıma kapasitesi ve eğim koşullarına dayanıklılık, cihazın sistem üzerindeki simülasyonunun gerçekçi ve güvenilir olmasını garanti eder.

3. Sonuçlar

Sonuç olarak, debriyaj sistemindeki boyutsal ölçüler ve teknik gereksinimler dikkate alınarak yapılan bilgisayar destekli sayısal analizler, baskı montajında diş açar cıvata kullanımının sisteme olan etkilerini kapsamlı bir şekilde simüle etmiştir. Bu analizler sonucunda, cıvatalar üzerindeki yükleme koşullarını değerlendirmek için yapılan gerilme kuvveti, moment ve toplam deformasyon analizleri, elde edilen verilerle birlikte sistem performansını değerlendirmeye olanak sağlamıştır. Toplam deformasyon analizi sonucu, Şekil 8'de gösterilmiş olup, analize ait sayısal veriler ise Tablo 1'de yer almaktadır. Analizde, model üzerindeki deformasyon miktarları renk ölçeği ile ifade edilmektedir.

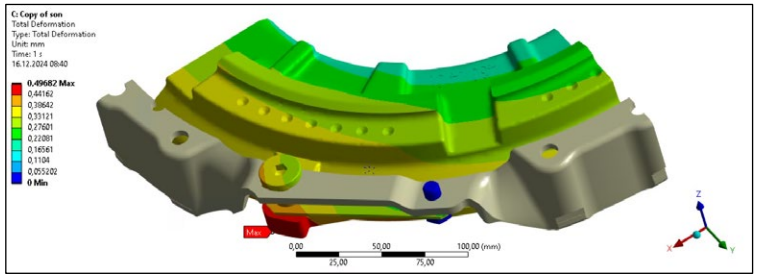

Şekil 8. Toplam Deformasyon Analizi Sonucu

Görseldeki kırmızı bölgeler, en fazla deformasyona uğrayan alanları temsil eder ve bu alanın deformasyon miktarı 0,49682 mm olarak belirlenmiştir. Diğer taraftan, mavi bölgeler minimum deformasyonu, yani 0 mm'yi ifade etmektedir. Skaladan görüldüğü üzere, deformasyonun en yüksek olduğu bölge kırmızı renk ile işaretlenmiştir. Bu bölgeler, analizde kritik bölgeler olarak değerlendirilmelidir, çünkü bu alanlarda deformasyonun yüksek olması, yapının dayanıklılığı ve performansı açısından önemli bir risk oluşturabilir.

Tablo 1. Toplam Deformasyon Analizi Sonucu Sayısal Verileri

Time [s]	Minimum [mm]	Maximum [mm]	Average [mm]
0.2	0.0	0.31186	0.24049
0.4	0.0	0.3531	0.25969
0.6	0.0	0.39598	0.2794
0.9	0.0	0.47196	0.31618
1.0	0.0	0.49682	0.3284

Sistem üzerindeki toplam gerilme analizi sonucu Şekil 9'da görülmektedir. Görselde, maksimum gerilme değeri 384,23 MPa olarak belirlenmiş ve bu nokta kırmızı ile işaretlenmiş. Analizden elde edilen sayısal veriler Tablo 2'de görülmektedir. Bu bölgede, yapının gerilme konsantrasyonu en yüksektir. Minimum gerilme ise 0,0091635 MPa ile mavi tonlarda, yapının diğer bölgelerinde gözlemlenmiştir.

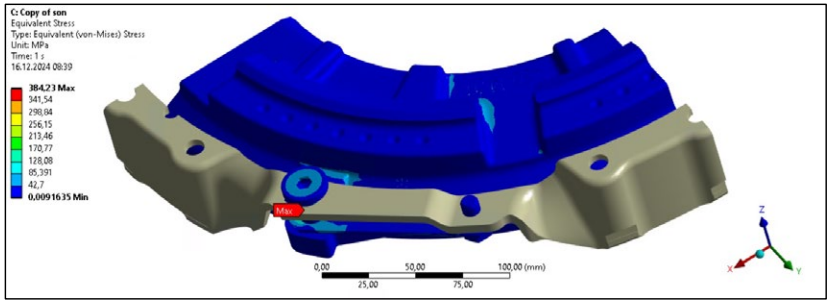

Şekil 9. Toplam Gerilme Analizi Sonucu

Yüksek gerilmenin bulunduğu bu alan, genellikle bağlantı noktaları, keskin köşe veya geometrik sınırlamaların neden olduğu bölgelerde ortaya çıkar. Eğer maksimum gerilme bölgesindeki gerilme değeri, kullanılan malzemenin akma dayanımını aşarsa, bu bölgede plastik deformasyon veya olası bir kırılma riski bulunabilir. Bu durumda, tasarımın yeniden gözden geçirilmesi, malzemenin değiştirilmesi veya ilgili bölgede yükü azaltacak tasarım değişiklikleri yapılması gerekebilir.

Tablo 2. Toplam Gerilme Analizi Sonucu Sayısal Verileri

Time (s)	Minimum (MPa)	Maximum (MPa)	Average (MPa)
0.2	2.0984e-003	78.016	5.7711
0.4	3.8894e-003	146.79	11.181
0.6	5.5879e-003	226.67	16.663
0.9	8.3604e-003	343.46	25.211
1.0	9.1635e-003	384.23	28.04

Cıvataların Üzerindeki Gerilme Analizi Sonucu Şekil 10'daki gibidir.

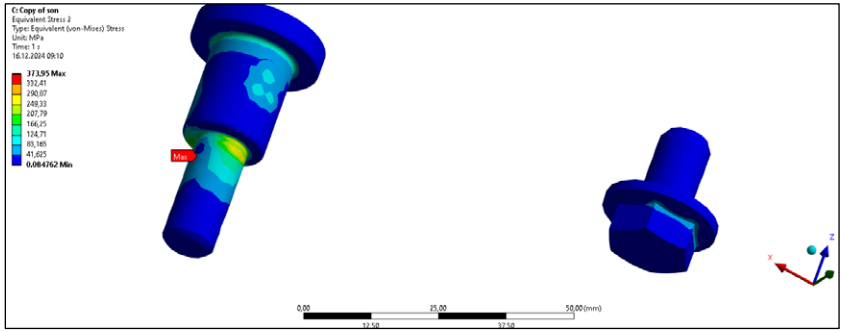

Şekil 10. Cıvataların Üzerindeki Gerilme Analizi Sonucu

Tablo 3'te görüntülenen analiz sonuçlarına göre, maksimum Von-Mises gerilmesi 373,95 MPa olarak belirlenmiştir, bu da cıvatanın üzerinde en fazla gerilmenin yoğunlaştığı bölgeyi gösterir. Minimum değer ise 0,084762 MPa olup, bazı bölgelerde yüklemenin olmadığını veya çok düşük olduğunu belirtir. Analiz, sol taraftaki cıvatanın daha yoğun bir yüklenme ve gerilme yaşadığını, sağ taraftaki cıvatada ise daha düşük yük birikimi olduğunu ortaya koymaktadır. Maksimum gerilme noktası, analizde kırmızı renkle işaretlenmiş olup, bu bölge cıvatanın kesit değişim yerinde yoğunlaşmıştır. Geometrik düzensizlikler nedeniyle bu tür bölgelerde gerilme yığılmaları sıkça görülür. Sonuç olarak, bu analiz, cıvatanın kritik bir bölgesinde yüksek gerilme olduğunu göstermektedir. Daha güvenli bir tasarım için malzeme, geometri ve yükleme koşullarının optimize edilmesi önemlidir. Von-Mises gerilmesinin azaltılması, cıvata ömrü ve güvenliği açısından kritik bir faktördür.

Tablo 3. Cıvataların Üzerindeki Gerilme Analizi Sonucu Sayısal Verileri

Time [s]	Minimum [MPa]	Maximum [MPa]	Average [MPa]
0.2	1.7728e-002	62.168	8.868
0.4	3.6063e-002	124.32	18.082
0.6	5.4316e-002	199.24	27.98
0.9	7.6954e-002	327.25	42.822
1.0	8.4762e-002	373.95	48.079

Belirtilen sınır koşulları altında gerçekleştirilen montaj testinde, cıvataların fonksiyonelliği doğrulanmış ve bağlantı üzerindeki direnç sıkma torku değeri belirlenmiştir. Ayrıca çalışılması gereken yüzey sertliği ve delik çapı gibi parametreler kesinleştirilmiştir. Ürün performansını ifade eden sıyırma/sıkma tork oranı gibi parametreler hesaplanmıştır. Test sonuçlarına göre, levha kalınlığı da dikkate alınarak, 9.30 mm çapında ve sıyırma torkunun sıkma torkuna oranının 3.5 olduğu koşullarda çalışılabileceği tespit edilmiştir. Testlerden elde edilen Tork-Açı grafiği Şekil 11'de sunulmuştur.

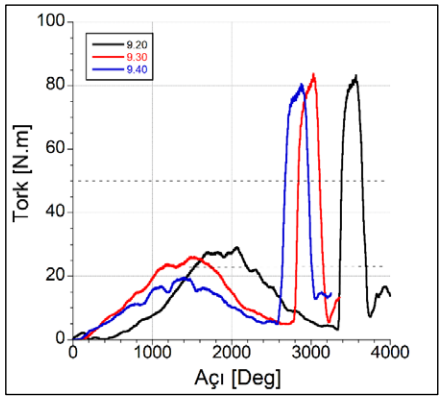

Şekil 11. Tork - Açı Grafiği

Diş açar cıvata montajı yapılmış test levhalarının görselleri ise Şekil 12'de görülmektedir.

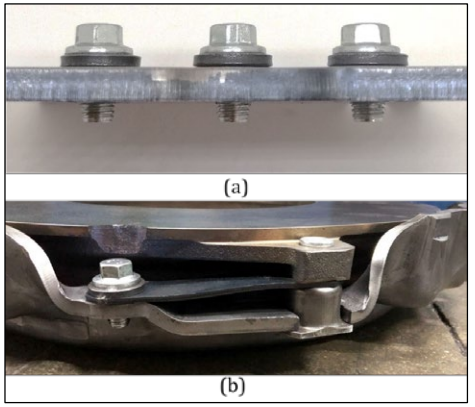

Şekil 12. Diş Açar Cıvatanın Montajlandığı (a) Test Levhası, (b) Debriyaj Sistemi

Şekil 3'te yer alan 1 numaralı montaj bölgesindeki karşı parçanın dökme demir malzemeden olması nedeniyle, bu bölgede kilitleme kimyasalı ile birlikte standart metrik cıvata kullanımı tercih edilmiştir. Diş açar cıvatalar, dökme demirin ufalanma eğilimi ve görece yüksek sertlik değerleri nedeniyle bu koşullarda uygun bulunmamaktadır. Diş açar cıvata denemesi yapılan dökme demir ürün Şekil 13'teki gibidir.

Şekil 13. Diş açar cıvata denemesi yapılan dökme demir ürün

Aracın 1. viteste gerçekleştirilen dinamometre test cihazından alınan sürtünme katsayısı-cycle grafiği, Şekil 14'te gösterilmektedir. Bu grafikte, özellikle 300 çevirim (cycle) sonrasındaki veriler dikkate alınmaktadır, çünkü bu noktada malzeme tam temas haline ulaşarak, ideal çalışma koşullarına uygun bir duruma gelmiştir. Bu aşama, malzemenin çalışma performansını değerlendirmek ve uzun vadeli dayanıklılığını analiz etmek için kritik bir zaman aralığıdır.

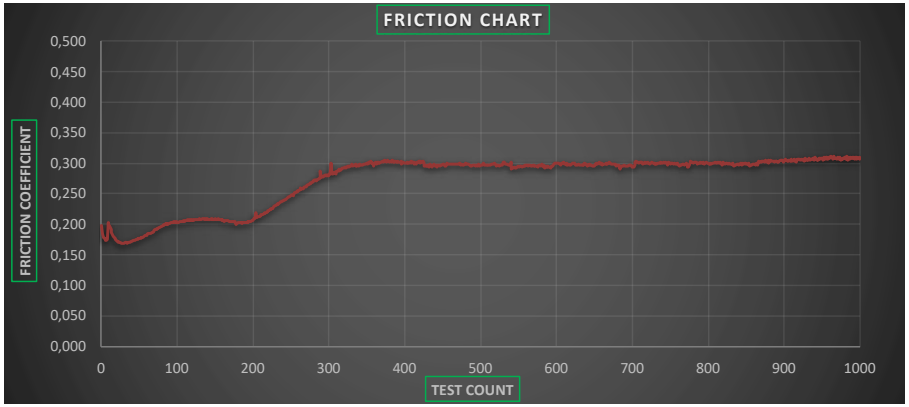

Şekil 14. Sürtünme Katsayısı Grafiği

Grafikte, bir sistemin sürtünme katsayısının test sayısına bağlı olarak nasıl değiştiği gösterilmektedir. Başlangıçta sürtünme katsayısı yaklaşık 0.200 seviyesindedir ve testlerin ilk aşamalarında belirgin bir artış eğilimi sergilemektedir. Özellikle 300. cycle kadar olan süreçte, sürtünme katsayısındaki bu artış, yüzeylerin birbirine uyum sağlaması ya da temas koşullarının iyileşmesiyle açıklanabilir. Bu dönemde sürtünme katsayısı hızlı bir şekilde yükselmektedir. 300. cycle itibaren, sürtünme katsayısının yaklaşık 0.350 seviyesine ulaştığı ve bu değerden sonra daha stabil bir seyir izlediği görülmektedir. Bu durum, sistemin kararlı bir sürtünme davranışı sergilemeye başladığını ve yüzeyler arasındaki etkileşimin artık oturduğunu göstermektedir.

Son olarak, grafik toplamda 1000 cycle boyunca sürtünme katsayısındaki değişimleri detaylı bir şekilde sunmaktadır. Kararlı bölgeye geçiş, sistemin malzeme seçimi ve yüzey performansının uzun vadeli dayanıklılığını değerlendirme açısından önemli bir bulgu sunar. Bu tür analizler, mekanik sistemlerin güvenilirliğini artırmak ve çalışma koşullarına uygun malzeme kullanımını doğrulamak için kritik bir role sahiptir.

10.9 dayanım sınıfındaki bir cıvata için dayanım gerilmesi 900 N/mm^2 olarak belirlenmiştir. Ancak, cıvatanın maruz kalacağı maksimum gerilme değeri 373.95 N/mm^2'dir. Bu durumu değerlendirmek için kullanılan güvenlik faktörü (αeem) hesaplanabilir. Hesaplama şu şekilde yapılır:

$$\sigma_{eem}=\sigma_e D/S \; ; \qquad (1)$$

$$(900\ N/mm^2)/(373.95\ N/mm^2)= 2.40$$

Sonuç olarak, güvenlik faktörü 1.72 olarak bulunur. Bu, cıvatanın maruz kalacağı maksimum gerilmenin yaklaşık 1.72 katına kadar güvenle dayanabileceğini gösterir. Bu hesaplama, cıvatanın güvenli bir şekilde kullanılabilirliğini ve dayanıklılığını değerlendirirken önemli bir parametre olarak kullanılır.

4. Değerlendirme ve Tartışma

Prototip üründeki debriyaj parçalarından çelik malzemeye sahip olan kafes parçasında diş açar cıvata kullanımının performans açısından uygun olduğu belirlenmiş ve sistem testlerinde herhangi bir sorunla karşılaşılmamıştır. Yapılan analizler ve testler, incelenen ürünlerin çelik malzeme kafes alt parçasında diş açar cıvatanın güvenli bir şekilde kullanılabileceğini göstermektedir.

Ancak dökme demir malzeme Baskı plakasında, yüksek diş açma torku ve dökme demirin kırılgan yapısı nedeniyle montaj parçasının ufalanarak malzeme kopması gözlemlenmiştir. Diş açar cıvatalar, dökme demirin yüksek sertlik değerleri ve ufalanma eğiliminden dolayı bu koşullarda uygun bulunmamaktadır. Bu nedenle dökme demir montaj parçalarında kendinden diş açar cıvatalar tavsiye edilmemektedir. Şekil 2'deki 1 numaralı montaj bölgesinde, karşı parçanın dökme demir olması nedeniyle, kilitleme kimyasalı kullanımı üzerinde çalışılmaktadır.

Teşekkür

Yazarlar, bu bilimsel araştırmanın her aşamasına sağladıkları katkılar ve desteklerinden dolayı Norm Fasteners Cıvata ve Dönmez Debriyaj firmalarına teşekkür eder.

References

[1] Kurt, U., Çelik, C., Eş, C., & Yıldız, Ö. (2023). Debriyaj Diskindeki SAE 1010 Malzeme Disk Kapağının Temperleme Isıl İşlemi ile Renklendirilmesinin Parçanın Mekanik Özellikleri Üzerine Etkisinin İncelenmesi. 3th Global Conference on Engineering Research.

[2] Dündar , A. (2022). Debriyaj Sistemlerinde Yastıklamalı Yay Üretim Prosesinin Araç Konforuna Etkisinin İncelenmesi. Bursa Uludağ Üniversitesi.

[3] Şenol, S., Yıldız, Ö., & Eş, C. (2023). Debriyaj Kafesi Tasarım Optimizasyonu ve Validasyonu. 3th Global Conference on Engineering Research.

[4] Savran, E., Vargelci, S., Catenaro, L., & Karpat, F. (2023). Bir otomobil braket tasariminin analizi ve değerlendirmesi. Uludağ Üniversitesi Mühendislik Fakültesi Dergisi, 28(2), 493-506.

[5] Deveci, Ö. O. (2020). Binek araç koltuk kızak bağlantı braketinin tasarımı ve ürün testlerinin gerçekleştirilmesi (Master's thesis, Bursa Uludag University (Turkey)).

[6] Stéphan, P., Mathurin, F., & Guillot, J. (2011). Analytical study of maximal tapping torque during forming screw process. Journal of Materials Processing Technology, 211(2), 212-221.

[7] Guillot, J., Stéphan, P., & Daidié, A. (2009). 3D Finite Element Modeling of an Assembly Process With Thread Forming Screw. Journal of Manufacturing Science and Engineering, 131, 041015-1.

[8] Stéphan, P., Mathurin, F., & Guillot, J. (2012). Experimental study of forming and tightening processes with thread forming screws. Journal of Materials Processing Technology, 212(4), 766-775.

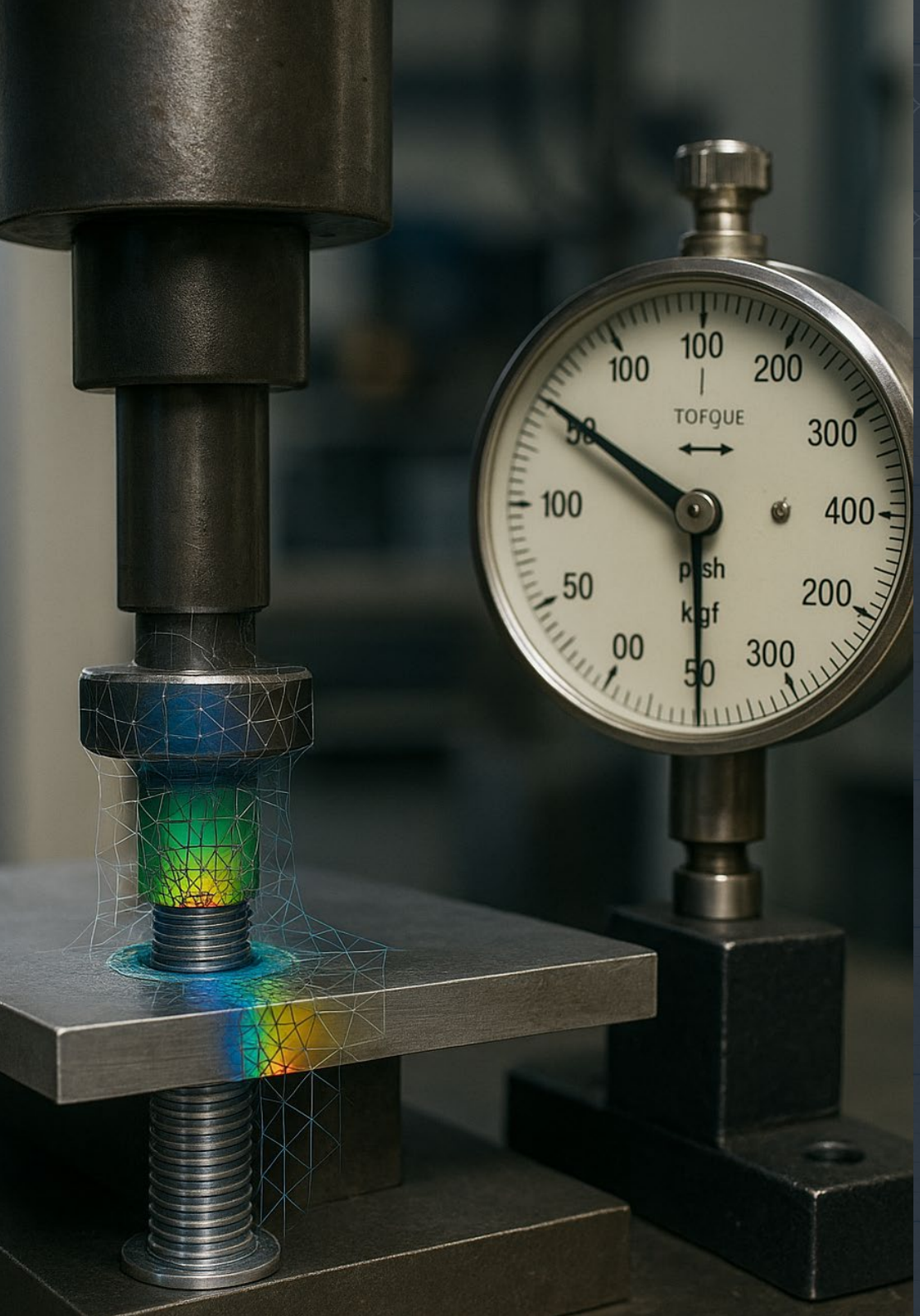

ÇAKMA CIVATALARIN PERFORMANS TESTLERİNİN SONLU ELEMANLAR PROGRAMIYLA İNCELENMESİ

Kağan DEMİRTAŞ
Tolga AYDIN
Umut İNCE

6. Ulusal Üniversite-Sanayi İşbirliği, Ar-Ge ve İnovasyon Kongresi

ÇAKMA CIVATALARIN PERFORMANS TESTLERİNİN SONLU ELEMANLAR PROGRAMIYLA İNCELENMESİ

KAĞAN DEMİRTAŞ[1], TOLGA AYDIN[1], UMUT İNCE[1]

[1]Norm Cıvata San. ve Tic. A.Ş. Ar-Ge Merkezi, AOSB, Çiğli, İzmir, Türkiye
Email*: kagan.demirtas@normfasteners.com

Özet

Çakma cıvatalar, kaynak cıvatalarına alternatif olarak otomotiv sektörü başta olmak üzere birçok endüstriyel alanda kullanılan, mekanik kilitleme sağlayarak çalışan bir bağlantı elemanı olarak öne çıkmaktadır. Kaynak cıvatalarının montajında, kaynak bölgesindeki ısıl girdi sonucu oluşan iç gerilmeler, sac metaldeki çarpılmalar, proses sırasında cıvata dişlerine cüruf sıçrama durumu ve kaynak ekipmanı gereksinimi gibi dezavantajlar bulunmaktadır. Çakma cıvataların sıralanan dezavantajların üstesinden gelmesi sebebiyle her geçen gün kullanımı artış göstermektedir.

Çakma cıvataların incelenen temel performans parametreleri, cıvatanın kullanım yerine bağlı olarak, sac metal - çakma cıvata bağlantısının radyal ve eksenel yüklere karşı gösterdiği dirençtir. Bu parametrelerin ölçülmesi amacıyla literatürde tork dayanımı ve itme dayanımı testleri mevcuttur. Çalışma kapsamında belirlenen bir çakma cıvatanın sac metale montaj işlemi ve ardından performans testleri deneysel olarak gerçekleştirilmiştir. Ardından montaj işlemi ve performans testleri Simufact Forming sonlu elemanları programı ile modellenerek deneysel veriye yakınsayan simülasyon modelinin elde edilmesi amaçlanmıştır. Simülasyon modelindeki değişkenlerin simülasyon sonucuna etkileri incelenirken aynı zamanda test cihazındaki kompliyans parametresinin sonuçlara olan etkisi göz önünde bulundurulmuş, dikkate alınmadığı takdirde karşılaşılacak fark raporlanmıştır. İteratif simülasyon çalışmaları sonucunda nihai olarak simülasyon modeli ile test verisinin birbirine yakınsadığı gözlemlenmiştir. Çalışma sonucunda herhangi bir çakma cıvatanın mukavemeti bilinen sac metal malzemesine çakılması işlemindeki kritik değer olan çakma kuvvetinin ve performans değerlerinin simülasyon ortamında hassas bir şekilde ve doğrulukla öngörülebilmesi mümkün olmuştur.

Anahtar Kelimeler: Çakma cıvata, sayısal benzetim, kompliyans

1. Giriş

Piyasada, özellikle otomotiv endüstrisinde, sac metallerle birlikte kaynak cıvataları sıklıkla kullanılmaktadır. Kaynak cıvatalarının kullanım amacı, bağlantı elamanlarından bir tanesinin kaynak işlemi ile sabit hale getirilip diğerinin montajını kolaylaştırmaktır. Sac metale kaynaklanan bu tip cıvataların en büyük dezavantajı, kaynaklanan bölgede yüksek ısıl girdi sebebiyle oluşan iç gerilmeler ve proses sırasında cıvata dişlerine cüruf sıçrama ihtimalidir. Bu ve buna benzer dezavantajlar sebebiyle günümüzde kaynak cıvatalarına alternatif olarak sac metaller ile birlikte otomotiv başta olmak üzere çeşitli endüstriyel alanlarda çakma cıvatalar kullanılmaktadır. Literatürdeki tanımına göre kendi kendine sabitlenen bağlantı elemanları olarak çakma cıvata, şaft çapı bağlantı elemanının baş kısmından daha küçük olan bir sac metale bağlantı için uygun bir çözüm sunmaktadır. Çakma cıvataları temel olarak sac metalde önceden açılan belirli çaptaki deliklere yerleştirilmektedir[1].

Bahsedilen uygulama uygun bir pres aracılığı ile cıvata kafasına kuvvet uygulanması şeklinde gerçekleştirilmektedir. Pres ile cıvata kafasına uygulanılan kuvvet sonucunda plaka malzemesi çakma cıvata geometrisindeki açıklıklara plastik şekillenerek dolmaktadır. Sac metaldeki bu plastik şekillenme sayesinde mekanik kilitleme sağlayan bir bağlantı sağlanmış olmaktadır. Bir sac metale sabitlenen bağlantı elemanlarının tasarımında, bu elemanların düzgün bir şekilde monte edildiğinde ana malzeme içinde dönmesini önleyecek tasarım özellikleri bulunmaktadır. Örneğin, tork dayanımını artırmak için tırtıklı sabitleme halkası gibi özellikler, döner kuvvetlere karşı dayanımı iyileştirirken itme dayanımını da artırmaktadır. Bu nedenle, kendi kendine sabitlenen bağlantı elemanları monte edildikleri şasi, panel, braket veya diğer bileşenlerin kalıcı bir parçası haline gelmektedir [1].

Kendi kendine sabitlenen bağlantı elemanları konusunda literatürde bulunan bir çalışmada bu tip bir bağlantı elemanı tasarımı gerçekleştirilmiştir. Bu tasarımda tasarım unsurlarının yüksekliği, çapı, ve derinliği gibi parametreler kontrol faktörleri olarak belirlenmiştir. Tasarımın ardından Taguchi Yöntemi'nin ortogonal dizilim tablosu ve sonlu elemanlar analizi (FEA) kullanılarak yapılan simülasyonlarda, bağlantı elemanının sac metal malzemeye yerleşmesi esnasında malzeme doluluk oranını en çok etkileyen parametrelerin sırasıyla lob yüksekliği, oluk yüksekliği, lob çapı ve oluk derinliği olduğu tespit edilmiştir. Maksimum şekillendirme yükü üzerinde en etkili parametrenin oluk yüksekliği olduğu belirlenmiş, ancak bu yükü minimize eden kombinasyonun bağlantı elemanının işlevselliği açısından yeterli olmadığı görülmüştür. Optimum tasarım kombinasyonu olarak 2 mm oluk yüksekliği, 23 mm lob çapı, 1.5 mm lob yüksekliği ve 0.25 mm oluk derinliği seçilmiş ve bu tasarımın yüksek tork direnci ve birleşme gücünü sağladığı sonucuna ulaşılmıştır [2].

Kendi kendine sabitlenen bağlantı elemanlarının çalışma koşulları altında güvenilirliğini denetlemek için üç test uygulanabilmektedir: tork dayanım testi, itme dayanım testi ve çekme dayanım testi [1]. İtme dayanımı testi çakılmış olan cıvataya eksenel yönde, çakma işlemi sırasında uygulanan kuvvetin ters yönünde bir yük uygulanarak gerçekleştirilmektedir. Test sırasında cıvata, yerleştirildiği delikten çıkana kadar kuvvet artırılmaktadır. İtme dayanımı testi sonucunda elde edilen maksimum kuvvet değeri, cıvata-panel bağlantısının itme dayanımı dayanımını ifade etmektedir. Tork dayanımı testi cıvata-panel bağlantısının dayanabileceği maksimum tork değerini belirlemek amacıyla gerçekleştirilen bu testte, cıvataya belirli bir aparat aracılığıyla tork uygulanmaktadır [1]. Test sırasında ölçülen en yüksek tork değeri, bağlantının tork dayanımı dayanımını temsil etmektedir. Plaka malzemesi ile çakma cıvata arasında plastik şekillenme ile sağlanan bu bağlantıdan bahsedilen performans değerleri farklı bağlantı koşullarına göre hesaplanmaktadır.

Bu bağlamda, çakma cıvata üretimini gerçekleştiren firmalar tarafından çakma işleminin ve performans testlerinin doğru bir şekilde nasıl gerçekleştirilmesi gerektiğine dair çalışmalar gerçekleştirilmiştir. Şekil 1 a, b ve c'de sırasıyla çakma, çıkartma ve tork direnci testlerinin şematik gösterimleri görülebilmektedir. Mevcut çalışmalar bahsi geçen bağlantının testlerinin gerçekleştirilmesine yönelik olup bu testlerin bilgisayar ortamında paket programlar aracılığı ile sayısal benzetimi konusunda ciddi bir bilgi ve deneyim eksikliği bulunmaktadır. Bu doğrultuda doğrulanmış bir simülasyon modeli geliştirilmesi, farklı cıvata ve sac metal kombinasyonları ile gerçekleştirilen bağlantıların performans değerlerinin testlere ihtiyaç duymadan bilgisayar ortamında tahminlenmesinin önünü açmaktadır.

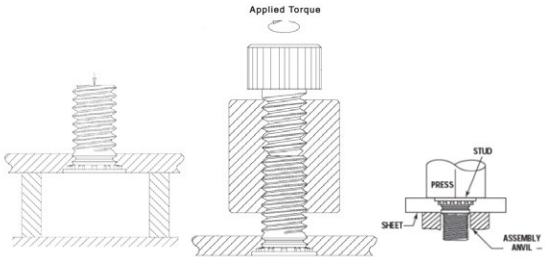

Şekil 1. Performans testleri (a) İtme dayanımı Testi, (b) Tork dayanımı Testi, (c) Çakma İşlemi [4]

Bu çalışma, çakma cıvata bağlantılarının çakma kuvveti ve performans değerlerinin sonlu elemanlar yöntemi kullanarak incelenmesini konu almakta ve en verimli modeldeki sınır koşullarının elde edilmesini amaçlamaktadır. Çalışmada, öncelikle referans bir çakma cıvata belirlenip bu cıvatanın çakılacağı sac metal panel ile birlikte deneysel testler gerçekleştirilmiş, ardından sonlu elemanlar çalışmasının sonuçları deneysel test verileriyle kıyaslanmıştır.

2. Materyal ve Metot

2.1 Testlerin Gerçekleştirilmesi

Çakma cıvataların performans verilerini denetlemek amacıyla sonlu elemanlar modelleri geliştirilmesi kapsamında öncelikle testler gerçekleştirilmiştir. Test verilenin ışığında simülasyon modelleri kurgulanmış ve kalibre edilmiştir. Bu doğrultuda çakma işlemi, tork dayanımı ve itme dayanımı testlerinin gerçekleştirilmesinde kullanılmak üzere gerekli ekipmanlar belirlenmiş ve temin edilmiştir. Çakma işlemi ve test süreçlerinde kullanılan ekipmanlar şu şekilde sıralanmaktadır: çakma işlemi için kullanılan referans çakma cıvata, cıvatanın montajının yapıldığı sac metal panel, çakma işleminde paneli desteklemek amacıyla kullanılan alt kalıp, İtme dayanımı testinde paneli destekleme işlevini üstlenen alt kalıp ve tork dayanımı testi için özel olarak tasarlanmış, cıvataya bir şaft aracılığıyla tork uygulanmasını sağlayan aparat. Bahsi geçen tüm test ekipmanları, Şekil 1'de gösterilmektedir.

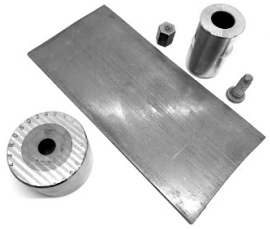

Şekil 2. Testlerde kullanılan ekipmanlar

Referans çakma cıvata ürünü olarak Norm Holding patentli çakma cıvatası olan 10.9 kalitedeki M12x47 FastiNorm® seçilmiştir. Panel malzemesinin belirlenmesi ve boyutlandırılmasında ise dikkate alınan temel parametreler; cıvataların panel üzerinde çakılacağı deliklerin sayısı, delik çapları ve delik merkezleri arasındaki mesafedir. Panel boyutlarının belirlenmesinde delikler arasındaki mesafe, çakma prosesi sırasında oluşabilecek deformasyon riskini minimize etmek

amacıyla önemli bir kriter olarak değerlendirilmiştir. Delik merkezlerinin birbirine çok yakın olması durumunda, çakma işlemi sırasında bir deliğin yanındaki diğer delik deformasyona maruz kalabilmektedir. Bu nedenle delikler arasındaki minimum mesafe, tavsiye edildiği üzere 2d+1 (d: delik çapı) formülüyle hesaplanmış ve en az 27 mm olarak belirlenmiştir. Ancak, çakma işlemi sırasında panelin altında kullanılacak alt kalıbın (alt kalıp) boyutları göz önüne alınarak delikler arasındaki mesafe 40 mm olarak tasarlanmıştır. Sac metal panel üstünde cıvatanın yerleşeceği deliklerin çapı ise referans olarak seçilen çakma cıvatanın unsurlarının çapı gözetilerek 13mm olarak belirlenmiştir.

Panel seçiminde dikkate alınan diğer bir önemli unsur ise sertlik değeridir. Çakma işlemi sırasında cıvatanın unsurlarında deformasyon oluşmaması için panel sertliğinin, cıvata sertliğinden daha düşük olması gerekmektedir. Panel sertlik değerinin belirlenmesinde, piyasada bulunan çakma cıvata ürünlerinin teknik veri dokümanları ve otomotiv firmalarının şartnameleri referans alınmıştır. Bu dokümanların incelenmesi sonucunda, tüm üreticiler tarafından panel sertliği için 147 HV veya daha düşük değerlerin uygun olduğu belirtilmiştir [3]. Panel malzemesinin sertliği ve diğer özellikleri, bahsedilen kriterler doğrultusunda 5 mm et kalınlığına, 200 HV sertlik değerine ve C45 çelik malzeme özelliklerine sahip olacak şekilde belirlenmiştir. Şekil 3'te kullanılan sac metal panelin teknik resmi görülebilmektedir.

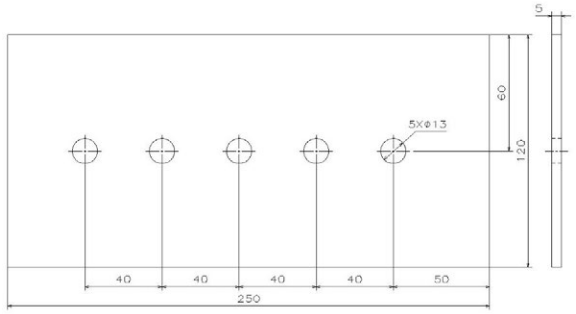

Şekil 3. Çakma cıvataların çakılacağı sac metalin teknik resmi

Çakma testi, ilerleme kontrollü bir yöntem kullanılarak gerçekleştirilmiştir. İlerleme kontrollü testin tercih edilmesinin temel nedeni, test sırasında cıvatanın kafa altının panelin üst yüzeyine temas ettiği noktada işlemi sonlandırmaktır. Test programının hazırlanması aşamasında, ilerleme verisi test cihazına manuel olarak girilmiştir. Çakma testi ve test tamamlandıktan sonra elde edilen panel ve cıvata durumu Şekil 4 ve Şekil 5'te sunulmaktadır.

Şekil 4. Çakma testi düzeneği

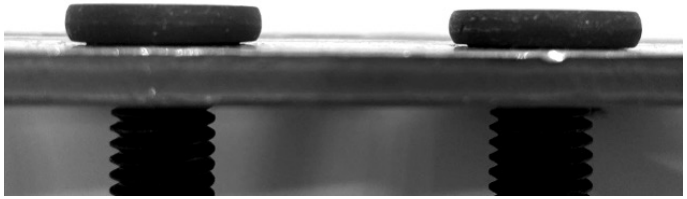

Şekil 5. Cıvataların sac metal panele çakıldıktan sonraki görüntüsü

Şekil 4'te gösterilen test düzeneği kullanılarak toplamda 5 çakma testi gerçekleştirilmiştir. Cıvatanın sac metal panele doğru bir şekilde yerleştirilebilmesi için uygulanan yükün, test cihazının üst çenesinin ilerleme mesafesine bağlı olarak değişimi Şekil 6'da sunulmuştur. Şekil 6'daki grafikte, "Test 1" adıyla gösterilen eğri dikkate alınmamış ve diğer testlerin ortalamaları alınarak bir ortalama eğri oluşturulmuştur. Çakma kuvveti, grafikte görülen ortalama test sonucunun son strok değerindeki kuvvet olarak tanımlanmıştır. Bu doğrultuda, çakma kuvveti, 3,67 mm strok değerinde 116,80 kN olarak belirlenmiştir.

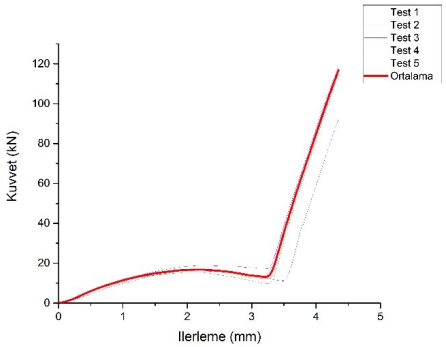

Şekil 6. Çakma testi sonuçları

Çakma testlerinin tamamlanmasının ardından, kurgulandığı üzere çakılan cıvatalara itme dayanımı testi yapılması amacıyla testler için gerekli düzenek kurulmuştur. İtme dayanımı testlerinde, çakma testlerinde kullanılan aynı test düzeneği tercih edilmiştir. Bu doğrultuda, Şekil 7'de gösterildiği şekilde testler gerçekleştirilmiştir. İtme dayanımı testi 5 farklı bağlantıya uygulanmıştır.

Şekil 7. İtme dayanımı testi düzeneği

Çakma cıvatalarında, beklenen durum, cıvatanın minimum deformasyon ile panel malzemesini deforme etmesidir. İtme dayanımı testi sonrasında cıvatanın unsurlarındaki deformasyon seviyesi kontrol edilmiş ve deformasyonun istenilen seviyede kaldığı belirlenmiştir.

İtme dayanımı test sonuçları, eksenel bası yükünün test cihazının üst çenesinin ilerleme mesafesine bağlı olarak değişimini göstermektedir ve bu değişim Şekil 8'de sunulmaktadır. Kırmızı eğri, yapılan 5 testten 4'ünün ortalamasını yansıtmaktadır; "Test 5" ortalamaya dahil edilmemiştir. İtme dayanımı değeri, cıvatanın hangi kuvvet ile çakıldığı delikten çıkacağını ifade eden kuvvet değeri olarak tanımlanmakta olup, bu değer "Ortalama" isimli eğriden okunmuştur. Eğrinin maksimum kuvvet değeri, İtme dayanımı değeri olarak kabul edilmiştir ve bu değer 0,32 mm ilerleme değeri için 12,44 kN olarak belirlenmiştir.

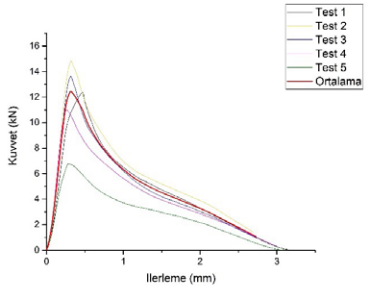

Şekil 8. İtme dayanımı testi sonuçları

Çakma ve İtme dayanımı testleri tamamlandıktan sonra, çalışma kapsamındaki son test olan tork dayanımı testi gerçekleştirilmiştir. Literatürde tanımlandığı şekilde, bu test, cıvatanın panel üzerine sabitlenmesinin ardından, cıvatanın şaft kısmına tork uygulanarak yapılmıştır. Bahsedilen torkun uygulanmasında, yüksek hassasiyetli bir cihaz olan Atlas Copco ST Wrench kullanılmıştır.

Test öncesinde, cıvatanın çakıldığı panel, bir mengene aracılığıyla sıkıştırılarak sabitlenmiş ve ardından test aparatı cıvataya yerleştirilmiştir (Şekil 9). Diğer testlerde olduğu gibi, Tork dayanımı testi de 5 numune üzerinde gerçekleştirilmiş olup, test sonuçları uygulanan torkun, sıkıcının taradığı açıya bağlı olarak değişimi şeklinde Şekil 10'da sunulmuştur.

Şekil 9. Tork dayanımı testi

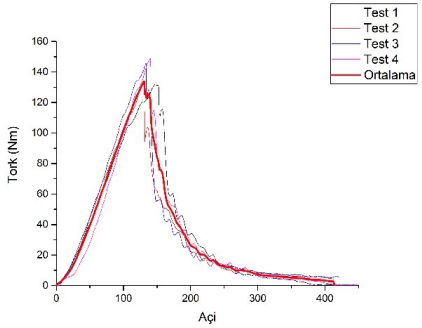

Şekil 10. Tork dayanımı testi sonuçları

2.3 Sonlu Elemanlar Analizi Çalışmaları

Çakma, İtme dayanımı ve tork dayanımı testleri gerçekleştirildikten sonra, simülasyon çalışmaları başlatılmıştır. Çakma prosesinin simülasyonu, çalışmanın en kritik aşaması olup, elde edilen veriler doğrultusunda itme dayanımı ve tork dayanımı simülasyonlarına yön verilecektir. Çakma işleminin simülasyonunun doğru bir şekilde yapılabilmesi için kritik faktörler arasında, malzeme modelinin doğru bir şekilde tanımlanması, cıvatanın geometrisinin ölçümlerle uyumlu şekilde modellenmesi, sürtünme modelinin belirlenmesi ve simülasyon modelinin titizlikle hazırlanması yer almaktadır.

Simülasyon çalışmalarında kullanılan malzeme modeli, deneysel olarak gerçekleştirilen testler sonucunda elde edilen verilere dayanmaktadır. Panel malzemesinin akış özellikleri, sabit strain rate (0,001 1/s) ve değişken sıcaklık değerleri altında belirlenmiştir. Sıcaklık aralıkları olarak 25°C, 50°C, 100°C, 150°C ve 200°C değerleri belirlenmiş ve bu sıcaklıklar altında malzemenin akış eğrileri çıkarılmıştır. Elde edilen akış eğrileri, Şekil 11'de görsel olarak sunulmaktadır.

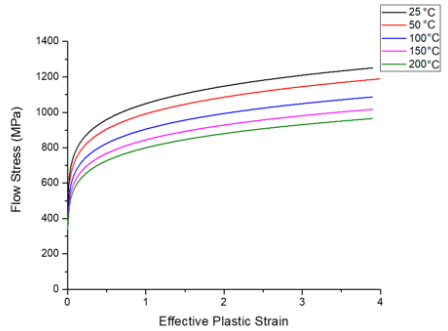

Şekil 11. Sac metal malzemesi için oluşturulan akış eğrileri

Malzeme modelinin oluşturulmasının ardından testlerde kullanılan geometriler modellenmiştir. Çalışma kapsamında gerçekleştirilen tüm simülasyonlarda katı modeller, cıvata geometrisi dikkate alınarak, 90 derece simetrik olacak şekilde modellenmiştir. Gerçekleştirilen simülasyon, plastik şekillenme sürecini modelleyen bir çalışmadır ve bu süreçte şekillenen yapı, iş parçası olarak tanımlanan sac metal panel malzemesidir. Simülasyonda, alt kalıp ve çakma cıvata rijit elemanlar olarak, panel ise iş parçası olarak tanımlanmıştır. Panel geometrisinin çevresine, iç çap ölçüsü panelin dış çap ölçüsüne eşit olan rijit bir halka (ring) yerleştirilmiştir. Bu halkanın amacı, çakma işlemi sırasında meydana gelen deformasyon esnasında panel malzemesinin radyal yöndeki deformasyonunu sınırlandırmaktır. Tüm geometriler, simülasyon ortamında Şekil 11'de görüldüğü şekilde konumlandırılmıştır. İş parçası olan panel malzemesine ait ağ yapısı, yüksek doğruluk elde etmek amacıyla hexahedral eleman tipi kullanılarak oluşturulmuştur. Bu ağ ağ yapısı da Şekil 11'de detaylı olarak gösterilmektedir.

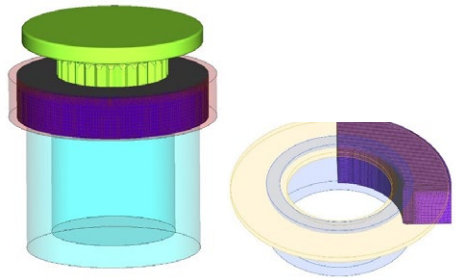

Şekil 11. Çakma simülasyonu öncesi yerleşim ve ağ yapısı

Belirtilen sınır koşullarında gerçekleştirilen simülasyonlarda Şekil 12'deki Kuvvet-İlerleme değerleri elde edilmiştir.

Gerçekleştirilen simülasyonun sonuçları değerlendirildiğinde, çakma işleminin başlangıç aşamasında ve tırtır boyunca ilerleyen grafiğin ilk kısmında, simülasyon sonuçlarının tutarlı ve yakınsak olduğu görülmektedir. Ancak, cıvatanın kafa altı uzvunun panel malzemesiyle temas ettiği ve kuvvetlerin daha keskin bir şekilde artış gösterdiği ikinci kısımda, simülasyon sonuçlarının test verilerinden belirgin şekilde sapma gösterdiği tespit edilmiştir.

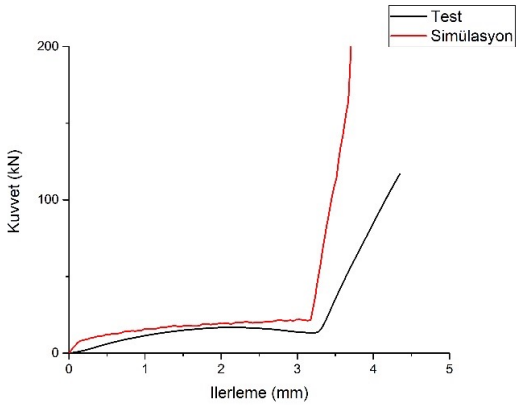

Şekil 12. Gerçekleştirilen simülasyon sonuçları ile test sonuçlarının karşılaştırması

Simülasyon verilerindeki bu farkın, cıvatanın rijit olarak modellenmesinden kaynaklandığı değerlendirilmiştir. Bu doğrultuda cıvata, elastoplastik olarak modellenip simülasyon tekrar edilmiştir. Söz konusu düzenleme sonrasındaki sonuçların deneysel test verileri ile karşılaştırılması Şekil 13'te sunulmaktadır.

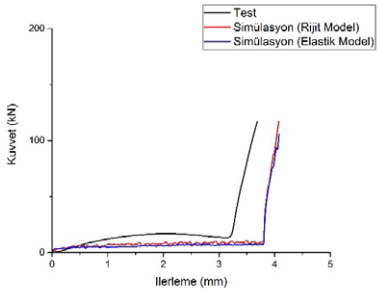

Şekil 13. Rijit ve elastoplastik cıvata ile gerçekleştirilen simülasyonun test sonuçları ile karşılaştırılması

Sonuçlardan da görülebileceği gibi cıvatanın deforme edilebilir olup olmamasının sonuçlara belirgin bir etkisi yoktur. İlave olarak elastoplastik modellenmiş cıvata ile çalışmak simülasyon süresini oldukça uzatmaktadır. Bu koşullar altında çalışmalara rijit cıvata modeli ile devam edilmiştir. Simülasyon sonuçları ile test sonuçlarının özellikle kafa altı uzvun panele temasının başlamasından sonrasını ifade eden grafiğin ikinci kısımda ıraksaması problemini çözmek için farklı çözüm yolları değerlendirilmiştir. Bu sebeple test koşulları ve test cihazı ele alınmış, burada bir hata meydana gelip gelmediği sorgulanmıştır.

Mekanik testler sırasında deformasyonun gözlendiği parçalar yalnızca test numuneleri değildir. Bir test makinesi kuvvet uygulandığında, tüm sistem -çerçeve, yük hücresi, tutucular, bağlantılar ve numune- belirli bir dereceye kadar elastik deformasyona uğramaktadır. Diğer bir deyişle test esnasında test cihazı sabit katsayılı lineer bir yay gibi davranır. Test yazılımı yer değiştirmeyi ölçerken, ham yer değiştirme verisini alır, bu da ölçülen yer değiştirmenin aslında toplam sistem deformasyonunun toplamı olduğu anlamına gelmektedir. Sadece numunenin yer değiştirmesini belirlemek için,

makinenin kompliyans değeri (yük çerçevesi, yük hücresi ve tutucuların neden olduğu deformasyonlar) bu ölçümden çıkarılmalıdır. Yer değiştirmeyi ölçmek için ekstansometre kullanımı, daha doğru bir çözümdür çünkü ölçümler doğrudan numuneden alınmaktadır. Proje kapsamında gerçekleştirilen test koşullarında ekstansometre kullanılamamıştır. Ekstansometreler kullanılamadığında, daha doğru yer değiştirme ölçümleri elde etmek için kompliyans yapılmış ölçüm değerleri kullanılmalıdır. Bu bağlamda bahsedilen işlemin testler esnasında kullanılan test cihazında ve sonuçlarda gerçekleştirilmesine karar verilmiştir.

Öncelikle test cihazının çeneleri birbirlerine temas edecek şekilde yerleştirilmiş ve test cihazı belirli bir yüke kadar bası yönünde çalıştırılmıştır. Bu halde yapılan test sonucunda Şekil 14'de görülen kuvvet-yer değiştirme grafiği elde edilmiştir. Bu grafik bize belirli yük altında makinenin bileşenlerinin yer değiştirme miktarını vermektedir. Ardından bu eğriye lineer fit uygulanmış ve eğimi alınmıştır.

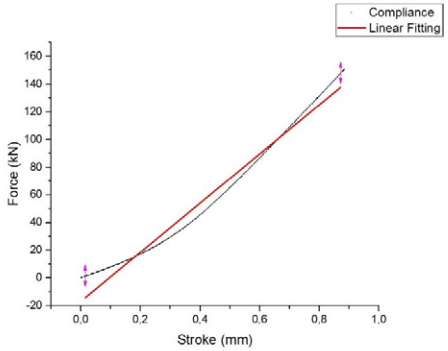

Şekil 14. Çeneleri boş şekilde basılmış test cihazından alınan eğri

Test sonuçlarının yer değiştirme verilerine yapılan işlemler şu şekildedir:

$$\tan\alpha = K = \frac{F}{\delta_C} \tag{1}$$

$$\delta_C = \frac{F}{K} \tag{2}$$

$$\delta_S = \delta_R - \delta_C \tag{3}$$

δ_S, δ_R ve δ_C sırasıyla numunenin deformasyonu, makinenin test sonrasında verdiği toplam deformasyon ve test cihazının kendi bileşenlerinin deformasyonudur.
Kompliyans uygulaması ile elde edilen deformasyon sonuçlarını ve simülasyon verilerini içeren grafik, Şekil 15'de sunulmaktadır. Grafik incelendiğinde, kompliyans uygulamasının test verilerinin özellikle ikinci kısmındaki eğimi belirgin bir şekilde değiştirdiği gözlemlenmiştir. Bu aşamada eğimin artmasıyla birlikte, test sonuçlarının simülasyon verileriyle önemli ölçüde uyumlu ve yakınsak bir hale geldiği tespit edilmiştir.

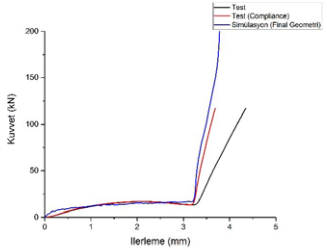

Şekil 15. Kompliyans uygulanmış test sonuçları ile simülasyon verilerinin karşılaştırması

Elde edilen sonuçlar değerlendirildiğinde, test verilerinin son strok değerine karşılık gelen kuvvet değeri ile simülasyon sonuçlarının tam anlamıyla istenilen düzeyde örtüşmediği görülmektedir. Bu grafiklerden elde edilen en önemli parametre, test verisindeki son strok değerine karşılık gelen çakma kuvvetidir.

Simülasyon verilerinin test sonuçlarına daha fazla yakınsamasını sağlamak amacıyla sürtünme modeli yeniden ele alınmış ve kombine bir sürtünme modeli kurgulanmıştır. Bu yeni sürtünme modeli ile elde edilen nihai sonuçlar Şekil 16'da sunulmaktadır. Bu aşamada, çakma simülasyonunun test verileriyle önemli ölçüde uyum sağladığı ifade edilebilir. Gerçekleştirilen çakma testlerinde, 3,67 mm strok değerine karşılık gelen çakma kuvveti 116,80 kN olarak ölçülmüştür. Simülasyon sonuçlarında ise aynı strok değerinde 126 kN çakma kuvveti elde edilmiştir.

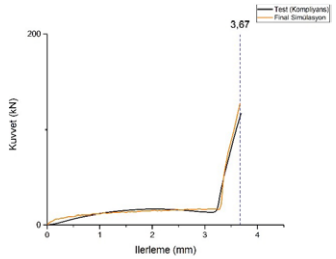

Şekil 16. Final simülasyonu ile test sonuçlarının karşılaştırılması

Çakma simülasyonunun başarıyla tamamlanmasının ardından, itme dayanımı testi simülasyonu kurgulanmıştır. Çakma simülasyonunda elde edilen veriler, doğrudan İtme dayanımı simülasyonuna aktarılmıştır. Bu aşamada, çakma simülasyonundan farklı olarak yalnızca uygulanan kuvvetin yönü tersine çevrilmiş, diğer tüm simülasyon parametreleri ve ayarları sabit tutulmuştur.

İtme dayanımı simülasyonundan elde edilen sonuçların test verileri ile karşılaştırması Şekil 17'de sunulmaktadır. Test sonuçlarına göre 12,44 kN olarak ölçülen İtme dayanımı değeri, simülasyon sonuçlarında 11,82 kN olarak elde edilmiştir. Şekil 17'de görüldüğü üzere, simülasyon verileri test sonuçlarının ortalaması ile büyük ölçüde örtüşmekte ve kesikli çizgi ile gösterilen bireysel test sonuçlarının sınırları içinde kalmaktadır.

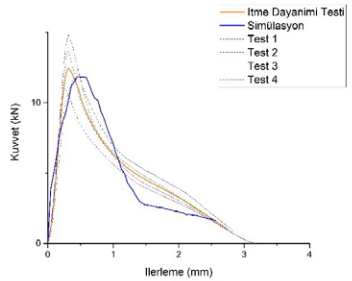

Şekil 17. İtme dayanımı simülasyonu ile test verilerinin kaşılaştırılması

Çalışmanın son aşamasında Tork dayanımı testinin simülasyonu gerçekleştirilmiştir. Simülasyonun tamamlanmasının ardından, test sonuçları ve simülasyon verileri Şekil 18'de sunulan grafikte karşılaştırılmıştır. Grafikte görüldüğü üzere, maksimum değer olan Tork dayanımı değeri test sonuçlarında 133,85 Nm olarak ölçülmüş, simülasyon sonuçlarında ise bu değer 136,46 Nm olarak elde edilmiştir. Bu sonuçlar, simülasyon verilerinin Tork dayanımı değerine başarıyla yakınsadığını göstermektedir.

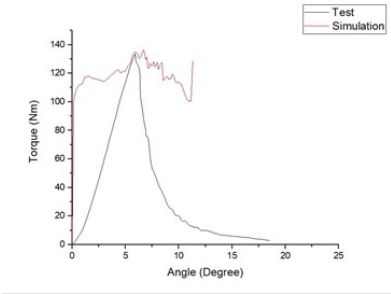

Şekil 18. Tork dayanımı testlerinin sonuçları ile simülasyon sonuçlarının karşılaştırması

3. Sonuçlar

Bu çalışma kapsamında elde edilmesi hedeflenen en önemli çıktı, herhangi bir çakma cıvatanın belirli sertlik ve mukavemet değerlerine sahip panel malzemesine çakılması sırasında kritik öneme sahip çakma kuvvetinin yanı sıra itme dayanımı ve tork dayanımı gibi performans parametrelerinin simülasyon ortamında hassasiyet ve doğrulukla öngörülebilmesidir. Çalışma, ileride gerçekleştirilecek araştırmalara rehberlik edecek nitelikte olup, çakma işleminin belirli koşullar altında modellenmesine dair kapsamlı bir yöntem sunmaktadır.

Teşekkür

Yazarlar, bu bilimsel araştırmanın her aşamasına sağladıkları katkı ve desteklerinden ötürü Norm Holding firmalarına teşekkür eder.

References

[1] DAUD, N. A. M. (2019). EFFECT OF HOLE SIZE, SHEET THICKNESS AND MATERIAL TYPE TO THE PERFORMANCE OF THE SELF-CLINCHING FASTENER (Doctoral dissertation, Universiti Sains Malaysia).

[2] Byun, H.-S., & Kim, G.-Y. (2013). Optimization design of the clinch stud using the finite element analysis and the Taguchi method. Journal of the Korea Academia-Industrial Cooperation Society, 14(7), 3135-3141. https://doi.org/10.5762/KAIS.2013.14.7.3135

[3] PennEngineering. (2022). FH™ self-clinching studs and pins datasheet. Retrieved from https://www.pemnet.com

[4] PennEngineering. (2019). Testing clinch performance. Retrieved from https://www.pemnet.com

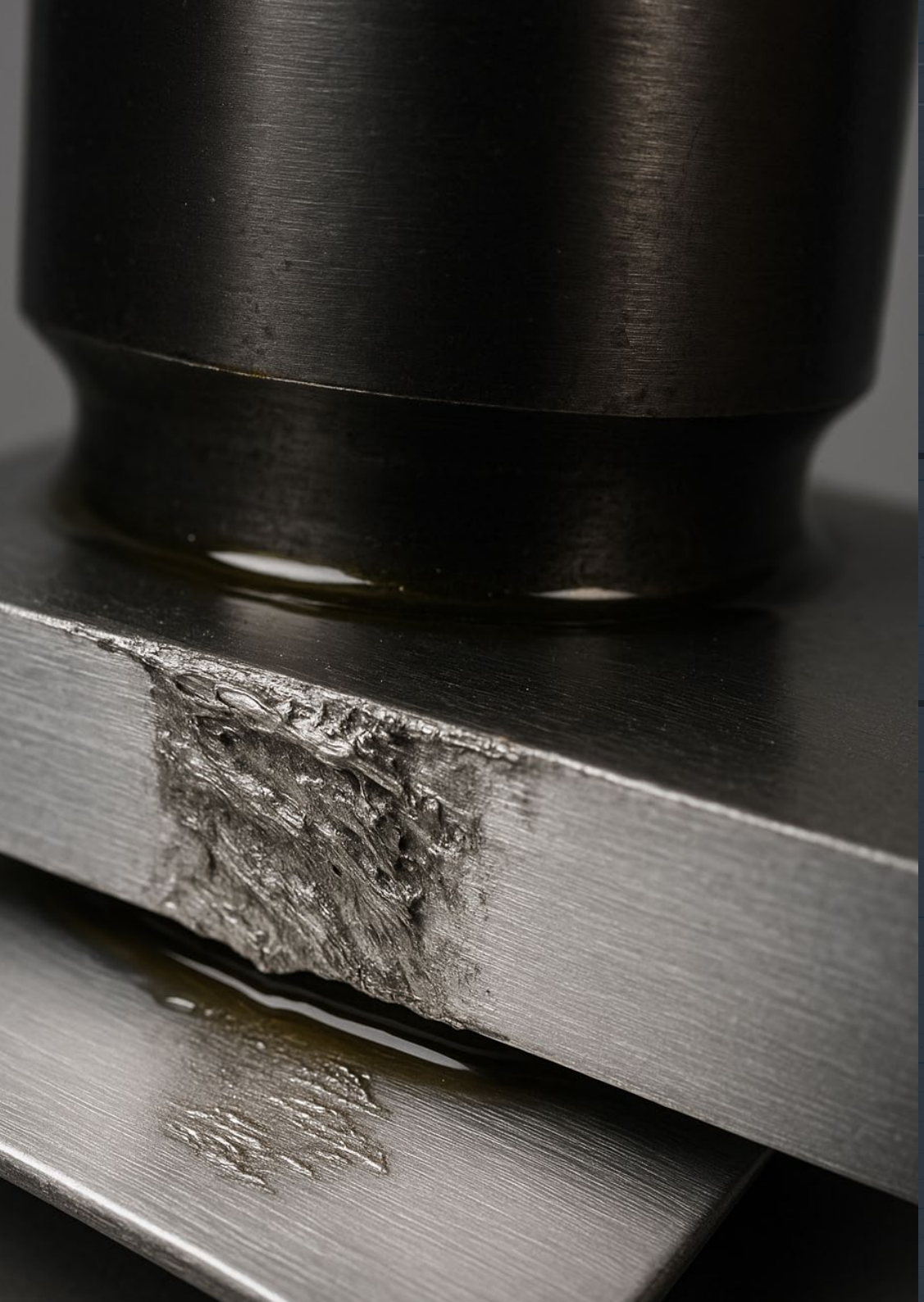

A REVIEW ON GALLING OF ALUMINUM IN COLD FORMING PROCESSES

Hatice SANDALLI YILDIZ
Mert ÖZDOĞAN

Düzce Üniversitesi Bilim ve Teknoloji Dergisi

A REVIEW ON GALLING OF ALUMINUM IN COLD FORMING PROCESSES

Hatice SANDALLI YILDIZ1[a,*], Mert SANDALLI[a]

[1]Norm Fasteners Co., Izmir, TURKEY
[*]Corresponding author's e-mail address: hatice.sandalli@normfasteners.com

Abstract

As world's sustainability becomes the most influential topic, aluminum and its alloys are becoming the preferred material of the automotive industry because they allow vehicle weight to be reduced without compromising safety. Thus, aluminum has taken its place in the global industry as an alternative material that can be used instead of steel. The main drawback of forming aluminum at room temperature is galling. This phenomenon in cold forming of aluminum not only affects the quality of the produced parts but also the lifespan of production tools. This paper reviews the galling of aluminum alloys during bulk and sheet cold forming processes along with friction conditions. The available testing methods in order to simulate the actual cold forming process are introduced. Effect of process parameters such as lubrication, tool surface finish and tool coatings are discussed in detail.

Keywords: Galling, Aluminum alloys, Cold forming

SOĞUK ŞEKİLLENDİRME PROSESLERİNDE ALÜMİNYUMUN YAPIŞMA AŞINMASI ÜZERİNE BIR İNCELEME

Özet

Sürdürülebilirlik dünyanın en etkili konusu haline gelirken, alüminyum ve alaşımları, güvenlikten ödün vermeden araç ağırlığının azaltılmasına olanak sağladığı için otomotiv sektörünün tercih edilen malzemesi haline gelmektedir. Böylece alüminyum çelik yerine kullanılabilecek alternatif bir malzeme olarak küresel endüstride yerini almaktadır. Alüminyumun oda sıcaklığında şekillendirilmesinin ana dezavantajı adhesiv aşınmadır. Alüminyumun soğuk şekillendirilmesindeki bu olay, yalnızca üretilen parçaların kalitesini değil, aynı zamanda üretim takımlarının ömrünü de etkiler. Bu çalışmada, sürtünme koşullarıyla birlikte kütlesel ve sac soğuk şekillendirme işlemleri sırasında alüminyum alaşımlarının adhesiv aşınmasını incelemektedir. Gerçek soğuk şekillendirme sürecini simüle etmek için mevcut test yöntemleri tanıtılmaktadır. Yağlama, takım yüzey kalitesi ve takım kaplamaları gibi proses parametrelerinin etkisi detaylı olarak tartışılmaktadır.

Anahtar Kelimeler: Yapışma aşınması, Alüminyum alaşımları, Soğuk şekillendirme

1. Introduction

Human activities throughout the centuries impacted the world that we live in. Among these, global warming became one of the most influential topic in recent years where carbon dioxide (CO_2) content in the atmosphere increased by 50% in less than 200 years ago. Naturally, countries took precautions to prevent the emission of more CO_2 into the atmosphere and released stringent legislative regulations. These precautions motivated companies to push their limits for innovative ideas to find carbon free alternatives for already existing applications. In this sense, automotive industry has focused on electric vehicles to overcome these regulations and contribute to world's sustainability. A report from the mobility of the future study by MIT Energy Initiative [1] revealed that an average CO_2 emission for petrol car is at least 350 gr where it decreases for hybrid cars around 260 gr per mile. Best carbon emissions are observed for fully battery-electric vehicles with only 200 gr. This shows that we can significantly decrease the carbon emission by only changing the type of fuel. However, electric cars have their own downsides and the biggest problem to be solved in these vehicles is the driving range. The simplest solution for such problem is to reduce overall weight of the car. This has two significant effects: firstly, many forces acting on a vehicle are directly related to its weight. A decrease in mass diminishes required driving force and thus yields to reduced energy consumption. Secondly, a lighter car is considered safer due to its lower inertia, meaning that it needs a shorter distance to halt than its heavier alternative [2].

The weight reduction is generally related to the material change and especially in lightweight cars; aluminum alloy is the main material choice [3-5]. Aluminum alloys possess a desirable combination of characteristics, including extended durability, low weight, high strength-to-weight ratio, malleability and exceptional resistance to corrosion. Additionally, 95-98% of aluminum can be recycled repeatedly with a high quality, which is another important criterion for sustainability [6]. Due to these desirable properties, many lightweight car designs and parts, in Figure 1, are introduced with already existing or improved aluminum alloys [7-8].

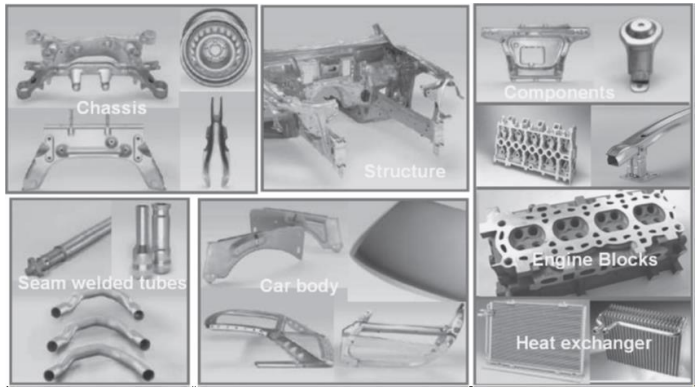

Figure 1. Aluminum alloy applications for light-weight cars[9]

Wrought alloys are classified into a two specific groups. First one is the non heat treatable alloys in which solid solution, strain hardening and dispersion hardening are the main methods to get required strength enhancements. This group consists of 1xxx, 3xxx, 4xxx and 5xxx series alloys. Other group is heat treatable alloys and their strengthening mechanisms are solution heat treatment and controlled aging. This group includes 2xxx, some of 4xxx, 6xxx and 7xxx series alloys [10]. Within aluminum alloys, 6xxx group have been widely researched due to its favourable properties such as heat treatability, robustness and weldability. When all 6xxx series aluminum alloys compared, it can be seen that the 6082

alloy within this series is the most common one due to its attractive properties such as higher mechanical properties, excellent corrosion resistance and convenience for T6 aging [11]. Wrought aluminum designation system with major alloying elements and their features is given in Table 1.

Table 1. Wrought alloy designation system [10]

Alloy Series	Major Alloying Element	Features
1xxx	Pure aluminum, 99%	Electrical conductivity
2xxx	Copper	Increased strength
3xxx	Manganese	Food safe
4xxx	Silicon	Lower melting point
5xxx	Magnesium	High corrosion resistance
6xxx	Magnesium and Silicon	Heat-treatable
7xxx	Zinc	High Strength

Metal forming is broadly used in automotive industry to manufacture parts with various size and shapes by plastically deforming the materials. This plastic deformation can be categorized into two group as bulk deformation and sheet metalworking with their own sub-groups [12]. Among the bulk deformation tecniques, forging is the most common metal forming technique, which uses compression forces in order to shape the work piece material between dies. Traditional forging is classified as hot, warm and cold forging according to application temperature. Cold forging is performed at temperatures below the recrystallization temperature of the work piece material, generally at room temperature, while hot forging is performed at temperatures above it. Warm forging is carried out at the temperatures between hot and cold forging application temperatures. The mentioned forging techniques have advantages and disadvantages compared with each other. In order to produce machine parts with hot forging, the work piece must be heated up to a certain temperature and this heating causes additional energy consumption. On the other hand, forging loads required to plastically deform the material decreases significantly and risk of damage in the work piece minimizes with the heating of the material. Better mechanical properties in the final product can be obtained with the cold forging thanks to the phenomenon of strain hardening. In addition, cold forging is a net-shape-forming technique, so generally there is no additional process required to obtain final shape of the product. In addition, this technique is suitable for mass production [13,14]. Due to these favourable properties, many vehicle parts such as nuts, bolts, bushes, joints and many more are manufactured by this forming method.

Despite its beneficial mechanical features, cold forming of aluminum is a challenging process due to its complicated nature. For instance, aluminum has tendency of sticking to tools during a cold forming process that can decrease the overall quality of the manufactured part. The work piece material that sticks to the tool surface undergoes hardening through oxidation, work hardening and grain refinement during the operation. Subsequently, it scratches the softer work piece material throughout the rest of the forming, which is commonly known as galling [15]. An example is shown in Figure 2. As a result of galling, surface finish of the manufactured parts deteriorates [16,17] and even in some severe cases, it can abrade the tool itself. There are many effecting factors on galling such as temperature, surface roughness, lubrication, sliding distance and contact pressure [18,19].

Figure 2. Cylinder that galled on removal from a conforming cylinder [20]

In literature, the majority of the studies related with cold forming of aluminum alloys are focused on the galling and the friction conditions between work piece and cold forming tool. In this review, the examination of the galling phenomenon in aluminum alloys is presented within the context of bulk and sheet cold forming processes, along with considerations of friction conditions. Various testing methods designed to simulate the cold forming process are also presented. Furthermore, the review delves into a detailed discussion of the effect of process parameters, including lubrication, tool surface finish and tool coatings.

Heinrichs and Jacobson (2009) investigated the effect of surface parameters on the tendency of galling during forming of aluminum using tool steel in laboratory tests. In this study, the parameters were selected as tool material, tool surface roughness and work piece surface preparation. AA6082 (1.2 %Si and 0.8 Mg), aluminum alloy, was used as a work piece material and samples were prepared by two different pre-treatments. First, aluminum samples were soft annealed, lubricated and extruded to 100 mm long cylinders with a diameter of 10 mm. Then, in order to obtain different surface quality, extruded cylindrical rods were separated into two equal groups. First group was soft-annealed and lubricated again whilst second group was only pickled. After these preparations, hardness of the soft-annealed and pickled samples were measured as 35 HV and 60 HV, respectively. To simulate the galling and the friction conditions between the work piece and the tool during cold forming, a load-scanner equipment was used in the sliding-contact tests. Brief illustration of their test set up is illustrated in Figure 3. Principle of the test was as follows, tool steel slides over the aluminum samples and deforms the contact surface. This sliding motion was performed in two different parts as single and multiple strokes. Then, contact surfaces were investigated by using scanning electron microscopy. The procedure was followed for both pickled and lubricated surfaces. Current testing method is proved to be an effective way to examine galling of various tool steels and is used in other studies as well [21,22]. Authors concluded that lubrication significantly effects galling. Experiments revealed that unlubricated surfaces were susceptible to galling even in the smoothest tool surfaces and it cannot be avoided. Similar outcome was obtained for the cases where lubrication wears off and maximum friction coefficient increases immediately. Another finding was about the occurrence of galling. It can be observed in both smooth and rough surfaces as thin layer and/or lumped together where aluminum transfer (galling) was not necessarily a function of high friction coefficient. Around the scratches in rough tool surfaces galling occured in which aluminum deposits in and over these surface impurities. Thus, author suggested that in the forming process of aluminum, tool materials with smooth surfaces and proper lubrication were key parameters in terms of alleviating the adhesive wear [23].

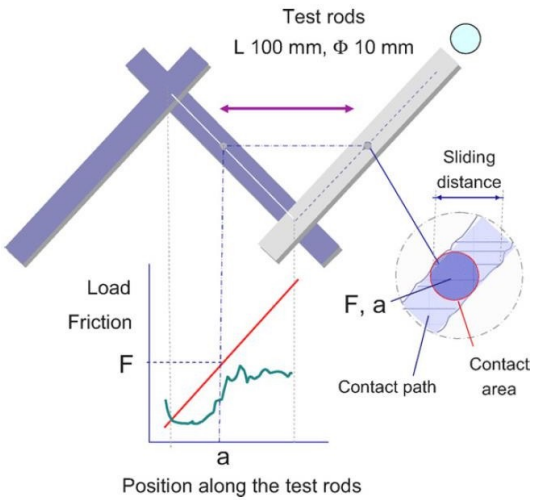

Figure 3. Sketch showing the test set up [23]

Heinrichs and Jacobson (2010) investigated the effect of coating on the AA6082 aluminum's tendency of galling during cold forming. Various coatings, namely diamond like carbon (DLC), titanium aluminum nitride (TiAlN), titanium nitride (TiN) and titanium carbonitride (TiCN), were applied on 8 tool samples by using physical vapor deposition (PVD) technique as single layer or as multilayer combinations and compared with the uncoated tool. Briefly, these coatings are widely used in industrial applications for their superior characterictics such as high hardness, low friction, chemical inertness and self-lubrication. Due to these qualifications, they are widely used in forming and machining of metal parts [24-28] and special attention is given to it in this study. Coatings like TiN, TiCN, and TiAlN are generally used for tool life and performance purposes by decreasing the friction between work piece- tool contact in the literature. Technical data about the applied coatings in the paper are given in Table 2.

Table 2. Main alloying elements and hardness of the tested tool steels [29]

Tool steel	Steel type	Hardness
Grade A	5Cr-Mo-V	50
Grade B	5Cr-Mo-V	55
Grade C	9V,4.5Cr-Mo-W	60

Influence of different coatings were examined by comparing results of the tests with uncoated tool. H13 was selected as tool material and two sets of tools were prepared in which the first group has higher roughness while other tools have smoother surface. Regarded surface roughnesses of the tools are given in Table 3.

Table 3. Roughness parameters of the rougher surfaces (white light interferometry) [29]

	Mean Ra (nm)	Mean Rt (nm)	Mean Rq (nm)
Grade A	280	2900	350
Grade B	270	3200	340
Grade C	250	2900	310

The AA6082 samples were prepared with two different pre-treatment same as the authors previous study [23] and tests were carried out by using a load scanning rig. Conducted tests revealed that there is a significant difference between pre-lubricated and unlubricated pickled aluminum samples in the sense of friction performance. The effect of tool roughness was minimal in pre-lubricated aluminum rods and in some cases coating performance was same with the uncoated tools. On the other hand, some of the DLC coatings in unlubricated and pickled aluminum samples yielded to maximum performance in comparison by keeping low friction for more than 200 strokes. For the same conditions, other coatings and uncoated tools could keep low friction for less than 10 strokes. The occurence of galling under high loads was also different in pre-lubricated samples where aluminum deposition observed as large bulky flakes on top of the tool rod where it was more integrated with the surface in pickled ones. In any circumstances the lubrication was found as the most important factor in terms of galling and friction conditions. Authors also highlighted that there is no clear correlation between hardness of the coating and the aluminum's galling tendency. Coatings with a higher hardness than aluminum oxide could or could not mitigate aluminum adhesion which leads to a unreliable outcomes. Even in combination of hard coating with a smooth surface could fail to prevent galling which shows that the chemical adherence is also an important parameter [29].

In order to examine the effect of tool defects on occurrence of galling, Heinrichs and Jacobson (2011) conducted another study. They used two layered DLC coated tools, first layer was Me-Doped and the second layer was hydrated DLC. Controlled defects with various sizes on the tool surfcaes were created with Berkovich, Vickers and spherical diamond tips. In order to create less controlled defects SiC grinding paper was also used. Illustration of these surface defects are given in Figure 4. They followed same experimental procedures with their previous studies where sliding-contact test wih a load scanner equipment was used for investigating the galling and the friction conditions. AA6082 and AISI H13 were selected as work piece and tool material, respectively. The aluminum samples were not lubricated to get worst contact conditions possible. The tool materials were prepared with six different depts, scaling from nano to micro scale and one sample was left polished for comparison. Results of the sliding- contact test revealed that the effect of surface irregularities was negligible in the sense of friction coefficient at the first stroke. But, scanning electron microscope (SEM) image of the tool surface showed that aluminum was deposited inside dents which could excite galling in following strokes. Authors examined the transferred aluminum to tool by using electron spectroscopy for chemical analysis (ESCA) and found that transferred aluminum was mostly in the form of aluminum oxide and could not cover the whole tool surface. This could be achieved only if aluminium was transferred gradually while sliding, with each thin film being extensively oxidized before the subsequent film was transferred. One interesting finding was the hardness increment of deposited aluminum. Before experiment, hardness of the aluminum sample was 60 HV. After first stroke, it increased to 65 HV and after multiple strokes it became 95 HV. Authors explained this occurrence by mechanical entrapment of aluminum inside the dent. In first stroke, aluminum deposited into the dent in a blotchy manner. Then, rod slided back along the path and removed the tip of deposited aluminum while remaining metal was trapped inside the dent. This removing process highly sheared the top surface of trapped aluminum in which the metal was plastically deformed and authors believe that this repetitive passage could harden the aluminum. Even though these dented areas increased the friction locally, they had insignificant effect on the overall friction. In brief, the results of the study emphasized that the adherence of aluminum on the tool surface initially occurs around the scratches, and with a good surface finish of the tool, it can be avoided. However, this initial adherence didn't have a significant effect on tool life compared to overal surface finish [30].

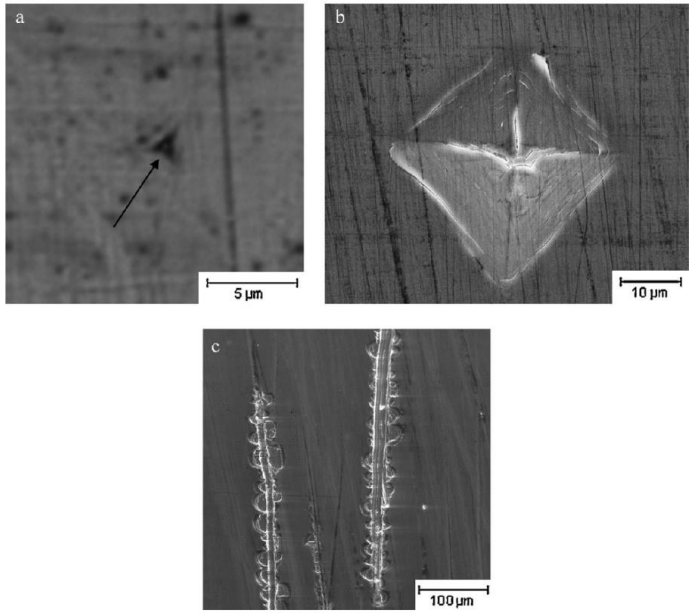

Figure 4. Image of (a) nanoindentation with depth 160 nm (optical microscopy), (b) microindentation with depth 5.6 m (SEM) and (c) scratches from 240 grit paper on the surface of a coated tool rod. [30]

Le Mercier et al. (2017) investigated the galling of Al6082-T6 aluminum alloy during cold forging process. Upsetting-sliding test (UST) was used for replicating metal-metal interface interactions, such as sliding velocity, contact pressure and temperature to evaluate the amount of deposited aluminum to tool surface. Schematic representation of the test set-up is illustrated in Figure 5 and the tested configuration is given in Table 4. Three trials were conducted for each test configuration in which a single tool and unworn aluminum sample surface was used. Cylindrical aluminum samples were lubricated with molybedenum disulphide. Combination of SEM and surface profilometry was used for surface analysis. This combined method was used and proved by Nosar [31] to be an efficient way of comprehending the mechanisms for controlling the transfer of materials. The main idea of this method came from the nature of topographical distinction between ground and polished surfaces. Surface topography image of the latter for steel tool consists of peaks with hard phase particles on nanoscale whereas grounded surfaces are characterized with macroscale scratches caused by abrasive particles such as SiC. Nosar [31] found that the optical surface profilometer alone was not adequate to define polished surface topography due to this difference and emphasized the importance of SEM addition to profilometer analysis for correctly identifying surfaces. Le Mercier performed this combined method to characterize topographies and make a quantitative analysis about galling. According to findings of the study, it was revealed that galling was observed in every test conditions and its regime was depend on the sliding velocity. At sliding velocities of 100 and 200 mm/s, the coefficient of linear regression was almost the same, indicating the same galling mechanism. At lower sliding velocities, such as 20 mm/s, a different linear regression coefficient was obtained, suggesting a different mechanism. Furthermore, a noteworthy relationship between wear volumes and the friction ratio has been emphasized which underscores the significance of considering a parameter that represents friction in adhesive wear models. The wear volumes exhibit similar trends as those noted in the friction ratio [17].

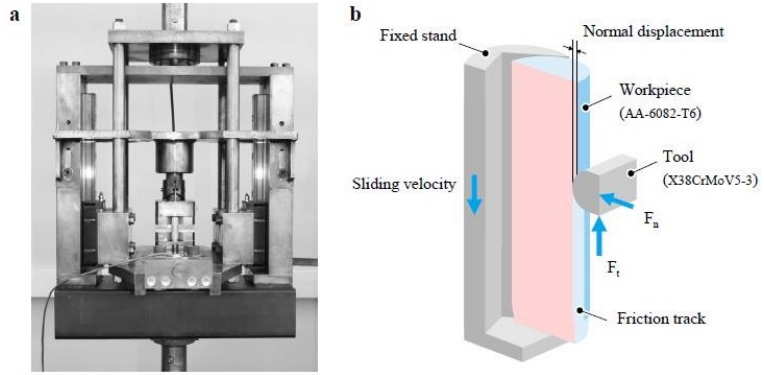

Figure 5. (a) Upsetting sliding test device, (b) Schematic diagram of the test [17]

Table 4. Tested configurations [17]

Tool/Test configuration	1	2	3	4	5	6	7	8	9	10
Sliding velocity (mm.s-1)	20	20	20	100	100	100	200	200	200	200
Normal displacement (µm)	30	60	100	30	60	100	30	40	60	100

Pujante (2013) conducted an experimental study on AA2017 aluminum balls with temperature ranging from 30-450°C to examine the effect of temperature on wear behaviour. They used ball-on-disc sliding test with H13 tool steel where AA2017 ball was securely affixed within a holder connected to an oscillating electro-mechanical drive. This drive exerted pressure against a fixed tool steel disc, which was in turn positioned atop a heating block. The applied load was kept constant during each test and the coefficient of friction was measured. Tests were conducted for three set of tool samples with varying surface roughnesses and orientations. All experiments were conducted at 30°C, 150°C, 250°C, 350°C and 450°C. Backscattered electron imaging and confocal microscopy were used to monitor groove depths and other wear induced formations for 10s and 300s duration which corresponded to 250 and 7500 sliding cycles respectively. In 250 cycle, groove depths were measured to be similar in all temperatures which was around 2-3µm. From 30-250°C tool abrasion was not observed and there were thin layer of aluminum alongside with lumps up to 30 µm due to metallurgical junction between metal- metal contact. But they were all removed later with repetitive sliding motion. However, at higher temperatures (350-450°C) tool abrasion was apparent. At those temperatures, deposited aluminum was converted into aluminum oxide and assisted abrasive wear mechanicsm on tool surface. In 7500 cycle, grooves were more deeper around 10µm without any material transfer, lumps of aluminum were detected but later abraded, for just above the room temperature. After 2500 cycle, coefficient of friction was stabilized. In between 150-250°C, material transfer was more pronounced and lumps that formed during the initial stages of the tests became a sites for nucleation growth and accelerated further material transfer. At the highest temperatures, 350-450°C, case groove depths were measured as 20µm which is the highest depth in all cases. Abrasion was so severe that it even removed material from tool steel. Authors didn't focus on the material loss from the tool but they reminded that H13 metal could operate around these temperatures without any disturbances caused by softening. So, this material loss could not be explained by thermal softening of the tool steel. In overall, conducted experiments demonstrated that temperature had significant effect on the wear behavior and it is an important parameter for forging process of aluminum. Authors also examined the effect of surface finish in some extend, but they concluded that its effect was negligible due to low surface roughness [32].

Pruncu et al. (2018) investigated the material transfer mechanism from Al6082 T6 alloy to tool steel under upset-

ting-sliding tests. The test set-up is shown in Figure 4. The tests were performed with various contactor penetration depths ranging from 0.04 to 0.18 mm and two different sliding velocities as 10 mm/s and 60 mm/s, respectively. Samples were separated into two groups, with one of the groups being lubricated with MoS_2 to prevent early damage. The results of lubricated and unlubricated samples were compared. Additionally, a new contactor was used for each test. The amount of transfered aluminum on contactor was assessed by measuring the initial and final thicknesses of the sample. In order to do that, maximum 10-point height method was used within the study. The results of the study revealed that, the amount of transferred material tended to increase with increasing plastic deformation. At high plastic deformation levels, the transferred material almost covered whole contact surface of the contactor. Even for low plastic deformation levels, aluminum adherence to contactor surface was observed. The transfer mechanism was explained as the initiation of aluminum adherence to the tool and the delamination of aluminum particles. As the deformation continued, the initial interactions between aluminum and the tool at the microscopic level gradually shifted towards interactions between aluminum to aluminum. The results of the study also highligted that, as the amount of transferred aluminum increased, the coefficient of friction was also increased. When the tests were performed with MoS_2 lubricant, the effect of transferred aluminum on coefficient of friction was low since metal to metal contact was minimized with the use of lubricant [33].

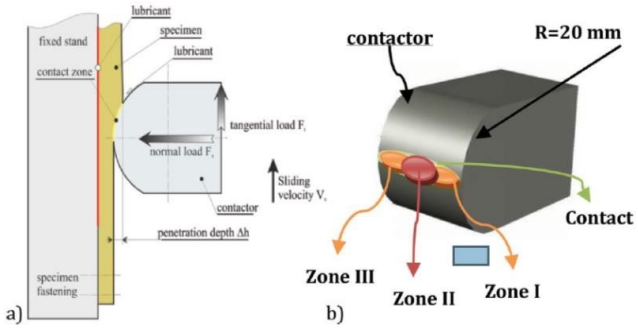

Figure 6. (a) Schematic view of the upsetting-sliding test and (b) zones of analysis considered for the contactor surface [33]

Vidales et al. (2023) studied the wear behavior of Al5754 with a focus on surface roughness and tool geometry. The authors also investigated the effect of coating and lubrication on the wear behavior. Experiments conducted in two parts: in the first part, effect of surface roughness and geometry of tools was studied while in the second part, performance of coating with various lubricants was examined. To analyze the effect of surface roughness, a modified version of scratch test was used in which aluminum ball was rubbed on the unworn surface of tools. Schematic diagram of scracth test is illlustrated in Figure 7 and test parameters are given in Table 5. The tool surfaces were prepared with different surface finishes as polished, machined and sand blasted. In order to investigate the wear and friction behavior of coated balls, ball-on-disc test with a tribometer was used. Tests were performed both with and without lubricants to reveal the effect of lubrication. The balls were manufactured with WC/Co and coated with two different bi-layered DLC coatings. The tests parameters and lubricant details are given in Table 6 and Table 7, respectively. Ball-on-disc tests with lubricants were carried out with the submerged system in lubricant. This was not an accurate simulation of the industrial operations. To simulate the real process and to verify the lab results, semi-industrial tests was also conducted. During these tests, two different punch geometries, straight or back-tapered were used. Additionally, within the study, used industrial punching tools provided by a company, was also investigated with field emission scanning electron microscopy (FE-SEM), energy dispersive X-ray (EDX) and infinite focus microscopy to reveal failure modes. These punching tools were used for the trimming of Al5754 parts. Through the surface investigation of industrial tools, the authors observed that the most visible damage was the galling on the side faces of the tools. The minimum aluminum adherence was observed with the

polished tools, while highest adherence was observed with the machined tools. Although sand blasted tools had highest roughness within all tools, they showed less adherence than machined tools because of the anisotropy in surface roughness. Coating irregularities, such as micro-droplets, found to be adhesion provoker where thin aluminum layer was observed on polished tool with low friction coating. The results of the study also indicated that, the applied bi-layered DLC coatings showed similar behavior in terms of friction without lubrication during lab tests. When the lubricants were applied to the system, friction decreased regardless of the type of lubricant used. The best results in terms of galling was obtained with the use of back-tapered and polished punching tools coated with a-C:H/Cr DLC. In brief, tool surface roughness had an important effect on aluminum adhesion and with the combination of suitable tool geometry and coating, aluminum adherence could be reduced significantly [34].

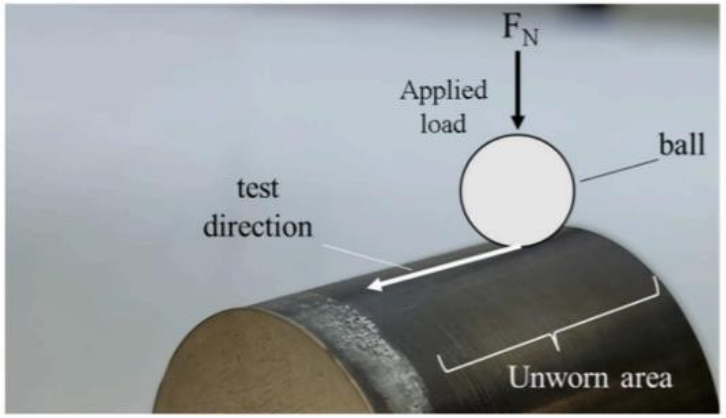

Figure 7. Scratch test schematic diagram. [34]

Table 5. Experimental parameters of modified scratch test [34]

Ball	Ø2.5 mm 99% Al
Load	1 N
Length	10 mm
Speed	20 mm/min

Table 6. Friction test parameters [34]

Spherical Indenter	Ø10 mm-coated WC/Co balls
Disc	Ø40 mm x 3 mm of aluminum 5754
Load	10N
Test environment	Dry & Lubricated
Total distance	85.5 m
Speed	95 mm/s

Table 7. Lubricant characteristics [34]

Lubricant	**Formulation**	**Viscosity** (ISO 40°C)	**Weld Load** (kg)
LUB 1	Mineral Oil + Ester additives	130 cSt	180
LUB 2	Mineral Oil + Ester additives	150 cSt	760
LUB 3	Ester Base + Additives	110 cSt	320

In literature, many experimental studies were performed to understand the effecting factors on aluminum adherence and friction conditions. However, there are a few studies related with the numerical approach to predict these phenomenon [35-37]. Given that cost of tools in metal forming processes can account for as much as 30% of the overall production cost [38] and considering that wear, galling, and friction conditions significantly shorten the lifespan of these tools, it becomes crucial to investigate numerical approaches for predictive purposes [39,40].

A simple example can be given for numerical investigation of maximum contact pressure on die-blank interfaces. Finite element modeling can be utilized to model contact pressure distribution over these parts and its response might yield to a favorable result to comprehend tool wear [41,42]. Similarly, coupling the friction models into finite element analysis is a favored method for evaluating friction [43,44] to increase die life in cold forming process. In this sense, there are several numerical studies related to galling of aluminum alloys. For instance, a methodology on predicting the galling onset was proposed by Filali for AA6082-T4 aluminum alloy in cold forming. Strip reduction test (STR) was utilized to investigate lubrication and onset occurence of galling, then, obtained results were compared with finite element results. Ductile failure and adhesive wear mechanisms were related to each other in order to predict galling. First adhesion of soft material to harder surface was taken as the beginning of galling and authors assumed that this material transfer was achieved for a critical damage value at the contact region. Since adhesion wear is related to friction at the surfaces, they suggested that the damage model used for such problem must include the effect of shear stresses. For instance, classical damage models such as Lemaitre's and Gurson-Tvergaard-Needleman (GTN) could only predict galling under extreme contact conditions where excessive tensile stresses are observed. Because these methods only consider tensile stress at the contact area and required critical damage values could be achieved only under such extreme contact conditions which is not appliable to common forming processes. Friction model was derived from work piece-tool contact and it was controlled by the lubricant. Wilson's lubrication model was implemented for normalized thin-film thickness, z, to determine this contact conditions and modify the finite element model accordingly. Three seperate contact conditions were considered. If the contact was within a thick lubricant film, shearing of lubrication film was chosen as the main cause of friction stress and it was written as a function of lubrication viscosity. For thinner films, a shear stress factor was utilized to include the effect of surface roughness. In the thinnest case, two types of regimes were defined: mixed and boundary lubrication for direct and partial contact. Friction stresses were subsequently taken into account with parameters such as adhesion coefficient, fractional area of contact, contact pressures and strain rate. Comparison between purposed model and experiments showed general agreement with some deviations. Model had some errors in the sense of starting location of galling where it always predicted the location to be further than its experimental equivalent. Also, local adhesion of aluminum was found to be smaller than it was expected. Authors related these problems to mesh effect and Wilson model where it might overestimated ploughing friction stress. But in overall, their model was able to predict the onset of galling for both lubricated-unlubricated cases, and strip rupture due to traction [45].

2. Conclusion

The demand for aluminum and its alloys in the automotive industry is increasing day by day due to regulations aimed at reducing greenhouse gas emissions and improvements in electric vehicles. For both purposes, aluminum stands out as a lighter but durable material that can be used instead of steel. Despite its beneficial features, forming of aluminum at room temperatures is a challenging process due to complicated nature of the material. Aluminum has tendency of sticking to tools during cold forming processes that can decrease the overall quality of the manufactured part. Friction conditions and other forming parameters are crucial in order to delay the onset of the sticking. Many researchers have focused on the galling phenomenon that occurs during the forming of aluminum and its alloys and investigated the parameters that affect it. As a result of all the studies carried out, although galling cannot be completely prevented, critical and necessary conditions have been introduced to delay it. The effect of proper lubrication and coating is highlighted as a conclusion of studies. Also, DLC coatings gets attention of researchers and promise good results depending on the application. In addition to experimental studies, numerical studies are also presented to predict the galling onset before production and to reduce the trial and error.

References

[1] MIT Energy Initiative. 2019. Insights into Future Mobility. Cambridge, MA: MIT Energy Initiative.

[2] J. Bouquerel, B. Diawara, A. Dubois, A. Dubar, J.-B. Vogt, D. Najjar, "Investigations of the microstructural response to a cold forging process of the 6082-T6 alloy," Materials and Design, vol. 68, pp.245-258, 2015.

[3] A. Kumar, R.Maithani, A. Kumar, D. Kumar, S. Sharma, "An all-aluminium vehicle's design and feasibility analysis", Materials Today: Proceedings, vol.64, pp. 1244-1249, 2022.

[4] M. Goede, "Sustainable Production Technologies of Emission reduced Lightweight car concepts (SuperLIGHT-CAR)", TIP4-CT-2005-516465, 2009.

[5] M. Goede, M. Stehlin, L. Rafflenbeul, G. Kopp, E. Beeh, "Super Light Car–lightweight construction thanks to a multi-material design and function integration", European Transport Research Review, vol. 1, pp. 5–10, 2009.

[6] W.S. Miller, L. Zhuang, J. Bottema, A.J. Wittebrood, P. De Smet, A. Haszler, A.Vieregge, "Recent development in aluminium alloys for the automotive indusrty", Materials Science and Engineering A- Structural Materials Properties Microstructure and Processing, vol. 280, no. 1, pp.37- 49, 2000.

[7] J. Hirsch, "Automotive Trends in Aluminium-The European Perspective", Materials Forum, vol.28, pp. 15-23, 2004.

[8] J. Hirsch, "Aluminium Alloys for Automotive Application", Materials Science Forum, vol.242, pp. 33-50, 1997.

[9] J. Hirsch, "Aluminium in Innovative Light-Weight Car Design", MATERIALS TRANSACTIONS, vol.52, pp. 818-824, 2011.

[10] R. Howard, N. Bogh, D. S. MacKenzie, "Heat Treading Processes and Equipment," in Handbook of Aluminum: Volume 1 Physical Metallurgy and Processes, New York: Marcel Dekker, 2003, pp. 882.

[11] B. Karahan, U. İnce, S. Yurtdaş, N.E. Kılınçdemir, F.C. Ağarer, C. Kılıçaslan, "On the Cold Forging of 6082 H13 and T4 Aluminum Alloy Bushes" in 5th International Symposium on Innovative Technologies in Engineering and Science, Baku, 2017.

[12] P. C. Sharath, "Multi directional forging: an advanced deforming technique for severe plastic deformation," in Advanced Welding and Deforming, Elsevier, 2021, pp. 529-556.

[13] C. Kılıçaslan, U. İnce, "Soğuk Dövme Kalıplarında Meydana Gelen Kırılma Sebeplerinin Nümerik Olarak İncelenmesi", Mühendis ve Makina, vol. 57, pp. 65-71, 2016.

[14] M. B. Toparlı, "Soğuk Dövme Kalıplarında Ömür Artışı Elde Etmek için Baskın Hasar Mekanizmasının Belirlenmesi," Uludağ Üniversitesi Mühendislik Fakültesi Dergisi, vol. 24, pp. 157- 172, 2019.

[15] J. Heinrichs, M. Olsson, S. Jacobson, "Initiation of Galling in Metal Forming: Differences Between Aluminium and Austenitic Stainless Steel Studied In Situ in the SEM", Tribology Letters, vol.50, pp.431-438, 2013.

[16] J. Heinrichs, S. Jacobson, "Mechanisms of material transfer studied in situ in the SEM: Explanations to the success of DLC coated tools in aluminium forming," Wear, vol. 292, pp. 49-60, 2012.

[17] K. Le Mercier, M. Dubar, K. Mocellin, A. Dubois, L. Dubar, "Quantitative analysis of galling in cold forging of a commercial Al-Mg-Si alloy," in International Conference on the Technology of Plasticity, Cambridge, 2017.

[18] M. Hanson, "On adhesion and galling in metal forming", Ph.D. Dissertation, Faculty of Science and Technology, Uppsala University, 2008.

[19] V. Westlund, J. Heinrichs, S. Jacobson, "On the Role of Material Transfer in Friction Between Metals: Initial Phenomena and Effects of Roughness and Boundary Lubrication in Sliding Between Aluminium and Tool Steels", Tribology Letters, vol. 66, pp. 1-15, 2018.

[20] K. G. Budinski, S. T. Budinski, "Interpretation of galling tests", Wear, vol. 332-333, pp. 1185- 1192, 2015.

[21] B. Podgornik, S. Hogmark, J. Pezdirnik, "Comparison between different test methods for evaluation of galling properties of surface engineered tool surfaces", Wear, vol. 257, pp. 843-851, 2004.

[22] M. Hanson, A. Gaard, P. Krakhmalev, S. Hogmark, J. Bergström, "Comparison of two test methods for evaluation of forming tool materials", Tribotest, vol. 14, pp. 147-158, 2008.

[23] J. Heinrichs, S. Jacobson, "Laboratory test simulation of galling in cold forming of aluminium," Wear, vol. 267, PP. 2278-2286, 2009.

[24] M. H. Sulaiman, R. N. Farahana, K. Bienk, C. V. Nielsen, N. Bay, " Effects of DLC/TiAlN- coated die on friction and wear in sheet-metal forming under dry and oil-lubricated conditions: Experimental and numerical studies", Wear, vol.438-439, 2019.

[25] A. Ghiotti, S. Bruschi, "Tribological behaviour of DLC coatings for sheet metal forming tools", Wear, vol. 271, pp. 2454-2458, 2011.

[26] C. Kayış, E. A. Diler, H. Sandallı, F.C. Ağarer, "Effects of TiN/CrN, CrAlN, and TiN Coatings on the Performance of AISI M2 Tool Steel", Düzce University Journal of Science & Technology, vol. 10, pp. 1344-1358, 2022.

[27] J. Heinrichs, S. Jacobson, " Mechanisms of Transfer of Aluminium to PVD- Coated Forming Tools", Tribology Letters, vol. 46, pp. 299-312, 2012.

[28] J. Heinrichs, S. Jacobson, "Evaluation of TiB2 coatings in cold forming of aluminium", Surface Engineering, vol. 28, pp. 517-525, 2012.

[29] J. Heinrichs, S. Jacobson, "Laboratory test simulation of aluminium cold forming- influence from PVD tool coatings on the tendency to galling," Surface & Coating Technology, vol. 204, pp.3606- 3613, 2010.

[30] J. Heinrichs, S. Jacobson, "The influence from shape and size of tool surface defects on the occurence of galling in cold forming of aluminium," Wear, vol. 271, pp.2517-2524, 2011.

[31] N. S. Nosar, M. Olsson, "Influence of tool steel surface topography on adhesion and material transfer in stainless steel/tool steel sliding contact", Wear, vol. 303, pp. 30-39, 2013.

[32] J. Pujante, L. Pelcastre, M. Vilaseca, D. Casellas,. B. Prakash, "Investigations into wear and galling mechanism of aluminium alloy-tool steel tribopair at different temperatures", Wear, vol. 308, pp. 193-198, 2013.

[33] C. I. Pruncu, T. T. Pham, A. Dubois, M. Dubar, L. Dubar, "Morphology of Surfcae Integrity as Effect of Cold Forging of Aluminum Alloy", Tribology Transactions, vol. 61, pp. 632-639, 2018.

[34] E. Vidales, N. Cuadrado, E.Garcia-Llamas, J. T. Garitano, I. Aseguinolaza, M. Carranza, M. Vilaseca, G. Ramirez, "Surface roughness analysis for improving punching tools performance of 5754 aluminium alloy", Wear, vol. 524-525, 2023.

[35] J. Tenner, K. Andreas, A. Radius, M. Merklein, "Numerical and experimental investigation of dry deep drawing of aluminum alloys with conventional and coated tool surfaces", in International Conference on the Technology of Plasticity (ICTP), Cambridge, 2017.

[36] M. P. Pereira, W. Yan, B.F. Rolfe, "Contact pressure evolution and its relation to wear in sheet metal forming", Wear, vol. 265, pp. 1687-1699, 2008.

[37] W. Dong, L. Xu, Q. Lin, Z. Wang, "Experimental and numerical investigation on galling behavior in sheet metal forming process", International Journal of Advanced Manufacturing Technology, vol.88 (1-4), pp. 1101-1109, 2016.

[38] M. Hawryluk, "Review of selected methods of increasing the life of forging tools in hot die forging processes", Archives of Civil and Mechanical Engineering, vol.16, pp.845-866, 2016.

[39] X. Yang, Y. Hu, L. Zhang, Y. Zheng, D. J. Politis, X. Liu, L. Wang, "Experimental and modelling study of interaction between friction and galling under contact load change conditions", Friction, vol.10, pp.454-472, 2022.

[40] Y. Hou, W. Zhang, Z. Yu, S. Li, "Selection of tool materials and surface treatments for improved galling performance in sheet metal forming", The International Journal of Advanced Manufacturing

[41] W. Yan, E. P. Bus so, N. P. O'Dowd, "A micromechanics investigation of sliding wear in coated components", Proceedings of the Royal Society of London. Series A: Mathematical, Physical and Engineering Sciences, vol.456, pp.2387-2407, 2000.

[42] W. Yan, "Theoretical investigation of wear-resistance mechanism of superelastic shape memory alloy NiTi", Materials Science and Engineering: A, vol.427, pp.348-355, 2006.

[43] J. Hol, M.V. Cid Alfaro, M. B. De Rooij, T. Meinders, "Advanced friction modeling for sheet metal forming", Wear, vol.286-287, pp.66-78, 2012.

[44] F. Klocke, D. Trauth, A. Shirobokov, P. Mattfeld, "FE-analysis and in situ visualization of pressure-, slip-rate-, and temperature-dependent coefficients of friction for advanced sheet metal forming: development of a novel coupled user subroutine for shell and continuum discretization", The International Journal of Advanced Manufacturing Technology, vol.81, pp.397-410, 2015.

[45] O. Filali, A. Dubois, M. Moghadam, C. V. Nielsen, L. Dubar, "Numerical prediction of the galling of aluminium alloys in cold strip drawing", Journal of Manufacturing Processes, vol.73, pp.340- 353, 2022.

FARKLI DAYANIM SINIFLARINDAKİ BAĞLANTI ELEMANLARININ TİTREŞİM ÖLÇÜMLERİYLE YORULMA ÖMRÜNÜN TAHMİNLENMESİ

Tolga AYDIN
Mahmut PEKEDİS

Hodja Akhmet Yassawi 8th International Congress on Scientific Research

FARKLI DAYANIM SINIFLARINDAKİ BAĞLANTI ELEMANLARININ TİTREŞİM ÖLÇÜMLERİYLE YORULMA ÖMRÜNÜN TAHMİNLENMESİ

Tolga Aydın[1,2], Mahmut Pekedis[3]

[1]1Ege University, Fen Bilimleri Enstitüsü, Makine Mühendisliği Ana Bilim Dalı, İzmir, Türkiye
[2]R&D Engineer, Norm Cıvata San. ve Tic. A.Ş., A.O.S.B., Çiğli, İzmir, Türkiye
ORCID ID: https://orcid.org/0000-0002-4979-1486
tolga.aydin@normfasteners.com, tolgaaydin@gmail.com, +90 542 785 07 92
[3]Doç. Dr., Ege Üniversitesi, Mühendislik Fakültesi, Makine Mühendisliği Bölümü, İzmir, Türkiye
ORCID ID: https://orcid.org/0000-0002-3350-0277
mahmut.pekedis@ege.edu.tr, + 90 232 311 4970

Özet

Cıvataların çalışma koşullarında hasara uğramasının temel sebebi genellikle, uygulanan yükün statik dayanım sınırın üstüne bir gerilme yaratmasından ziyade yorulma kaynaklı etkenlerin baskın olduğu durumlardır. Soğuk şekillendirme yöntemi ile imal edilen cıvataların, aynı lot içerisinde üretilmiş belirli adet cıvata örneklemi test edilse dahi, yorulma testi sonuçlarında bir saçılım ortaya çıkmaktadır. Bu belirsiz durum farklı sektörlerde, özellikle emniyet parçalarında, güvenlik riski doğurmaktadır. Saçılım oranını net olarak tahminleyebilecek bir mühendislik yaklaşımı da bulunmamaktadır. Aynı özelliklere sahip cıvatalar için belirli standardizasyon ve mühendislik denklemleri kullanılarak o cıvata tipi ve yükleme koşuluna ait yorulma ömürlerine yönelik çıkarımlar yapılabilmektedir. Buna karşın, cıvatanın servis verdiği cihaz üzerinde yapılan periyodik bakımlarda yahut ilk montaj aşamasında cıvatanın yorulma ömrüne dair bir çıkarım tekil olarak yapılamamaktadır. Tekil olarak yorulma testi yapılabilmekte ancak test sonucu tahribatla sonuçlanmaktadır. Cıvataya herhangi bir hasar vermeden, tekil olarak yorulma ömrünü tahmin edebilen bir yöntem ya da cihaz literatürde güncel olarak bulunmamaktadır. Bu çalışmada, cıvataların titreşim ölçümlerine karşı davranışının tahribatsız olarak ölçülüp verilerin mühendislik denklemleri kullanılarak işlenip yorulma ömrünün tekil olarak tahmin edilebilirliği incelenmiştir. Çalışma kapsamında, cıvatalar üzerinde titreşim ölçümleri; shaker, ivmeölçer ve strain gage gibi komponentler vasıtasıyla gerçekleştirilip ölçümü yapılan cıvatalar yorulma testlerine tabi tutulmuştur. Titreşim ölçümleriyle yorulma çevrimleri arasındaki ilişki; doğal frekans değerleri, frekans tepki fonksiyonları, güç spektrum yoğunlukları vb. parametrelerin yorulma ömürleriyle uyumu kontrol edilerek raporlanmıştır. Yapılan çalışma, titreşim davranışlarıyla yorulma ömrü arasında bir korelasyon tespit ettiği takdirde, sadece yorulma ömrünü tahminlemek için değil, katlanma vb. şekillenme kusurlarının bir kalite – kontrol yöntemi olarak hasarsız tespit edilebilirliğine yönelik araştırma alanı oluşturmak adına da önem taşımaktadır.

Anahtar Kelimeler: Cıvata yorulması, titreşim, doğal frekans, bağlantı parçası.

Abstract

The primary cause of bolt failure under operational conditions is typically fatigue-related factors, rather than the applied load exceeding the static strength limit. Even when a certain number of cold-forged bolts manufactured in the same batch are subjected to fatigue testing, the results exhibit considerable scatter. The present state of uncertainty shows a potential security risk in a number of industrial sectors, with particular implications for the safety components. The lack of a clear engineering approach to predict the scattering rate makes it difficult to identify the fatigue behaviour of a single component. For bolts with comparable properties, standardisations and engineering equations can be employed to infer the fatigue life according to the bolt type and loading condition. Conversely, the fatigue life of the bolt cannot be inferred individually during periodic maintenance on the assembly area or during the initial assembly phase. Individual fatigue tests can be performed, but the results are inevitably accompanied by bolt failure. There is currently no method or device in the literature that can predict the individual fatigue life without any damage to the bolt. In this study, the vibration measurements of bolts were processed using engineering equations in order to investigate the individual predictability of fatigue life. Within the scope of the study, vibration measurements on bolts were carried out using components such as a shaker, accelerometer and strain gage, and fatigue tests of measured bolts are performed. The relationship between the aforementioned measurements and the fatigue life cycles of the bolts was then evaluated, with particular focus on the compatibility of parameters such as natural frequency values, frequency response functions and power spectrum densities with fatigue life. Should a correlation between vibration behaviour and fatigue life be identified, the study would be of significant value not only in terms of predicting fatigue life but also in establishing a research area for the non-destructive detection of deformation defects such as folding, etc. as a quality control method.

Keywords: Bolt fatigue, vibration, natural frequency, fastener.

WEAR PROPERTIES OF TUNGSTEN CARBIDE COBALT (WC-CO) HARDMETAL MATERIALS AFTER BORIDING PROCESS

Kübra ÖZTÜRK
Bahadır UYULGAN
Umut İNCE

50. Avrupa Isıl İşlem ve Yüzey Mühendisliği Konferansı ve Isıl İşlem ve Yüzey İşlemleri Derneği, ECHT 2024 - A3TS

WEAR PROPERTIES OF TUNGSTEN CARBIDE COBALT (WC-CO) HARDMETAL MATERIALS AFTER BORIDING PROCESS

Kübra Öztürk[1,2,a*], Bahadır Uyulgan[1,b], Umut İnce[2,c]

[1]1Department of Metallurgical and Materials Engineering, Dokuz Eylul University, İzmir, Turkey
[2]R&D Center, Norm İzmir Cıvata San. ve Tic. A.Ş., AOSB, İzmir, Turkey
[a]kubra.ozturk@normfasteners.com, [b]bahadir.uyulgan@deu.edu.tr, [c]umut.ince@normfasteners.com

Abstract

The performance of die systems utilized in fastener production through the cold forming method is directly tied to surface characteristics, significantly impacting production costs. Metal-ceramic composite materials with varying WC-Co content are widely used in cold forming process. The crucial features influencing the effective and enduring use of these dies materials at the desired performance levels are wear resistance and fatigue resistance. The boriding process enhances surface properties by diffusing boron atoms into the surface of the material at high temperatures, creating a high-hardness boron layer at surface. This study aims to investigate the effect of pack-boriding treatment on the wear properties of WC-Co material with a 19% Co content used in die inserts. Two sets of samples were subjected to pack-boriding with EKABOR-2 boron powder at 1000°C and 950°C for 4 hours. After pack boriding process, pin-on-plate wear test were conducted to samples under dry and oily conditions. The borided samples were characterized using optical microscopy and X-ray diffraction (XRD). X-ray diffraction analysis confirmed the effectiveness of the boriding process by identifying peaks associated with CoB, Co_2B, and W_2CoB_2 phases in the borided layer of the samples. The results were compared for each set of values, confirming that the boride layer significantly improved wear properties on the sample surfaces.

Keyword: Cold forming, WC-Co, Pack Boriding, Wear.

CORRELATION ANALYSIS FOR PREDICTING COLD FORGING PUNCH FATIGUE LIFE IN FASTENER PRODUCTION

Can İÇMEZ
Tolga AYDIN
Burak HIZLI
Samed ENSER
Umut İNCE

Hexagon Live Virtual Manufacturing 2024 Congresszentrum Marburg - Germany

CORRELATION ANALYSIS FOR PREDICTING COLD FORGING PUNCH FATIGUE LIFE IN FASTENER PRODUCTION

Abstract

Fastener production presents unique challenges in metal forming, particularly concerning the durability of cold forging dies subjected to high stresses. Cold forging at room temperature increases the forming difficulty due to work hardening after each operation. Hence, prior simulation analysis is crucial for assessing product accuracy and tool life before mass production. At Norm Fasteners, design and simulation studies are conducted before manufacturing to ensure quality. This study aims to correlate punch forming simulations using Simufact Forming software with real-world tool life data to calibrate and enhance the accuracy of cold forging punch analyses. The study examines cold forging punches utilized in the past two years, selecting those with low tool life based on total product quantity and average tool life. Simufact Forming simulations analyze the accuracy of product forms and conduct die analysis for punches involved in forging socket forms. Maximum tensile and compressive stresses from die analyses are compared with punch tool life data obtained from production. Analysis reveals a correlation between tool life and compressive stress, offering a predictive metric for punch life. The correlation between simulation results and real-world tool life data provides valuable insights for predicting cold forging punch life in fastener production, enhancing efficiency and reliability in manufacturing processes.

EFFECT OF BORIDING ON FATIGUE LIFE OF WC-CO DIE INSERTS IN COLD FORMING

Kübra ÖZTÜRK
Bahadır UYULGAN
Burak HIZLI
Umut İNCE

Tenth International Conference on Engineering Failure Analysis (ICEFA 2024)

EFFECT OF BORIDING ON FATIGUE LIFE OF WC-CO DIE INSERTS IN COLD FORMING

Kübra Öztürk[1,2,a*], Bahadır Uyulgan[1,b], Burak Hızlı[1,2,c] and Umut İnce[2,d]

[1]1Department of Metallurgical and Materials Engineering, Dokuz Eylul University, İzmir, Turkey
[2]R&D Center, Norm İzmir Cıvata San. ve Tic. A.Ş., AOSB, İzmir, Turkey
[a]kubra.ozturk@normfasteners.com, [b]bahadir.uyulgan@deu.edu.tr, [c]burak.hizli@normfasteners.com, [d]umut.ince@normfasteners.com

Abstract

Cold forming dies constitute the foundation of the entire cold forming process; thus, enhancing their life is essential to increase process efficiency in cold forming. Boriding heat treatment improves the mechanical and wear properties of materials by diffusing boron atoms into the surface of the materials. This study aims to investigate the effect of pack-boriding treatment on the fatigue life of WC-Co material with a 19% Co content used in die inserts. Three sets of samples were subjected to pack-boriding with EKABOR-2 boron powder at 1000°C, 950°C, and 900°C for 4 hours in each temperature condition. After boriding heat treatment, three-point bending fatigue testing were conducted on the samples. Goodman-Haigh diagrams were obtained from the experimental results to be utilized in predictive die life calculations for respective boriding condition. For comparison, samples without boriding heat treatment were used as a reference. X-ray diffraction analysis confirmed the effectiveness of the boriding process by identifying peaks associated with CoB, Co_2B, and W_2CoB_2 phases in the borided layer of the samples. Following the fatigue tests, the fracture surfaces of the samples were examined using scanning electron microscopy (SEM) to reveal the microstructural changes induced by the boriding heat treatment.

Keyword: Cold forming, WC-Co, Pack Boriding, Fatigue life

A CASE STUDY OF FASTENER PRODUCTION WITH FINITE ELEMENT SIMULATIONS

Alper KARAKAŞ
Prof. Dr. Binnur GÖREN KIRAL
Hatice SANDALLI YILDIZ

BURSA 2nd INTERNATIONAL CONFERENCE ON MATHEMATICS AND ENGINEERING

A CASE STUDY OF FASTENER PRODUCTION WITH FINITE ELEMENT SIMULATIONS

Alper Karakas, Prof. Dr. Binnur GOREN KIRAL, Hatica SANDALLI YILDIZ

Norm Somun San. ve Tic. A.Ş.
alper.karakas@normfasteners.com – 0009-0000-8659-1822
Dokuz Eylül University
binnur.goren@deu.edu.tr– ORCID ID
Norm Somun San. ve Tic. A.Ş.
hatice.sandalli@normfasteners.com – 0000-0002-5550-8480

Abstract

In today's technology finite element simulations are used in variety of industrial applications in order to identify the potential areas of failure in the both production part and tools, thereby reducing the trial-and-error period during production. Thanks to these simulations, engineers can investigate complex structures under different conditions, such as varying loads and temperatures with different material properties, allowing for a comprehensive understanding of their behavior.
Wheel nuts are fasteners used in the industry, especially to connect the rims of motor vehicles and trailers to the hub flanges. Although wheel nut production can be carried out by many manufacturing methods, as in other fasteners, in terms of speed and cost, it is preferred to produce it by cold forging method. The aim of this study is to examine the difficulties experienced in the production of wheel nuts, which are very difficult and costly to produce by cold forging method due to their geometry, and to design and analyze the optimum dies using the finite element method. As the method to be used, it is planned to determine the appropriate design with the support of the finite element program (Simufact forming).

Keywords: Fasteners, cold forging, tooling design, finite element simulations

APPLICATION OF FINITE ELEMENT ANALYSIS IN FASTENER INDUSTRY

Hatice SANDALLI YILDIZ
Burak Berk ARINCI
Ege ŞAHİN

5th INTERNATIONAL CONGRESS ON ENGINEERING AND SCIENCES

APPLICATION OF FINITE ELEMENT ANALYSIS IN FASTENER INDUSTRY

Hatice SANDALLI YILDIZ[1], Burak Berk ARINCI[1], Ege SAHIN[1]
[1]Norm Somun San. ve Tic. A.Ş., İzmir/Türkiye

Abstract

Finite element analysis (FEA) is an effective and commonly used numerical technique that has evolved into an essential tool for modelling and simulating various problems. It is widely used in many engineering processes due to the significant advantages it offers. Among these advantages, the most significant are reducing trial-and-error process, which in turn reducing production time and material usage. As in other industries, FEA is applied in fastener production. Generally, the forging process of billet material in closed dies in investigated in order to determine the material flow, contact conditions and flow defects. Besides of this, FEA can be used for many applications regarding the production and assembly of fasteners.

In this study, FEA was performed as a case study in order to investigate material flow during cold forging process of a fastener, to determine the hardness distribution, to simulate the riveting process and the compression process of the fastener. For cold forging analysis, low carbon steel was used as billet material and to obtain the final form of the fastener, the billet was forged in multi-stations. During the forging process, the hardness of the billet was increased due to deformation hardening and with the use of FEA, the hardness distribution within the billet at each stations were investigated. After cold forging analysis, the riveting analysis was performed to investigate whether cracks will occur in the product during riveting. As a final step, compression tests were carried out to check whether there would be permanent deformation in the part under a certain load.

Keywords: Cold forging, fastener production, finite element analysis

DEVELOPMENT OF A FINITE ELEMENT MODEL FOR PERFORMANCE TESTS OF SELF-CLINCHING NUTS

Hatice SANDALLI YILDIZ
Burak Berk ARINCI
Ege ŞAHİN

5th INTERNATIONAL CONGRESS ON ENGINEERING AND SCIENCES

DEVELOPMENT OF A FINITE ELEMENT MODEL FOR PERFORMANCE TESTS OF SELF-CLINCHING NUTS

Hatice SANDALLI YILDIZ[1], Burak Berk ARINCI[1], Ege SAHIN[1]
[1]Norm Somun San. ve Tic. A.Ş., İzmir/Türkiye

Abstract

Self clinching nuts are the nuts that are mounted onto a sheet metal by pressing. After this process, the nuts become an integral part of the metal. The nut is mounted onto the sheet metal through plastic deformation of either the sheet metal or the nut itself during the pressing. By using this type of nuts, in addition to achieving stronger connections, more environmentally friendly alternatives to welded fasteners can be obtained. Self clinchning nuts are becoming increasingly popular in automotive industry for various purposes such as to facilitate the mounting of bolts to sheet metal.

The nuts in question should be able to withstand push-out to prevent the nut from being pushed out of the sheet metal under the influence of external forces, and to resist torque to stay securely aligned with the sheet metal. Generally, in the case of using self-clinching nuts, the mounting conditions such as material and the thickness of the sheet metal, the diameter of the hole on the sheet metal are specified. The expected performance criteria for the specified conditions are also defined. In fastener industry, when responding to customer demands, it is critical that the product not only be formed according to technical drawing, but also meets the expected performance criteria.

In this study, finite element models are developed to simulate the performance tests of self-clinching nuts in order to determine whether the nuts will satisfy the expected the performance criteria.

Keywords: Self-clinching nuts, Finite element models, Push-out tests, Torque-out tests

DESIGN OF INNOVATIVE DIE SYSTEM FOR BREAKAGE PROBLEM AT LOW CYCLES ENCOUNTERED IN COLD FORGING

Burak Berk ARINCI
Hatice SANDALLI YILDIZ

8th International Congress on Engineering Sciences and Multidisciplinary Approaches

DESIGN OF INNOVATIVE DIE SYSTEM FOR BREAKAGE PROBLEM AT LOW CYCLES ENCOUNTERED IN COLD FORGING

Burak Berk ARINCI[1], Hatice SANDALLI YILDIZ[1]
[1]Norm Fasteners Somun, İzmir, Türkiye
[2]Norm Fasteners Somun, İzmir, Türkiye
ORCİD: ID/0000-0003-2286-3117, burak.arinci@ normfasteners.com
ORCİD: ID/0000-0002-5550-8480, hatice.sandalli@normfasteners.com

Abstract

The cold forging process involves shaping cylindrical materials by forging them across multiple stations within a series of dies. Various issues can arise during cold forging, primarily due to high loads in the stations, inappropriate material choices, and increased stress on tooling components caused by design factors. These issues can be mitigated through finite element analysis (FEA) conducted during the design phase, thereby preventing time and financial losses while enhancing production efficiency. The importance of engineering-based optimizations to maintain financial competitiveness and improve efficiency is growing steadily.

This study investigates a novel spacer system, developed using finite element analysis, to address spacer consumption issues observed in the production of long-length bushes. A major cause of spacer problems, particularly at backward extrusion stations, is the high tonnage applied to the fixed die side, which transfers excessive stress to the extension ejector. This stress often exceeds the resistance limits of the spacer, leading to failure. Using finite element analysis, high-speed steel was initially selected as the spacer material but was found inadequate in terms of strength. Consequently, a new spacer structure was designed.

The new spacer system incorporates a combined structure of high-speed steel and carbide material, utilizing a shrink-fit approach to transfer stress from the spacer to the carbide material. This design significantly improved the mechanical limits of the spacer system, ensuring that the stresses from the backward extrusion ejector remained within safe limits. The analysis highlighted the importance of considering shrink-fit rates and material compatibility for optimal performance of the designed spacer system.

Keywords: Cold forging, Die Systems, Hybrid die

NORM
FASTENERS

www.normfasteners.com